Western University

Scholarship@Western

1990

Generalized Design of Damping Control

M. Sainath Moorty

Follow this and additional works at: https://ir.lib.uwo.ca/digitizedtheses

Recommended Citation

Generalized Design of Damping Control

by

M.Sainath Moorty

Department of Electrical Engineering

Submitted in partial fulfillment
of the requirement for the degree of
Master of Engineering Science

Faculty of Graduate Studies
The University of Western Ontario
London, Ontario
April 1990

Abstract

This thesis establishes new guidelines to aid a system planning engineer in the process of improving the small signal stability of power systems. These guidelines help in designing controllers to increase the positive damping of poorly damped or unstable electromechanical modes of oscillations. Design strategies for damping controllers on generators (called power system stabilizers) and on Static Var Compensators (called supplementary controls) are described. The same procedure can be used for designing damping controllers on other dynamic devices like HVDC link, Flexible AC Transmission System (FACTS) elements etc.

In this thesis the particulars of the appropriate system representation and the use of various analysis techniques are treated in detail. Also, in this thesis certain new techniques and innovations to the existing techniques for the small signal stability investigations and design of damping control on a power system are introduced, namely, modal torque calculations, use of voltage participation and observability factors and innovations to the standard pole placement technique of designing damping control to make it more robust.

Modal torque calculations, used to determine in a qualitative and quantitative manner the dynamic interaction between various devices and

their effect on system stability, is shown to be a very powerful for small signal stability studies.

A systematic procedure for the selection of a suitable location to place damping control is presented considering the controllability and observability of the device and feedback signal respectively, for the mode under consideration (the mode whose damping is to be enhanced). The controllability and observability aspects using the well known state participation factors are augmented by the use of a new sensitivity index called the voltage participation factor and a novel method for calculating the observability of a potential feedback signal to the mode under consideration respectively. The effectiveness of this procedure for the selection of a suitable site is validated through a case study of a test system.

The effectiveness of the standard pole placement technique used for the design of the damping control is enhanced from robustness considerations by certain innovations with regard to selecting the new location for the mode under consideration and the constraints placed on the phase characteristics of the damping control compensation network.

The proposed guidelines developed for the generalized procedure of designing damping control is validated through an extensive case study of a 39-bus test system presented in this thesis.

Acknowledgments

I would like to acknowledge the support, encouragement and patience my supervisor, Dr. R.M.Mathur, has shown to me during the course of this thesis work. In his capacity as my supervisor, Dr.R.M.Mathur's guidance has been invaluable.

I deeply appreciate the help received from Dr.P.Kundur, G.Rogers, D.Y.Wong, and the rest of the staff at the Specialized System Studies Department - System Planning Division of Ontario Hydro. I would specially like to thank Dr.P.Kundur (Head; Specialized System Studies) in allowing me the opportunity to work in his department and introduce the topic of small signal stability to me. I would also like to thank Graham Rogers and David.Y. Wong, who, as my theoretical and programing 'gurus', took time off their busy schedule to teach me the intricacies of the subject of small signal stability.

I am indebted to Dr. Sachchidanand (Visiting Professor from I.I.T. Kanpur, India) for the valuable discussions we had which helped crystalize certain concepts used in this thesis. His guidance and help in preparing the draft of this thesis is very much appreciated.

Table of Contents

List of Tables

List of Figures

List of Appendices

Nomenclature

All of the symbols used in this thesis have been defined in the text at appropriate places. Definitions of some important symbols are reproduced here.

ω_o : Base angular speed (radians/second)

H : Inertia constant of synchronous machine in per unit

D : Damping constant of synchronous machine in per unit

[A] : Matrix A or vector [A]

$[A]^T$: Transpose of matrix [A] or vector [A]

$\Delta(.)$: Small deviation in the quantity (.)

SVC : Static Var Compensator

PSS : Power System Stabilizer

HVDC: High Voltage Direct Current

I,i : Current

V,v : Voltage

P,Q : Real and reactive power respectively

λ : Flux linkage in per unit (Chapter 2); Eigenvalue elsewhere

ψ : Flux linkage per unit voltage

Z,Y : Impdence and admittance respectively

ζ : Damping ratio

Subscripts d,q and D,Q: Denote the direct (d,D) and quadrature (q,Q) components of the quantities refered to the machine rotor axis and the synchronously rotating reference frame respectively

Chapter 1.

Introduction

1.1   General

Electric power systems are the most complex structures mankind has ever built. They span vast geographical areas transmitting energy over large distances. The stability and integrity of this system is vital for the economy. The power system must be reliable and ensure good quality of electric energy supplied to the user. However, these systems are prone to disturbances. A disturbance may be small or large in magnitude. These disturbances lead to different type of changes in the system. These changes may allow the system to operate under a stable condition or make it unstable. The instability of a power system can be loosely classified into two categories a)Steady state or small disturbance instability and b)Transient instability. The conditions for the onset of these instabilities and the corresponding remedial actions have been widely documented in the literature [2].

The steady state stability or small disturbance stability of a power system is defined as follows [24]:

A power system is steady state stable for a particular steady state operating condition if, following any small disturbance, it reaches a steady state operating condition which is identical or close to the pre-disturbance operating condition. This is also known as small disturbance stability of a power system.

In general the term small signal stability is interchangeably used for steady state stability [6]. Small signal instability is prone to occur in situations where the system is operating near its power limit, or if remote generation is involved, or if the system is trying to achieve an operating point which is inherently unstable. Incidents such as the Northeast Power Failure of 1965 demonstrate the consequences of small signal instability [3]. Ever since then there has been a growing interest in the study of power systems to improve the small signal stability.

1.2   Problem of small signal instability

Almost on a continuous basis the power system undergoes small changes due to random switching of the loads. The inherent nature of the system to try and meet the load requirements cause low frequency electromechanical oscillations. This is due to the dynamic interactions between the mechanical and electrical torques applied to the generator rotating system. These oscillations are reflected as variations in the speed, voltage, frequency etc. of the system. When these variations remain within narrow bounds, the system is said to be stable in the small signal sense. Conversely, if these variations increase with time, the system is unstable. The relative small signal stability of the system depends on how well the electromechanical modes of the system are damped. The behavior of the

electromechanical modes of oscillations can be analyzed in a linearized domain, since the cause of small signal instability is not due to large deviations but the inherent system conditions which lead to instability. The improvement of small signal stability is achieved by the proper design of controls so as to increase the damping of electromechanical modes of oscillation. This calls for a detailed analysis of the power system through appropriate modelling of its components as well as a systematic approach to the design of the controls.

1.3 System modelling

The modelling of a power system in dealing with small signal stability studies has been a well researched topic [1]. As mentioned earlier small signal stability studies involve the analysis of the small signal (linear) behavior of the power system about an operating point. This has led to the development of linearized system models in the state space framework. The time frame of interest in the analysis of the small signal stability is between 1 to 10 seconds. By this time the stator quantities of the machines and the network voltages and currents would have reached the steady state and hence can be represented by algebraic equations [4]. A recent development in the representation of the power system is the use of component connection form to model all the dynamic devices in the system [1]. In this approach the development of the system model proceeds systematically with the development of individual subsystems or component models which are interfaced through appropriate variables. This makes modelling flexible and enables large, complex systems to be modelled conveniently [5].

1.4   Control system design philosophy

The basic steps in the design of a damping control are:

a)Selection of suitable location for installing the damping control

b)Choice of suitable feedback signal to the damping control.

c)Determination of damping control parameters.

Linear control theory can be used to design damping control for the damping of electromechanical modes of oscillations. There are many control system design techniques, ranging from classical control methods to optimal and adaptive. It is important to note that very few power utilities have incorporated designs using optimal or adaptive control methods; and where it has been used, it is on an experimental basis. The main shortcoming of the optimal design technique is its lack of robustness since the system can operate under a wide variety of operating conditions, thereby making an optimal design subjective [6]. Adaptive control generally requires an internal model of the system (state identification). The degree to which this model remains representative of the system limits the use of adaptive control. Traditionally, classical control methods have been used for design purposes in power systems. Techniques like root locus, frequency response and pole placement have been used, but mainly for the design of power system stabilizers (PSS) on generators.

Based on the feedback of signals like speed, frequency, or combination of these and other signals; a PSS is designed to provide a supplementary input to the excitation system. The excitation system acts

on this supplementary input and produces a torque. This torque has a component in phase with speed changes of the generator which aids the damping of the electromechanical modes of oscillation [7]. The frequency response technique is normally used to design the lead or lag network for providing the necessary phase compensation over the desired frequency range [6].

Damping of electromechanical modes of oscillation can also be achieved through the supplementary control of Static Var Compensators (SVC) [8]. For the proper design of SVC supplementary control it is necessary to take into account the system wide interaction between the generating systems. However, this may result in a single input/multi-output type situation and hence the frequency response technique used for the design of PSS cannot be directly applied. In this situation the design of the phase compensation network will become quite complex and may deteriorate into a trial and error procedure. A need therefore exists to develop a systematic procedure for the design of SVC supplementary control. In addition to frequency response, pole placement techniques have also been used for the design of damping control [8,9,10]. This approach for control design has the advantage that the complete system dynamics can be conveniently handled.

In a large system, the location of damping control (power system stabilizer, supplementary control on SVC, etc) plays an important role in establishing its effectiveness on damping electromechanical modes of oscillation. A suitable location can be determined, based on the state

participation factors [11,12]. State participation factors give the sensitivity of the eigenvalues to the diagonal elements in the state matrix. The magnitude of the state participation factor gives an indication of the contribution of that state to a particular mode of electromechanical oscillation (eigenvalue). In situations where state participation factors cannot provide adequate information, a need exists to develop alternative criterion using other system quantities.

To enhance the effectiveness of the damping control the proper selection of feedback signals to the damping controllers is important. Years of field experience coupled with detailed analysis has shown that speed, frequency, line power flows or combinations of these form satisfactory feedback signals to power system stabilizers [13]. In the selection of feedback signals for supplementary control on SVC one cannot rely on field experience as this is minimal. Some work done in this area pinpoint line currents, line active power, bus frequency, active current components as possible signals [14].

1.5   Objective and scope of the thesis

The above discussion points to a need to develop a systematic approach for the design of damping control taking into consideration the dynamic interaction between the various components of a power system. In an attempt to accomplish this, the specific objectives of this thesis are established as:

a)Develop a better understanding, on a quantitative basis, of the dynamic interactions between the various power system components and their effect on the system stability.

b)Develop an alternate criteria for the determination of a suitable location of the damping control. The need for this arises when the state participation factors may not provide adequate information.

c)Develop a generalized procedure based on the mode observability criterion to select the appropriate feedback signals for the damping control.

d)Develop a design strategy for increasing the robustness of a damping control. The robustness of the design ensures that the damping control will operate effectively under a wide range of operating conditions to increase the damping of electromechanical modes of oscillation.

This thesis proposes new guidelines for the systematic design of controllers for damping electromechanical modes of oscillation. Special attention is required for the design of supplementary controls on Static Var Compensators.

1.6   Outline of the thesis

Chapter 2 describes the development of the linearized power system model in the state space form. Standard techniques (state participation factors, mode shape determination, frequency response, residue and time response calculation) for the small signal stability analysis of power systems and design of control is described in Chapter 3. Certain shortcomings in these techniques are overcome by certain improvements and new techniques are brought forth in Chapter 4. Also, in Chapter 4, the

effect of various power system components on the small signal stability of the system is described. Here emphasis is laid on the quantitative assessment of the effect a device (like SVC) has on system stability. Also, the concepts of voltage participation factors and the observability of eigenvalues in various system signals is described.

The guidelines and procedures for the design of the damping control using a pole placement technique employing the residue method, is discussed in Chapter 5. Certain innovations for making the damping control more robust are also proposed in this chapter.

The structure and salient features of the Small Signal Stability (S^3) program developed for the purpose of conducting small signal stability investigations is described in Chapter 6. Also, case studies of a test system employing the proposed design procedures for damping control are reported in Chapter 6.

Chapter 7 summarizes the conclusions drawn from this thesis and submits the future scope of work.

Chapter 2.

Power System Modelling

2.1   General

This chapter describes the development of the system model in the state space framework for small signal stability analysis of power systems. The overall system model is developed in a modular fashion utilizing the various device (subsystem) models.

2.2   State space representation

A linear dynamic system described by state space equations has the following form,

$$[\dot{X}] = [A]\,[X] + [B]\,[u] \tag{2.001}$$

$$[y] = [C]\,[X] + [D]\,[u] \tag{2.002}$$

where, [X] is the state vector, a set of system variables which, when known, completely describes the system, [u] is the vector of applied inputs to the

system, [y] is the output vector, [A] is the system state matrix, [B] is the input matrix defining the distribution of the inputs into the system, [C] is the output matrix defining the linear combination of the states forming each output and [D] is the feedforward matrix defining the linear combination of the inputs forming each output.

The size of the vector [X] is equal to the number of states used to represent the system under consideration and matrix [A] is a square matrix whose size is equal to the number of states in the system modelled. Also, $[\dot{X}] = \frac{d}{dt} [X]$

2.3 System modelling - a macro view

The development of the power system model for small signal stability analysis requires appropriate representation of the dynamic behavior of the various constituent devices of the power system and the interaction between them. These constituent devices are generally generating system, reactive power control devices, HVDC transmission system, loads etc. One approach to model the system is to represent each individual device in the linearized state space framework about an operating point, as given below,

$$[\dot{X}_d] = [A_d] [X_d] + [B_d] [\Delta V_d] \tag{2.003}$$

$$[\Delta I_d] = [C_d] [X_d] - [Y_d] [\Delta V_d] \tag{2.004}$$

where, $[X_d]$ is the state vector of the device, $[\Delta V_d]$ is the vector of all the small signal changes in the bus voltages (p.u.) which are input to this device, $[\Delta I_d]$ is the vector of all the small signal changes in the current injections into the buses by this device (p.u.), $[A_d]$ is the individual device state matrix, $[B_d]$ is the bus voltage input distribution matrix, $[C_d]$ is the device output distribution matrix for the device states, and $[Y_d]$ is the device admittance matrix.

It can be seen that Equations (2.003) and (2.004) represent each device as a voltage controlled current source. As the various devices in the power system interact through the transmission network, their respective component models can now be conveniently interfaced through appropriate network variables (voltage and current). The transmission network is treated to be under steady state for small signal stability analysis and is represented in the linearized domain about an operating point, by the equation,

$$[\Delta I] = [Y_N] [\Delta V] \qquad (2.005)$$

where, $[Y_N]$ is the bus admittance matrix.

2.3.1 System State Matrix

The individual state space equations of the dynamic devices are stacked together in the following form,

$$[\dot{X}] = [A_{st}]\,[X] + [B_{st}]\,[\Delta V] \qquad\qquad (2.006)$$

$$[\Delta I] = [C_{st}]\,[X] - [Y_{st}]\,[\Delta V] \qquad\qquad (2.007)$$

where, [X] is the complete state vector for the power system, [ΔV] is the vector of the network small signal changes in the bus voltages (p.u.), [ΔI] is the vector of the network small signal changes in the current injections (p.u.) into the buses by the system devices, $[A_{st}]$ is the stacked state matrix built up from all the individual device state matrices in the block diagonal form, $[B_{st}]$ is the stacked device bus input matrix built up from all the individual device bus input matrices in the block diagonal form, $[C_{st}]$ is the stacked device output matrix built up from all the individual device output matrices in the block diagonal form, and $[Y_{st}]$ is the stacked device admittance matrix built up from all the individual device admittance matrices in the block diagonal form.

Combining Equations (2.005), (2.006) and (2.007), the overall system state matrix [A], can be derived as,

$$[A] = [\; A_{st} + B_{st}\,[Y_N + Y_{st}]^{-1}\,C_{st} \;] \qquad\qquad (2.008)$$

This modular approach known as the 'component connection form' provides flexibility and ease in formulating the overall power system model. By virtue of the fact that each device is represented separately and then interfaced, it is possible to represent the device to any desired degree of detail. Also, the approach extends the flexibility to conveniently augment

the system model to include the representation of any new device. The formation of the state matrix [A] for a sample power system is illustrated in Appendix (A1.1).

An important consideration in the development of the power system model is the proper interface of the various device dynamics. Since, each synchronous machine in a power system is represented on its individual direct (d-) and quadrature (q-) axes, these can be interfaced to the other power system components only if all the component models including the synchronous machine model can be transformed to a common reference frame. In this context, a discussion on the common reference frame (synchronously rotating reference frame) will be in order.

2.3.2 Synchronously rotating reference frame

The various power system components can be conveniently modelled using phase variables except synchronous machines which results in differential equations with time varying coefficients. To avoid these time varying elements, it is customary to express the machine equations in the direct (d-) and quadrature (q-) axes components using Park's transformation. The machine interface to the external system is then described through the terminal voltages and currents, which are referenced to the machine d- and q- axes. The direct (d-) axis lags the quadrature (q-) axis by 90° and is taken to be fixed on the machine rotor.

Thus, each machine model will result in a different set of direct (d-) and quadrature (q-) axes reference frame.

The proper interface of the machine models to the rest of the system which, may be represented in the phase variable domain, would require the transformation of all the device models to a common coordinate axes (reference frame). The common coordinate axes (direct axis D- and quadrature axis Q-) which form the synchronously rotating reference frame, are established with respect to the system slack bus. The direct (D-) axis coincides with angle reference of the slack bus and lags the quadrature (Q-) axis by 90°. The relationship between the phase variables and the D- and Q- axis reference frame is depicted in Figure (2.1).
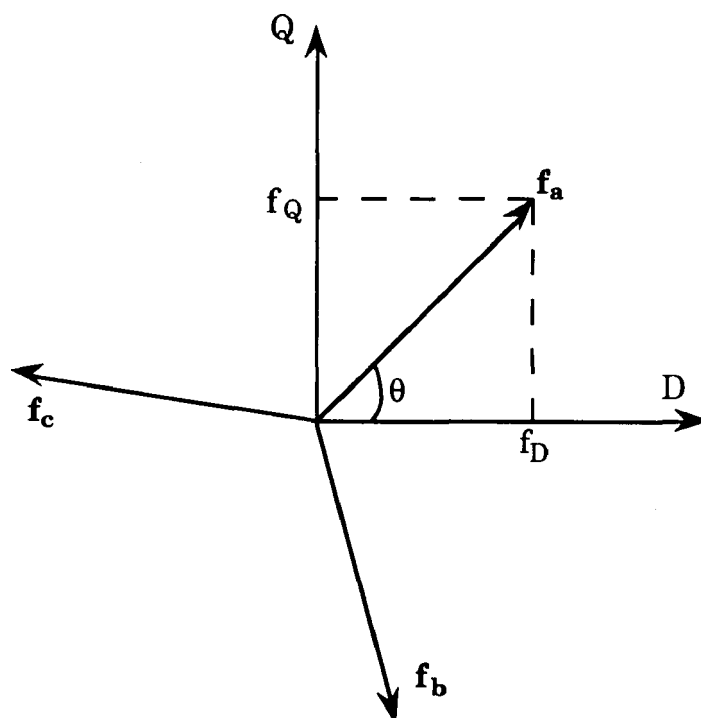
Figure (2.1): D-Q components of a phasor quantity

The phase variable (f_a, f_b, f_c where a,b,c denote the phases) are related to the D-Q components (f_D, f_Q) as follows [21],

$$\begin{bmatrix} f_a \\ f_b \\ f_c \end{bmatrix} = \begin{bmatrix} \cos\theta & \sin\theta \\ \cos(\theta-120) & \sin(\theta-120) \\ \cos(\theta-240) & \sin(\theta-240) \end{bmatrix} \begin{bmatrix} f_D \\ f_Q \end{bmatrix}$$

Since, the system is treated to be balanced for small signal stability analysis, there will not be any zero sequence component. In case of synchronous machine, the relationship between the machine d-q axes and the system common reference frame (D-Q axes) is shown in Figure (2.2).

The voltage equation describing a synchronous machine under steady state is given by,

$$\mathbf{E} = \mathbf{v_t} + \mathbf{i_t}\, r_a + j\, \mathbf{i_t}\, x_q \qquad\qquad (2.009)$$

where, all **boldface** quantities are phasors, $\mathbf{E}$, $\mathbf{v_t}$ and $\mathbf{i_t}$ are the phasor quantities respectively of the internal EMF, terminal voltage and current, of the machine expressed in per unit and r_a, x_q are respectively the stator resistance and quadrature (q-) axis reactance of the machine expressed in per unit. The (d-q) and (D-Q) components of the terminal voltage and current are related to the phase quantities as,

$$\mathbf{v_t} = v_d + jv_q \; ; \qquad\qquad \text{and} \qquad\qquad \mathbf{v_t} = v_D + jv_Q$$

$$\mathbf{i_t} = i_d + ji_q \; ; \qquad\qquad \text{and} \qquad\qquad \mathbf{i_t} = i_D + ji_Q$$

where, subscripts d, q, D, Q denote the (d- and q-) and (D- and Q-) component quantities (voltage and current) respectively.

Any quantity (f) expressed in the d-q components can be transformed as given below to the D-Q components and vice-versa, using the transformation matrix $[T_{cs}]$ which is derived from Figure (2.2).

$$|\mathbf{v_t}| = \sqrt{v_d^2 + v_q^2} = \sqrt{v_D^2 + v_Q^2}$$

$$|\mathbf{i_t}| = \sqrt{i_d^2 + i_q^2} = \sqrt{i_D^2 + i_Q^2}$$
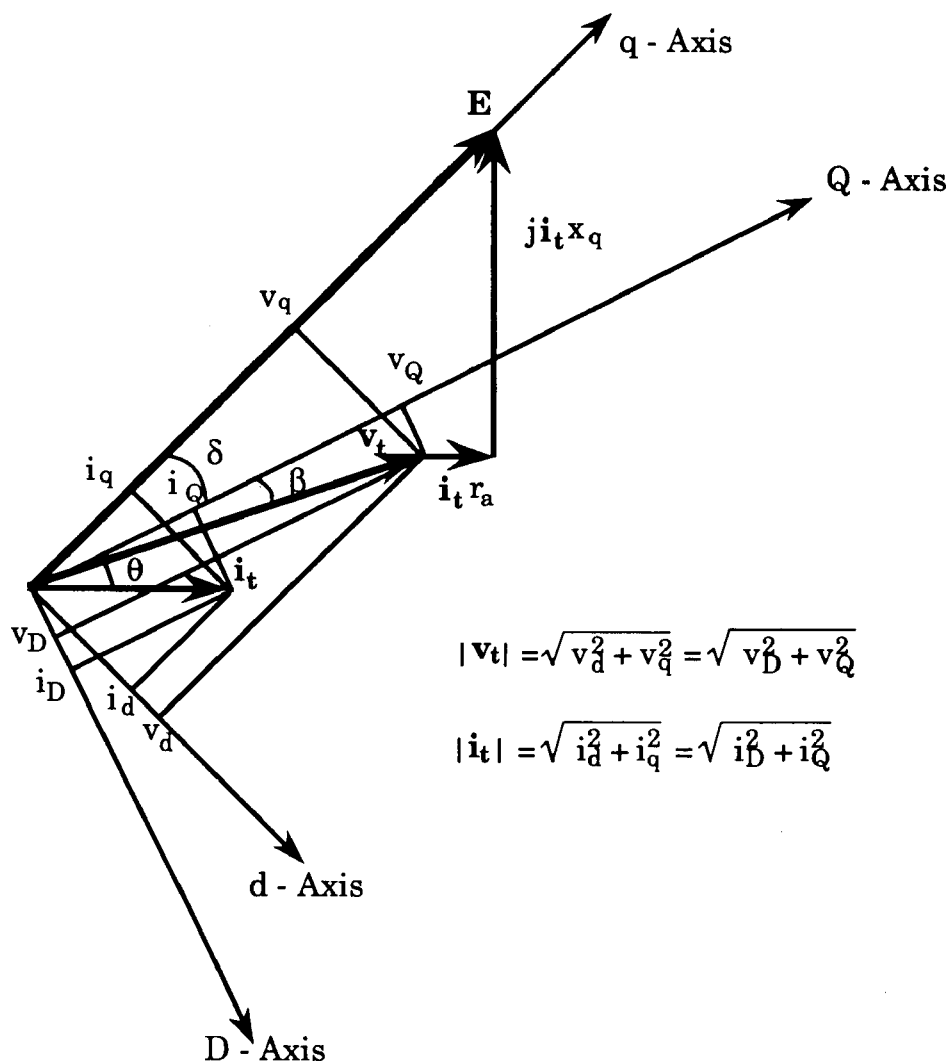
Figure (2.2): D-Q & d-q reference frames for a synchronous machine

$$[f_{DQ}] = [T_{cs}] [f_{dq}] \tag{2.010}$$

$$[f_{dq}] = [T_{cs}]^T [f_{DQ}] \tag{2.011}$$

where,

$$[f_{DQ}] = [\; f_D \quad f_Q \;]^T\;; \qquad [f_{dq}] = [\; f_d \quad f_q \;]^T\;; \quad \text{and} \quad [T_{cs}] = \begin{bmatrix} \cos \delta & -\sin \delta \\ \sin \delta & \cos \delta \end{bmatrix}$$

The determination of the angle δ between the machine reference frame and the system reference frame can be obtained from the equation given below.

$$\tan(\beta + \delta) = \frac{|i_t|\; x_q \cos \theta - |i_t|\; r_a \sin\theta}{|i_t|\; r_a \cos \theta + |i_t|\; x_q \sin\theta + |v_t|} \tag{2.012}$$

where, $\tan\beta = \frac{v_D}{v_Q}$, and θ is the power factor angle of the machine, and the load angle (90-β) is the bus voltage angle as obtained in the load flow calculations.

Expressing the machine terminal voltage and current in d-q and D-Q components using Equations (2.010) and (2.011), the following equations are obtained upon linearization,

$$[\Delta v_{DQ}] = [Tcs] [\Delta v_{dq}] + \begin{bmatrix} -v_Q \\ v_D \end{bmatrix} \Delta\delta \tag{2.013}$$

$$[\Delta i_{dq}] = [Tcs]^T [\Delta i_{DQ}] + [Tcs]^T \begin{bmatrix} i_Q \\ -i_D \end{bmatrix} \Delta \delta \qquad (2.014)$$

where,

$$[\Delta v_{DQ}] = [\Delta v_D \ \Delta v_Q]^T ; \qquad \text{and} \qquad [\Delta i_{DQ}] = [\Delta i_D \ \Delta i_Q]^T$$

In Equations (2.013) and (2.014) the operator Δ signifies a small change around an operating point.

2.4   System modelling - a micro view

The overall power system model is built up from the individual subsystem models for generating system, static var compensator, loads, transmission network, etc. Loads can be assumed to be of the constant impedance form and included as part of the transmission network which, in turn, is represented by algebraic equations as it is treated to be under steady state for small signal stability studies. The other dynamic devices (subsystems) which comprise of various constituent blocks can be represented through the models of these blocks depending on the degree of detail required.

A typical generating system model consists of the synchronous machine model and various other control systems like, the excitation system model for terminal voltage regulation, the power system stabilizer (PSS) model for damping enhancement, the prime mover model for mechanical power input regulation etc. The synchronous machine of the

generating system can be modelled in two ways, the classical model and the flux linkage model. The classical model of the synchronous machine is used when only the machine dynamics of the rotating system is considered adequate in representing the dynamics of the generating system. The flux linkage model of the synchronous machine is used when, apart from the dynamics of the rotating system, a need is felt, to represent the rotor dynamics, or/and the dynamics of the controls associated with the generating system.

The static var compensator (SVC) model comprises of the voltage regulator model (needed to maintain the specified bus voltage magnitude) and may include the supplementary control model (needed for damping enhancement).

The various control systems which are part of the devices, i.e. excitation system and PSS on the generating system and, the voltage regulator and supplementary control on the SVC, can be modelled in an identical manner. The modelling of the control system involves the formulation of the state space equations describing its dynamic behavior.

2.4.1 Control System model

A control system is built up of elementary blocks like lead, lag, washout, etc. Each of these control blocks can be represented by an individual state space equation of the form,

$$\dot{x} = a\,x + b\,u \tag{2.015}$$

$$y = c\,x + d\,u \tag{2.016}$$

where, x is the state variable of the control block, u is the input to the control block, y is the output of the control block and a,b,c,d are the coefficients of the state space equations. The method of representing individual elementary control blocks like lag, lead and washout are shown in Appendix (A1.2).

For a control system comprising of many blocks, the individual state space equations for each block are determined (in the form of Equations (2.015) and (2.016)), and are stacked together to get,

$$[\dot{X}_c] = [A]\,[X_c] + [B]\,[u] \tag{2.017}$$

$$[y] = [C]\,[X_c] + [D]\,[u] \tag{2.018}$$

where, $[X_c]$ is the state vector of the control system, [A], [B], [C], [D] are the matrices assembled from the stacking of the state space equations of each individual control block, [u] is the vector of the inputs to all the individual blocks, and [y] is the vector of the outputs from all the individual blocks.

The interconnection between the various control blocks, external inputs and the final control system output [z] is given by,

$$[u] = [L]\,[y] + [G]\,[U] \tag{2.019}$$

$$[z] = [M] [y] + [K] [U] \qquad (2.020)$$

In Equations (2.019) and (2.020) the vector [U] consists of suitable variables, whose linear combinations form the external inputs to the control system. The inputs to the control blocks [u], as seen from Equation (2.019) is the sum of the linear combinations of the external inputs defined by the relation [G][U] and the linear combinations of the outputs of the other control blocks present in the system defined by the relation [L] [y]. Depending on the external inputs to the control system and the control blocks to which they are applied, the coefficient matrix [G] is accordingly derived. Similarly, depending on the structural interconnections of the various blocks in the control system, the matrix [L] is formulated which defines the input/output relationship between the various blocks.

Based on the similar lines of deriving the matrices [L] and [G], matrices [M] and [K] can also be formed. The matrix [M] describes the contributions of the outputs of the various internal elementary blocks to each of the final outputs from control system, and [K] is the feedforward matrix describing the contributions of the external inputs to the final output of the control system.

From the above discussion it is seen that the identity of the input and output of each control block is maintained by separately defining the vectors [u] and [y]. This procedure of defining a separate input [u] and output vector [y], provides the flexibility to account for the structural changes in the control system being modelled.

Eliminating the vectors [u] and [y] from Equations (2.017) to 2.020), the final form of the state space equations of the control system is derived as,

$$[\dot{X}_c] = [A_c] [X_c] + [B_c] [U] \qquad\qquad (2.021)$$

$$[z] = [M_c] [X_c] + [K_c] [U] \qquad\qquad (2.022).$$

where,

$$[A_c] = [A + B L [I - D L]^{-1} C] ; \quad [B_c] = [B L [I - D L]^{-1} D G + B G];$$

$$[M_c] = [M [I - D L]^{-1} C] ; \text{ and } [K_c] = [M [I - D L]^{-1} D G + K]$$

The procedure outlined above for obtaining the control system state space equations is highly flexible as modifications can be easily incorporated. An example is given in Appendix (A1.3) to illustrate the development of a control system model.

2.5   Classical model of the synchronous machine

The classical model of a synchronous machine is the simplest form of representing its dynamics. This model is used if the detailed representation of a machine dynamics is not considered important for the analysis under consideration. In this model the assumptions made are that the field flux linkages are constant, the stator resistance is negligible, and the d- and q- axes transient reactances are equal. Thus, the machine

can be modelled as a voltage source **E** behind a transient reactance x_d' as shown in Figure (2.3).
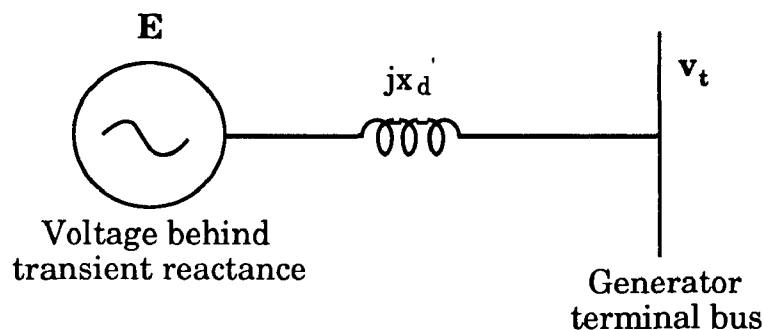
Figure (2.3): Classical model of the synchronous machine

In Figure (2.3), all the **boldface** quantities are phasors and v_t is the machine terminal voltage (p.u.).

2.5.1 State variables

The state variables chosen to derive the classical model of the synchronous machine are, the small changes in the angular velocity of the synchronous machine ($\Delta\omega$; p.u.) and the small changes in the rotor angle ($\Delta\delta$; p.u.). The rotor angle is defined as the angle between the machine direct (d-) axis and the common reference direct (D-) axis. Thus, the state vector of the classical machine is,

$$[X_{cl}] = [\ \Delta\omega \quad \Delta\delta\ ]^T \tag{2.023}$$

2.5.2 Initial equations for the state space formulation

The direct (d-) and quadrature (q-) axes terminal voltages of the synchronous machine neglecting the rate of change of stator and rotor flux linkages can be expressed as,

$$v_d = -\omega_0 \, \lambda_q \qquad\qquad (2.024)$$

$$v_q = \omega_0 \, \lambda_d \qquad\qquad (2.025)$$

where, v_d , v_q are the d-q axis components of the machine terminal voltage in per unit.

The dynamics of the rotating parts of the machine is described by the following equation which is derived in Appendix (A1.4).

$$I \, \omega_0 \, \frac{d}{dt}\omega = P_{base} \, (\, \omega_0 \, \lambda_q \, i_d - \omega_0 \, \lambda_d \, i_q \,) \qquad\qquad (2.026)$$

where, P_{base} is the base power of the system (MVA), ω_0 is the base angular speed of the system in radians/second, ω is the angular speed of the machine (p.u.), I is the moment of Inertia of the rotating parts of the synchronous machine in Kg-m^2, λ_d and λ_q are the direct (d-) and quadrature (q-) axes components of the stator flux linkages (p.u.).

The flux linkages (λ) can be expressed in per unit voltage (ψ), as,

$$\psi_d = \omega_0 \, \lambda_q \qquad\qquad (2.027)$$

$$\Psi_q = \omega_0 \, \lambda_d \tag{2.028}$$

Rewriting Equations (2.024) to (2.026) using Equations (2.027) and (2.028) gives,

$$v_d = -\Psi_q \tag{2.029}$$

$$v_q = \Psi_d \tag{2.030}$$

$$I \, \omega_0 \, \frac{d}{dt}\omega = P_{base} \, (\, \Psi_q \, i_d - \Psi_d \, i_q \,) \tag{2.031}$$

Linearizing Equations (2.029), and (2.030) gives,

$$\Delta v_d = -\Delta\Psi_q \tag{2.032}$$

$$\Delta v_q = \Delta\Psi_d \tag{2.033}$$

The d- and q- axes flux linkages are related to the stator d- and q- axes currents as,

$$\lambda_d = - L_d' \, i_d \tag{2.034}$$

$$\lambda_q = - L_d' \, i_q \tag{2.035}$$

where, L_d' is the d- axis transient inductance. Combining Equations (2.027) and (2.028), with Equations (2.034) and (2.035) results in,

$$\Psi_d = - x_d' \, i_d \tag{2.036}$$

$$\Psi_q = - x_d' \, i_q \tag{2.037}$$

Linearizing Equation (2.036) and (2.037) gives,

$$\Delta\psi_d = -x_d' \Delta i_d \qquad (2.038)$$

$$\Delta\psi_q = -x_d' \Delta i_q \qquad (2.039)$$

2.5.3 Derivation of the state space equations

Equation (2.031) is linearized as,

$$\frac{2H}{\omega_0} \dot{\Delta\omega} = [\; \psi_q \quad -\psi_d \;] \begin{bmatrix} \Delta i_d \\ \Delta i_q \end{bmatrix} + [\; -i_q \quad i_d \;] \begin{bmatrix} \Delta\psi_d \\ \Delta\psi_q \end{bmatrix} \qquad (2.040)$$

where, H is the inertia constant of the machine (p.u). The derivation of Equation (2.040) is given in Appendix (A1.4). Substituting $\Delta\psi_d$ and $\Delta\psi_q$ from Equation (2.038) and (2.039) in the above equation gives,

$$\frac{2H}{\omega_0} \dot{\Delta\omega} = [\; -E_d \quad -E_q \;] \begin{bmatrix} \Delta i_d \\ \Delta i_q \end{bmatrix} \qquad (2.041)$$

where, E_d and E_q are the d- and q- axes components of the voltage behind the transient reactance and can be expressed as,

$$E_d = -(\psi_q + x_d' i_q) \qquad (2.042)$$

$$E_q = \psi d + x_d' \, i_d \, .$$ (2.043)

The states $\Delta\omega$ and $\Delta\delta$ are related as,

$$\dot{\Delta\delta} = \Delta\omega$$ (2.044)

From Equations (2.032), (2.033), (2.038) and (2.039), the terminal voltage and current can be related as,

$$[\Delta v_{dq}] = [Z_d] \, [\Delta i_{dq}]$$ (2.045)

where, $[\Delta v_{dq}] = [\ \Delta v_d \quad \Delta v_q]^T;$ $\qquad\qquad [\Delta i_{dq}] = [\ \Delta i_d \quad \Delta i_q]^T$; and,

$$[Z_d] = \begin{bmatrix} 0 & x_d' \\ -x_d' & 0 \end{bmatrix} .$$

2.5.4 Transformation to the D- and Q- coordinates

In the state space equations derived above the terminal voltage and current are referenced to the d- and q- axes of the machine. It is necessary to transform these voltages to the D- and Q- axes of the system for proper interface of the machine to the system. Applying the transformation given by Equations (2.013) and (2.014) to the Equations (2.045), the terminal voltage and current in the D and Q coordinates are related by the following expression.

$$[\Delta i_{DQ}] = [C_{del}] \, \Delta\delta \ - \ [Y_d] \, [\Delta v_{DQ}] \tag{2.046}$$

where, $[\Delta v_{DQ}] = [\ \Delta v_D \quad \Delta v_Q]^T;$ $\qquad\qquad [\Delta i_{DQ}] = [\ \Delta i_D \quad \Delta i_Q]^T \ ;$

$$[C_{del}] = \left[\begin{array}{cc} \dfrac{E_D}{x_d{}'} & \dfrac{E_Q}{x_d{}'} \end{array}\right]^T ; \qquad \text{and} \qquad [Y_d] = - [Z_d]^{-1}$$

E_D and E_Q are the D- and Q- components of the voltage behind the transient reactance, and is given as,

$$E_D = v_D - xd' \, i_Q \tag{2.047}$$
$$E_Q = v_Q + xd' \, i_D \tag{2.048}$$

Transforming the terms in Equation (2.041) expressed in the d-q coordinates to the D- and Q- coordinates, and substituting for $[\Delta i_{DQ}]$ from Equation (2.046), gives,

$$\Delta\dot{\omega} = a_{12} \, \Delta\delta \ + [B_v] \, [\Delta v_{DQ}] \tag{2.049}$$

where,

$$a_{12} = \frac{\omega_0}{2\,H} \left(E_Q \, i_D - E_D \, i_Q \ - \frac{E_D{}^2 + E_Q{}^2}{x_d{}'} \right) ; \tag{2.050}$$

and, $[B_v] = \dfrac{\omega_0}{2\,H} \left[\begin{array}{cc} \dfrac{-E_Q}{x_d{}'} & \dfrac{E_D}{x_d{}'} \end{array}\right]$

2.5.5 Final state space equations

Equations (2.049), (2.045) and (2.047) can be put in the general form of Equations (2.003) and (2.004) to result in the following state space model of the classical representation of the generating system.

$$[\dot{X_d}] = [A_d] [X_d] + [B_d] [\Delta V_d] \tag{2.051}$$

$$[\Delta I_d] = [C_d] [X_d] - [Y_d] [\Delta V_d] \tag{2.052}$$

where, $[X_d] = \begin{bmatrix} \Delta\omega \\ \Delta\delta \end{bmatrix}$; $\qquad [\Delta V_d] = [\Delta v_{DQ}]$; $\qquad [\Delta I_d] = [\Delta i_{DQ}]$;

$[A_d] = \begin{bmatrix} 0 & a_{12} \\ 1 & 0 \end{bmatrix}$; $\qquad [B_d] = \begin{bmatrix} B_v \\ 0_{1\times 2} \end{bmatrix}$; $\quad$ and $\qquad [C_d] = [\, 0_{2\times 1} \quad C_{del}]$

2.6 Flux linkage model of the synchronous machine

A synchronous machine having three stator windings, one field winding and five equivalent damper windings - two along the direct (d-) axis and three along the quadrature (q-) axis, on the rotor are considered in deriving the detailed synchronous machine model using flux linkage representation. Figures (2.4a) and (2.4b), show the d- and q- axes equivalent circuits of the synchronous machine respectively [1,14,15].
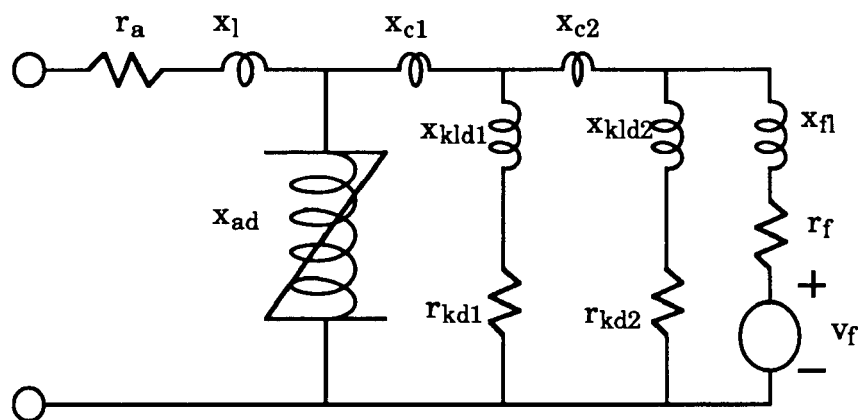
Figure (2.4a): Synchronous machine d- axis equivalent circuit
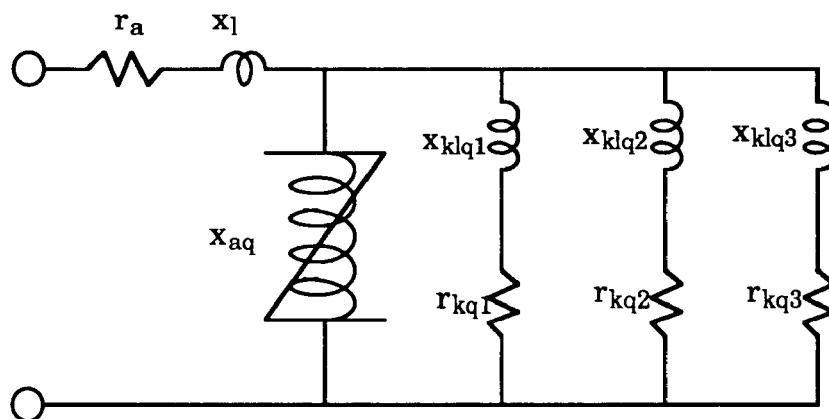
Figure (2.4b): Synchronous machine q- axis equivalent circuit

In Figures (2.4a) and (2.4b), the various quantities are,

r_a, x_l = Stator resistance and leakage reactance (p.u.), respectively.

r_f, x_f = Field winding resistance and leakage reactance (p.u.), respectively.

r_{kdi}, x_{kldi} = Damper winding resistance and leakage reactance (p.u.) in the d- axis equivalent circuit respectively. For i = 1, 2.

r_{kqj}, x_{klqj} = Damper winding resistance and leakage reactance (p.u.) in the q- axis equivalent circuit respectively. For j = 1 to 3.

In Figures (2.4a) and (2.4b), the unsaturated value of the mutual reactances on the d- and q- axes is given respectively as x_{ad} and x_{aq}. These mutual reactances are influenced by the saturation of the synchronous machine. If saturation is to be represented in the flux linkage model of the synchronous machine, then the saturation factors S_d, S_q and the incremental saturation factors S_{di} and S_{qi} have to be calculated. The determination of these factors is given in Appendix (A1.5). If saturation of the machine is not considered then,

$$S_d = S_q = S_{di} = S_{qi} = 1 \tag{2.053}$$

The following reactances are defined based on the equivalent circuits of Figures (2.4a) & (2.4b).

$$x_{ads} = x_{ad} \, S_d \tag{2.054a}$$

$$x_{aqs} = x_{aq} \, S_q \tag{2.054b}$$

$$x_{adsi} = x_{ad} \, S_{di} \tag{2.054c}$$

$$x_{aqsi} = x_{aq} \, S_{qi} \tag{2.054d}$$

$$x_d = x_l + x_{ads} \tag{2.054e}$$

$$x_q = x_l + x_{aqs} \tag{2.054f}$$

$$x_{di} = x_l + x_{adsi} \tag{2.054g}$$

$$x_{qi} = x_l + x_{aqsi} \tag{2.054h}$$

$$x_d{}' = x_l + \frac{x_{ads} \, x_{fl}}{x_{ads} + x_{fl}} \tag{2.054i}$$

$$x_{di}{}' = x_l + \frac{x_{adsi} \, x_{fl}}{x_{adsi} + x_{fl}} \tag{2.054j}$$

$$x_q{}' = x_q \tag{2.054k}$$

$$x_{qi}{}' = x_{qi} \tag{2.054l}$$

$$x_f = x_{adsi} + x_{fl} + x_{c1} + x_{c2} \tag{2.054m}$$

$$x_{fd1} = x_{adsi} + x_{c1} \tag{2.054n}$$

$$x_{fd2} = x_{adsi} + x_{c1} + x_{c2} \tag{2.054o}$$

$$x_{kd1} = x_{adsi} + x_{kld1} + x_{c1} \tag{2.054p}$$

$$x_{kd2} = x_{adsi} + x_{kld2} + x_{c1} + x_{c2} \tag{2.054q}$$

$$x_{d12} = x_{adsi} + x_{c2} \tag{2.054r}$$

$$x_{kq1} = x_{aqsi} + x_{klq1} \tag{2.054s}$$

$$x_{kq2} = x_{aqsi} + x_{klq2} \tag{2.054t}$$

$$x_{kq3} = x_{aqsi} + x_{klq3} \tag{2.054u}$$

$$x_{q12} = x_{aqsi} \tag{2.054v}$$

$$x_{q13} = x_{aqsi} \tag{2.054w}$$

$$x_{q23} = x_{aqsi} \tag{2.054x}$$

These reactances are used in the formulation of the state space equations of the synchronous machine. If fewer damper windings are to be considered in the machine representation, the d- and q- axis equivalent circuits can be modified by ignoring the appropriate damper winding branches.

2.6.1 State variables

In the flux linkage model of the synchronous machine the state variables chosen are, the small changes in the angular velocity of the machine ($\Delta\omega$ in per unit), small changes in the rotor angle ($\Delta\delta$ in per unit), the small changes in the field flux linkages ($\Delta\psi_f$ expressed in per unit voltage) and the small changes in the d- and q- axes damper winding flux

linkages ($\Delta\psi_{kdm}$ and $\Delta\psi_{kqn}$, expressed in per unit voltages). Thus, the state vector of the machine for the flux linkage representation is,

$$[X_g] = [\Delta\omega \quad \Delta\delta \quad \Delta\psi_f \quad \Delta\psi_{kdm} \quad \Delta\psi_{kqn}]^T \qquad (2.055)$$

The rotor angle $\Delta\delta$ is defined as the angle between the machine direct (d-) axis and the common reference (D-) axis.

2.6.2 Initial equations for the state space formulation

Park's equation for the synchronous machine neglecting the rate of change of stator flux linkages are given below [1,18,21].

$$v_d = -r_a i_d - \omega_0 \lambda_q \qquad (2.056)$$

$$v_q = -r_a i_q + \omega_0 \lambda_d \qquad (2.057)$$

$$v_f = r_f i_f + \frac{d}{dt}\lambda_f \qquad (2.058)$$

$$0 = r_{kdm} i_{kdm} + \frac{d}{dt}\lambda_{kdm}; \quad \forall\ m = 1,2. \qquad (2.059)$$

$$0 = r_{kqn} i_{kqn} + \frac{d}{dt}\lambda_{kqn}; \quad \forall\ n = 1\ \text{to}\ 3. \qquad (2.060)$$

The quantities v_d, v_q, i_d, i_q, ω_0, ω, λ_d, and λ_q have already been defined, with reference to the classical model of the synchronous machine. The other quantities not defined so far are,

v_f, λ_f, i_f = Field voltage, flux linkage and current (p.u.).

λ_{kdm}, i_{kdm} = m^{th} d - axis damper winding flux linkage and current (p.u.); where m=1,2.

λ_{kqn}, i_{kqn} = n^{th} q - axis damper winding flux linkage and current (p.u.); where n=1 to 3.

The dynamics of the rotating parts of the synchronous machine is described by the following equation derived in Appendix (A1.4).

$$I\,\omega_0\,\frac{d}{dt}\omega = P_{base}\,(\,T_m + \omega_0\,\lambda_q\,i_d - \omega_0\,\lambda_d\,i_q\,) \qquad (2.061)$$

In this equation all the terms except T_m have already been defined with reference to the classical model of the synchronous machine. T_m is the mechanical power input to the synchronous machine.

The flux linkages (λ) can be expressed in per unit voltage (ψ) as,

$$\psi_d = \omega_0\,\lambda_q \qquad (2.062)$$

$$\psi_q = \omega_0\,\lambda_d \qquad (2.063)$$

$$\psi_f = \omega_0\,\lambda_f \qquad (2.064)$$

$$\psi_{kdm} = \omega_0\,\lambda_{kdm}\,; \quad \forall\,m = 1,2 \qquad (2.065)$$

$$\psi_{kqn} = \omega_0\,\lambda_{kqn}; \quad \forall\,n = 1\text{ to }3 \qquad (2.066)$$

Using these equations, Equations (2.056) to (2.061) can be rewritten by expressing the flux linkages in per unit voltage. The resulting equations can be linearized and expressed as,

$$\Delta v_d = - r_a \, \Delta i_d - \Delta \psi_q \tag{2.067}$$

$$\Delta v_q = - r_a \, \Delta i_q + \Delta \psi_d \tag{2.068}$$

$$\omega_0 \, \Delta v_f = \omega_0 \, r_f \, \Delta i_f + \frac{d}{dt} \Delta \psi_f \tag{2.069}$$

$$0 = \omega_0 \, r_{kdm} \, \Delta i_{kdm} + \frac{d}{dt} \Delta \psi_{kdm} \tag{2.070}$$

$$0 = \omega_0 \, r_{kqn} \, \Delta i_{kqn} + \frac{d}{dt} \Delta \psi_{kqn} \tag{2.071}$$

$$\frac{2H}{\omega_0} \frac{d}{dt} \Delta \omega = \Delta T_m + \Delta \psi_q \, i_d - \Delta \psi_d \, i_q + \psi_q \, \Delta i_d - \psi_d \, \Delta i_q \tag{2.072}$$

The derivation of Equation (2.072) is given in Appendix (A1.4).

2.6.3 State space equations for the rotor flux linkage states $[\Delta \psi_{fkdq}]$

The relation between the flux linkages in the stator and rotor to the currents in the various windings is given below, by the matrix equations,

$$\begin{bmatrix} \Delta \psi_d \\ \Delta \psi_f \\ \Delta \psi_{kd1} \\ \Delta \psi_{kd2} \end{bmatrix} = \begin{bmatrix} x_{di} & x_{adsi} & x_{adsi} & x_{adsi} \\ x_{adsi} & x_f & x_{fd1} & x_{fd2} \\ x_{adsi} & x_{fd1} & x_{kd1} & x_{d12} \\ x_{adsi} & x_{fd2} & x_{d12} & x_{kd2} \end{bmatrix} \begin{bmatrix} -\Delta i_d \\ \Delta i_f \\ \Delta i_{kd1} \\ \Delta i_{kd2} \end{bmatrix} \tag{2.073}$$

$$
\begin{bmatrix} \Delta\psi_q \\ \Delta\psi_{kq1} \\ \Delta\psi_{kq2} \\ \Delta\psi_{kq3} \end{bmatrix} = \begin{bmatrix} x_{qi} & x_{aqsi} & x_{aqsi} & x_{aqsi} \\ x_{aqsi} & x_{kq1} & x_{q12} & x_{q13} \\ x_{aqsi} & x_{q12} & x_{kq2} & x_{q23} \\ x_{aqsi} & x_{q13} & x_{q23} & x_{kq3} \end{bmatrix} \begin{bmatrix} -\Delta i_q \\ \Delta i_{kq1} \\ \Delta i_{kq2} \\ \Delta i_{kq3} \end{bmatrix} \qquad (2.074)
$$

The d- and q- axes rotor flux linkages ($[\Delta\psi_{fkdq}]$) are related to the stator currents ($[\Delta i_{dq}]$) and rotor currents ($[\Delta i_{fkdq}]$) as,

$$
[\Delta\psi_{fkdq}] = - [X_x] [\Delta i_{dq}] + [x_{fkdq}] [\Delta i_{fkdq}] \qquad (2.075)
$$

where,

$$
[\Delta\psi_{fkdq}] = \begin{bmatrix} \Delta\psi_f & \Delta\psi_{kd1} & \Delta\psi_{kd2} & \Delta\psi_{kq1} & \Delta\psi_{kq2} & \Delta\psi_{kq3} \end{bmatrix}^T ;
$$

$$
[\Delta i_{fkdq}] = \begin{bmatrix} \Delta i_f & \Delta i_{kd1} & \Delta i_{kd2} & \Delta i_{kq1} & \Delta i_{kq2} & \Delta i_{kq3} \end{bmatrix}^T ;
$$

$$
[\Delta i_{dq}] = \begin{bmatrix} \Delta i_d & \Delta i_q \end{bmatrix}^T ;
$$

$$
[X_x] = \begin{bmatrix} x_{adsi} & x_{adsi} & x_{adsi} & 0 & 0 & 0 \\ 0 & 0 & 0 & x_{aqsi} & x_{aqsi} & x_{aqsi} \end{bmatrix}^T ; \text{ and}
$$

$$[x_{fkdq}] = \begin{bmatrix} x_f & x_{fd1} & x_{fd2} & 0 & 0 & 0 \\ x_{fd1} & x_{kd1} & x_{d12} & 0 & 0 & 0 \\ x_{fd2} & x_{d12} & x_{kd2} & 0 & 0 & 0 \\ 0 & 0 & 0 & x_{kq1} & x_{q12} & x_{q13} \\ 0 & 0 & 0 & x_{q12} & x_{kq2} & x_{q23} \\ 0 & 0 & 0 & x_{q13} & x_{q23} & x_{kq3} \end{bmatrix}$$

From Equation (2.075), the following equation is evident,

$$[\Delta i_{fkdq}] = [x_{fkdq}]^{-1} [\Delta \psi_{fkdq}] + [x_{fkdq}]^{-1} [X_x] [\Delta i_{dq}] \qquad (2.076)$$

Using Equations (2.069) to (2.071), the rate of change of rotor flux linkages can be expressed in the matrix form as,

$$[\Delta \dot{\psi}_{fkdq}] = [\omega_0 \, r_{fkdq}] [\Delta i_{fkdq}] + [\omega_{0f}] \Delta v_f \qquad (2.077)$$

where, $[\omega_0 \, r_{fkdq}]$ is a diagonal matrix with elements as,

$$[\omega_0 \, r_{fkdq}] = Diag \, [\omega_0 \, r_f \quad \omega_0 \, r_{kd1} \quad \omega_0 \, r_{kd2} \quad \omega_0 \, r_{kq1} \quad \omega_0 \, r_{kq2} \quad \omega_0 \, r_{kq3}] \text{ and}$$

$$[\omega_{0f}] = [\omega_0 \quad 0 \quad 0 \quad 0 \quad 0 \quad 0]^T$$

Substituting for $[\Delta i_{fkdq}]$ from Equation (2.076) in Equation (2.077), gives,

$$[\Delta \dot{\psi}_{fkdq}] = [A_{wxf}] [\Delta \psi_{fkdq}] + [Wxx_i] [\Delta i_{dq}] + [\omega_{0f}] \Delta v_f \qquad (2.078)$$

where, $[A_{wxf}] = [\omega_0 r_{fkdq}] [x_{fkdq}]^{-1}$;   and $[Wxx_i] = [\omega_0 r_{fkdq}] [x_{fkdq}]^{-1} [X_x]$

Equation (2.078) is the state equation for the rotor flux linkage states, $[\Delta\psi_{fkdq}]$.

2.6.4 State space equation for the speed and rotor angle states ($\Delta\omega$, $\Delta\delta$)

From Equation (2.072), the state equation for the speed state is,

$$\Delta\dot{\omega} = \frac{\omega_0}{2H} \Delta T_m - \frac{\omega_0}{2H} [-\psi_q \quad \psi_d] [\Delta i_{dq}] + \frac{\omega_0}{2H} [-i_q \quad i_d] [\Delta\psi_{dq}] \qquad (2.079)$$

where, $[\Delta\psi_{dq}] = [\Delta\psi_d \quad \Delta\psi_q]^T$

From Equations (2.073) and (2.074) the stator flux linkage changes in the d- and q- axes $[\Delta\psi_{dq}]$ can be expressed as a function of the stator d and q components of the changes in current $[\Delta i_{dq}]$ and the changes in the rotor flux linkages $[\Delta\psi_{fkdq}]$, i.e.

$$[\Delta\psi_{dq}] = [X_a] [\Delta i_{dq}] + [X_b] [\Delta\psi_{fkdq}] \qquad (2.080)$$

where, $[X_a] = \begin{bmatrix} -x_{di} & 0 \\ 0 & -x_{qi} \end{bmatrix} + [X_x]^T [x_{fkdq}]^{-1} [X_x]$; and

$[X_b] = [X_x]^T [x_{fkdq}]^{-1}$

Equations (2.081) and (2.082) are the state equations for the speed and rotor angle states. These equations involve quantities which correspond to the machine d-q axes. Equation (2.084) is the initial output equation.

2.6.5 Transformation to the D- and Q- coordinates

The machine state and output equations which are referenced to the d- and q- coordinate axes of the machine need to be transformed to the D- and Q- coordinates axes of the system for proper interface of the machine to the system. From Equations (2.013) and (2.014) the following expressions can be written for the voltage and current of the machine,

$$[\Delta v_{DQ}] = [T_{cs}] [\Delta v_{dq}] + \begin{bmatrix} -v_Q \\ v_D \end{bmatrix} \Delta \delta \qquad (2.085)$$

$$[\Delta i_{dq}] = [T_{cs}]^T [\Delta i_{DQ}] - [T_{cs}]^T \begin{bmatrix} -i_Q \\ i_D \end{bmatrix} \Delta \delta \qquad (2.086)$$

where,

$$[T_{cs}] = \begin{bmatrix} \cos \delta & -\sin \delta \\ \sin \delta & \cos \delta \end{bmatrix}; \qquad [\Delta v_{DQ}] = [\Delta v_D \quad \Delta v_Q]^T; \quad \text{and}$$

$$[\Delta i_{DQ}] = [\Delta i_D \quad \Delta i_Q]^T$$

Substituting for $[\Delta v_{dq}]$ from Equation (2.083) in Equation (2.085) gives,

$$[\Delta v_{DQ}] = - [Y_d]^{-1} [\Delta i_{DQ}] + [Cv_{del}] \Delta\delta + [Cv_f] [\Delta\psi_{fkdq}] \qquad (2.087)$$

where, $[Y_d] = - \{ [T_{cs}] [Z_a] \{[T_{cs}]^T\}^{-1} ; \qquad [Cv_f] = [T_{cs}] \begin{bmatrix} 0 & -1 \\ 1 & 0 \end{bmatrix} [X_b]$; and

$$[Cv_{del}] = [Y_d]^{-1} \begin{bmatrix} -i_Q \\ i_D \end{bmatrix} + \begin{bmatrix} -v_Q \\ v_D \end{bmatrix}$$

Therefore, the current ($[\Delta i_{DQ}]$) from Equation (2.087) is,

$$[\Delta i_{DQ}] = [C_{del}] \Delta\delta + [C_f] [\Delta\psi_{fkdq}] - [Y_d] [\Delta v_{DQ}] \qquad (2.088)$$

where, $[C_{del}] = [Y_d] [Cv_{del}]$; $\qquad$ and $\qquad [C_f] = [Y_d] [Cv_f]$

Equations (2.088) is the output current equation. Substituting for $[\Delta i_{dq}]$ using Equation (2.086) in Equation (2.081) and (2.078) gives,

$$\Delta\dot{\omega} = \frac{\omega_0}{2\,H} \Delta T_m - [Wt_{dqi}] [\Delta i_{DQ}] - A_{dw} \Delta\delta + [A_{dqf}] [\Delta\psi_{fkdq}] \qquad (2.089)$$

where, $[Wt_{dqi}] = [W_{dqi}] [T_{cs}]^T \qquad$ and $\qquad A_{dw} = - [W_{dqi}] [T_{cs}]^T \begin{bmatrix} -i_Q \\ i_D \end{bmatrix}$

and,

$$[\Delta\dot{\psi}_{fkdq}] = [A_{wxf}] [\Delta\psi_{fkdq}] + [Wtxx_i] [\Delta i_{DQ}] + [A_{df}] \Delta\delta + [\omega_{0f}] \Delta v_f \qquad (2.090)$$

where, $[Wtxx_i] = [Wxx_i] [T_{cs}]^T$ and $[A_{df}] = - [Wxx_i] [T_{cs}]^T \begin{bmatrix} -i_Q \\ i_D \end{bmatrix}$

2.6.6   Overall state space model of the synchronous machine

The state Equations (2.089), (2.082) and (2.090) can be combined in the form,

$$[\dot{X}_g] = [A_g] [X_g] + [W_i] [\Delta i_{DQ}] + [B_{tw}] \Delta T_m + [E_x] \Delta v_f \qquad (2.091)$$

where,

$[X_g] = [\Delta \omega \quad \Delta \delta \quad \Delta \psi_{fkdq}]^T$; $[W_i] = [-Wt_{dqi} \quad 0_{1 \times 2} \quad Wtxx_i]^T$;

$[B_{tw}] = [\dfrac{\omega_0}{2H} \quad 0_{7 \times 1}]^T$; $[E_x] = [0_{2 \times 1} \quad \omega_0 \quad 0_{5 \times 1}]^T$ and

$$[A_g] = \begin{bmatrix} 0_{1 \times 1} & A_{dw} & A_{dqf} \\ 1 & 0_{1 \times 1} & 0_{1 \times 6} \\ 0_{6 \times 1} & A_{df} & A_{wxf} \end{bmatrix}$$

Here $0_{n \times m}$ denotes a null matrix of size n×m .

The output current Equation (2.088) can be rewritten in terms of the state vector $[X_g]$ as,

$$[\Delta i_{DQ}] = [C_g] [X_g] - [Y_d] [\Delta v_{DQ}] \qquad (2.092)$$

where, $[C_g] = \begin{bmatrix} 0_{2 \times 1} & C_{del} & C_f \end{bmatrix}$

2.7   Exciter model

The exciter regulates the terminal voltage of the synchronous machine. Exciter dynamics is modelled by the generalized method of control system representation as described in Section (2.4.1). The block diagram of an exciter [16] is given in Figure (2.5).
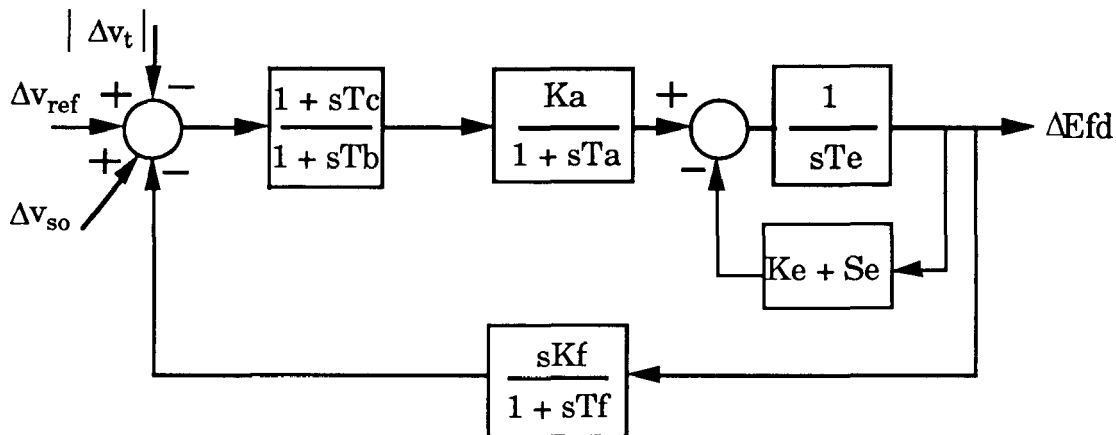
Figure (2.5): Exciter block diagram

In this figure the inputs $|\Delta v_t|$, Δv_{ref} and Δv_{so} denote small changes in the terminal voltage magnitude, reference voltage and output of PSS respectively, expressed in per unit. ΔEfd is the change in the output of the exciter in per unit and Se denotes the incremental saturation factor of the exciter DC machine. The steady state saturation factor SE is calculated from the following expression describing the saturation curve of the exciter DC machine [16].

$$SE = Aex \, \epsilon^{Bex \, Efd} \qquad (2.093)$$

where, Efd is the steady state output of the exciter and is calculated as shown in Appendix (A1.6). Aex, Bex are constants defining the saturation curve of the DC machine. The incremental saturation factor Se is obtained by linearizing Equation (2.093) as,

$$Se = Aex \, Bex \, \epsilon^{Bex \, Efd} \qquad (2.094)$$

2.7.1 Initial state space equations

Based on Equations (2.017) to (2.020) of Section (2.4.1), the initial state space equations of the exciter can be written as,

$$[\dot{X}_e] = [A_x] [X_e] + [B_x] [u] + [B_{ss}] \Delta v_{so} \qquad (2.095)$$

$$[y] = [C_x] [X_e] + [D_x] [u] + [D_{ss}] \Delta v_{so} \qquad (2.096)$$

$$[u] = [L_x] [y] + [G_x] [U] \qquad (2.097)$$

$$\Delta Efd = [M_x] [y] + [K_x] [U] \qquad (2.098)$$

$[X_e]$ is the state vector of the exciter. Vectors $[U]$ and $[z]$ of Equations (2.019) and (2.020) are defined in case of exciter as,

$$[U] = [\Delta\omega \quad \Delta v_D \quad \Delta v_Q \quad \Delta i_D \quad \Delta i_Q \quad \Delta v_{ref}]^T \qquad (2.099)$$

$$[z] = \Delta Efd \qquad (2.100)$$

It can be seen that the vector [U] contains variables whose linear combinations defines the external inputs to the exciter. From the block diagram of the exciter given in Figure (2.5) it is seen that the external inputs are $|\Delta v_t|$, Δv_{ref} and Δv_{so}.

The steady state terminal voltage magnitude of the synchronous machine $|v_t|$ can be expressed as a function of its D-Q components as,

$$|v_t| = \sqrt{v_D^2 + v_Q^2} \qquad (2.101)$$

where, v_D, v_Q are the direct (D-) and quadrature (Q-) axes components of the terminal voltage v_t. Linearizing Equation (2.101), the expression for the small changes in the terminal voltage magnitude $|\Delta v_t|$ is given as,

$$|\Delta v_t| = \left[\frac{v_D}{|v_t|} \quad \frac{v_Q}{|v_t|} \right] [\Delta v_D \quad \Delta v_Q]^T \qquad (2.102)$$

$|\Delta v_t|$ can be expressed as a function of the vector [U] using Equation (2.099) and (2.102) as,

$$|\Delta v_t| = [0 \quad \frac{v_D}{|v_t|} \quad \frac{v_Q}{|v_t|} \quad 0 \quad 0 \quad 0][U] \qquad (2.103)$$

The input Δv_{ref} can also be expressed as a function of the vector [U] from Equation (2.099) as,

$$\Delta v_{ref} = [0 \quad 0 \quad 0 \quad 0 \quad 0 \quad 1][U] \qquad (2.104)$$

The remaining input Δv_{so}, is treated separately for the sake of ease in interfacing the exciter model to the PSS. The influence of the input Δv_{so} on the exciter is described by the vectors $[B_{ss}]$ and $[D_{ss}]$ in Equations (2.095) and (2.096). The formulation of these vectors is illustrated by an example in Appendix (A1.3).

The matrices $[A_x]$, $[B_x]$, $[C_x]$, $[D_x]$, $[L_x]$, $[G_x]$, $[M_x]$ and $[K_x]$ correspond to the matrices $[A]$, $[B]$, $[C]$, $[D]$, $[L]$, $[G]$, $[M]$ and $[K]$ of Equations (2.017) to (2.020). All these matrices except $[G_x]$ and $[K_x]$ can be determined based solely on the parameters of the various constituent exciter blocks and their interconnections. Matrices $[G_x]$ and $[K_x]$ can be formulated from the knowledge of external inputs and the constituent exciter blocks to which they are applied. For the block diagram of the exciter shown in Figure (2.5), where the external inputs $|\Delta v_t|$ and Δv_{ref} are applied to the first block, the matrix $[G_x]$ is derived, using Equations (2.103) and (2.104) as,

$$[G_x] = [\; 0_{nx \times 1} \quad G_{x1} \quad 0_{nx \times 2} \quad A_{v1}]$$

where, nx = number of exciter states;

$$[G_{x1}] = - \begin{bmatrix} \dfrac{v_D}{|v_t|} & \dfrac{v_Q}{|v_t|} \\ 0_{(nx-1) \times 1} & 0_{(nx-1) \times 1} \end{bmatrix} \qquad \text{and} \qquad A_{v1} = \begin{bmatrix} 1 \\ 0_{(nx-1) \times 1} \end{bmatrix}$$

The matrix $[K_x]$ is given by,

$$[K_x] = [0_{nx \times 6}]$$

The negative sign in $[G_{x1}]$ is due to the negative feedback of $|\Delta \dot{v}_t|$. The matrix $[K_x]$ is a null matrix due to the absence of feedforward paths from the external inputs to the output ΔEfd.

2.7.2 Final state space equations

Eliminating vectors $[u]$ and $[y]$ from Equations (2.095), (2.096), (2.097) and (2.098); the final state space equations of the exciter are obtained as,

$$[\dot{X}_e] = [A_e] [X_e] + [B_e] [U] + [B_{vso}] \Delta v_{so} \qquad (2.105)$$

$$\Delta Efd = [M_e] [X_e] + [K_e] [U] + K_{vso} \Delta v_{so} \qquad (2.106)$$

The matrices $[A_e]$, $[B_e]$, $[M_e]$ and $[K_e]$ correspond to the matrices $[A_c]$, $[B_c]$, $[M_c]$ and $[K_c]$ of Equations (2.021) and (2.022) respectively. Also,

$$[B_{vso}] = [B_x L_x [I_x - D_x L_x]^{-1} D_{ss} + B_{ss}]; \qquad \text{and} \qquad K_{vso} = M_x [I_x - D_t L_x]^{-1} D_{ss}$$

2.8 Power System Stabilizer (PSS) model

The Power System Stabilizer provides a supplementary input to the exciter in order to modulate the voltage reference, thus modifying the output of the exciter in a manner so that the damping of electromechanical

modes is increased. The PSS dynamics is modelled by the generalized method of control system representation as described in Section (2.4.1). Depending on the type of feedback signals used in PSS, three different types of PSS are considered here [1], which are,

i)Type-1: where the feedback signal to the PSS is the small change in the speed ($\Delta\omega$) of the synchronous machine in per unit.

ii)Type-2: where the feedback signal is the small change in the electrical power output (ΔPe) of the synchronous machine in per unit.

iii)Type-3: where the feedback signal comprises both the small changes in the speed and electrical power output of the synchronous machine in per unit.

The block diagrams of Type-1, Type-2 and Type-3 PSS are given in Figures (2.6a),(2.6b) and (2.6c) respectively. The output of all the three types of PSS is denoted by Δv_{so}.

2.8.1 Initial state space equations

Based on Equations (2.017) to (2.020) of Section (2.4.1), the initial state space equations of the PSS can be written as,

$$\left[\dot{X}_s\right] = [A_t] [X_s] + [B_t] [u] \qquad (2.107)$$

$$\frac{\Delta\omega}{(p.u)} \rightarrow \boxed{Sk} \; \boxed{\left(\frac{1 + sTsld1}{1 + sTslg1}\right)^2} \; \boxed{\left(\frac{1 + sTsld2}{1 + sTslg2}\right)^3} \; \boxed{\frac{sTq}{1 + sTq}} \; \boxed{\left(\frac{1 + sTlagn1}{1 + sTlagd1}\right)^3} \; \boxed{\left(\frac{1 + sTlagn2}{1 + sTlagd2}\right)^2} \; \frac{\Delta v_{so}}{\longrightarrow}$$
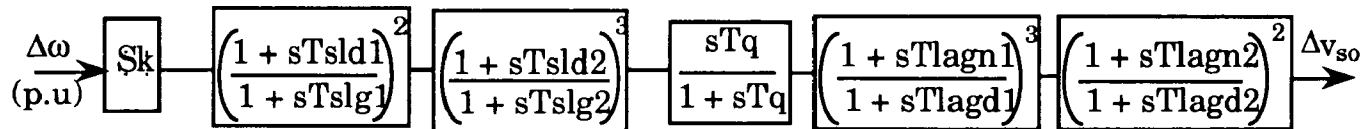
PSS with $\Delta\omega$ feedback (Type-1)

Figure (2.6a)

$$\frac{\Delta Pe}{(p.u)} \rightarrow \boxed{Pk} \; \boxed{\frac{sTp1}{1 + sTp2}} \; \boxed{\frac{1 + sTpld1}{1 + sTplg1}} \; \boxed{\frac{1 + sTpld2}{1 + sTplg2}} \; \boxed{\frac{sTq}{1 + sTq}} \; \boxed{\left(\frac{1 + sTlagn1}{1 + sTlagd1}\right)^3} \; \boxed{\left(\frac{1 + sTlagn2}{1 + sTlagd2}\right)^2} \; \frac{\Delta v_{so}}{\longrightarrow}$$
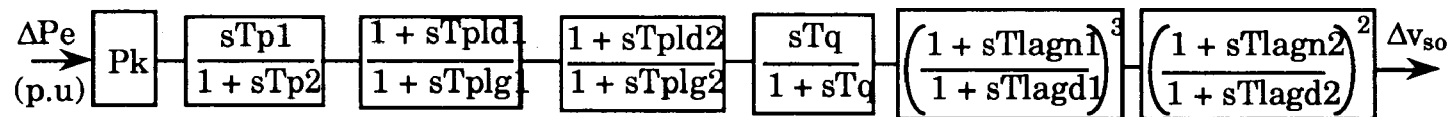
PSS with ΔPe feedback (Type-2)

Figure (2.6b)
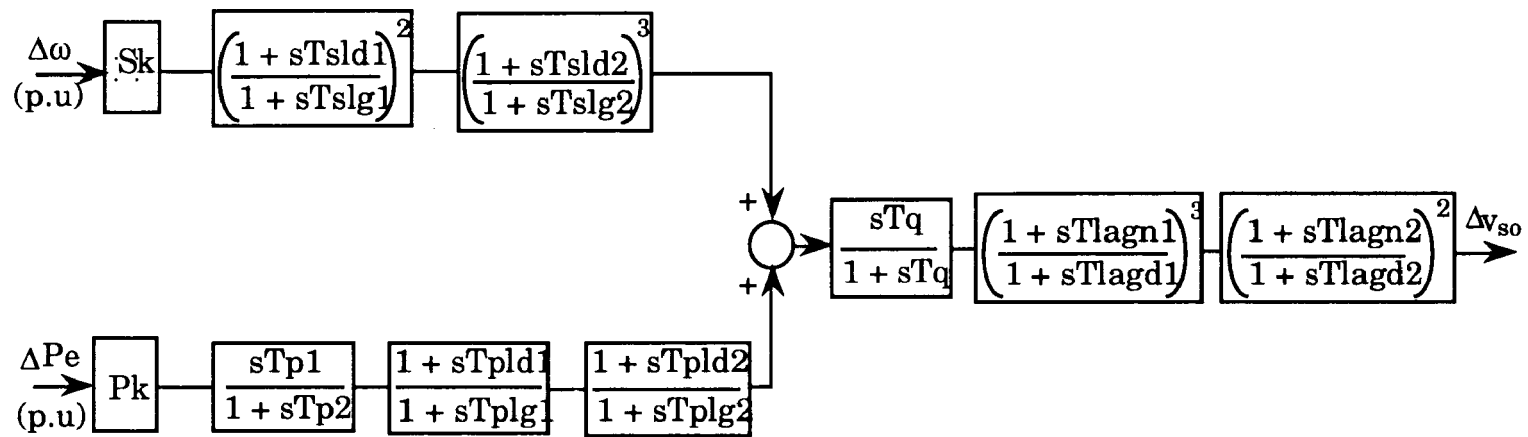
PSS with $\Delta\omega$ and ΔPe feedback (Type-3)

Figure (2.6c)

$$[y] = [C_t]\,[X_s] + [D_t]\,[u] \qquad\qquad (2.108)$$

$$[u] = [L_t]\,[y] + [G_t]\,[U] \qquad\qquad (2.109)$$

$$\Delta v_{so} = [M_t]\,[y] + [K_t]\,[U] \qquad\qquad (2.110)$$

$[X_s]$ is the state vector of the PSS. The vector $[U]$ is the same as in the case of exciter and is given by,

$$[U] = [\Delta\omega \quad \Delta v_D \quad \Delta v_Q \quad \Delta i_D \quad \Delta i_Q \quad \Delta v_{ref}]^T \qquad\qquad (2.111)$$

The vector $[z]$ of Equation (2.020) is defined in case of PSS as,

$$[z] = \Delta v_{so} \qquad\qquad (2.112)$$

It can be seen that the vector $[U]$ contains variables whose linear combinations defines the external inputs to the PSS. The two possible external inputs considered are $\Delta\omega$ and ΔPe. The input $\Delta\omega$ can be expressed as a function of the vector $[U]$ as,

$$\Delta\omega = [1 \quad 0 \quad 0 \quad 0 \quad 0 \quad 0]\,[U] \qquad\qquad (2.113)$$

The steady state electrical power output (Pe) of the synchronous machine can be expressed in terms of the D-Q components of the terminal voltage (v_D, v_Q) and current (i_D, i_Q) as,

$$Pe = v_D\,i_D + v_Q\,i_Q \qquad\qquad (2.114)$$

Linearizing Equation (2.114), the expression for the small change in electrical power output (ΔPe) is obtained as,

$$\Delta Pe = [i_D \quad i_Q] [\Delta v_D \quad \Delta v_Q]^T + [v_D \quad v_Q] [\Delta i_D \quad \Delta i_Q]^T \tag{2.115}$$

Expressing ΔPe as a function of the vector [U] gives,

$$\Delta Pe = [0 \quad i_D \quad i_Q \quad v_D \quad v_Q \quad 0] [U] \tag{2.116}$$

The matrices $[A_t]$, $[B_t]$, $[C_t]$, $[D_t]$, $[L_t]$, $[G_t]$, $[M_t]$ and $[K_t]$ correspond to the matrices [A], [B], [C], [D], [L], [G], [M] and [K] of Equations (2.017) to (2.020). All these matrices except $[G_t]$ and $[K_t]$ can be determined based solely on the parameters of the various PSS constituent blocks and their interconnections. Matrices $[G_t]$ and $[K_t]$ can be formulated from the knowledge of external inputs and the constituent blocks of the PSS to which they are applied. For the block diagrams of the PSS shown in Figure (2.6a), (2.6b) and (2.6c), the matrix $[G_t]$ and $[K_t]$ are derived using Equations (2.109), (2.110), (2.113) and (2.116); depending on the type of PSS.

i)Type-1   Here, $\Delta\omega$ is the feedback signal and hence,

$$[G_t] = [G_{t1} \quad 0_{ns \times 5}]$$

where, ns is the number of PSS states; and,

$$[G_{t1}] = [1 \quad 0_{1 \times (ns-1)}]^T ; \qquad \text{and} \qquad [K_t] = [0_{1 \times 6}]$$

ii)Type-2   Here, ΔPe is the feedback signal and hence,

$$[G_t] = [0_{ns \times 1} \quad G_{t1} \quad 0_{ns \times 1}]$$

where,

$$[G_{t1}] = \begin{bmatrix} i_D & i_Q & v_D & v_D \\ 0_{ns-1 \times 1} & 0_{ns-1 \times 1} & 0_{ns-1 \times 1} & 0_{ns-1 \times 1} \end{bmatrix} ; \qquad \text{and} \qquad [K_t] = [0_{1 \times 6}]$$

iii)Type-3   Here, both $\Delta \omega$ and ΔPe are the feedback signals. The initial state space Equations (2.107) to (2.110) for the PSS shown in Figure (2.6c) are formed by stacking the state space equations for each individual block in a sequential manner as explained in Section (2.4.1). If the blocks to which $\Delta \omega$ and ΔPe signals are applied are, say, respectively the first and the sixth block in the stack, then the matrices $[G_t]$ and $[K_t]$ are,

$$[G_t] = [G_{t1} \quad 0_{ns \times 1}]$$

where,

$$[G_{t1}] = \begin{bmatrix} 1 & 0_{1\times1} & 0_{1\times1} & 0_{1\times1} & 0_{1\times1} \\ 0_{4\times1} & 0_{4\times1} & 0_{4\times1} & 0_{4\times1} & 0_{4\times1} \\ 0_{1\times1} & i_D & i_Q & v_D & v_D \\ 0_{ns\text{-}5\times1} & 0_{ns\text{-}5\times1} & 0_{ns\text{-}5\times1} & 0_{ns\text{-}5\times1} & 0_{ns\text{-}5\times1} \end{bmatrix}; \quad \text{and} \quad [K_t] = [0_{1\times6}]$$

In all the PSS models (Type-1, Type-2 and Type-3) it is seen that the matrix $[K_t]$ is a null matrix. This is so because in all these models there is no feedforward path from the external inputs to the output Δv_{so}.

2.8.2 Final state space equations

Eliminating vectors [u] and [y] from Equations (2.107) to (2.110), the final state space equations of the PSS are obtained as,

$$\left[\dot{X}_s\right] = [A_s] [X_s] + [B_s] [U] \tag{2.117}$$

$$\Delta v_{so} = [M_s] [X_s] + [K_s] [U] \tag{2.118}$$

where, the matrices $[A_s]$, $[B_s]$, $[M_s]$ and $[K_s]$ correspond to the matrices $[A_c]$, $[B_c]$, $[M_c]$ and $[K_c]$ of Equations (2.021) and (2.022) respectively.

2.9 Overall state space representation of the generating system

Depending upon the details required, the generating system model can be formulated with any of the following three options,

i)Only machine dynamics considered.

ii)Machine and exciter dynamics are considered.

iii)Dynamics of machine, exciter and PSS are considered.

2.9.1   Generating system model considering only machine dynamics

If the requirement of the small signal stability investigation is satisfied by the classical representation of a synchronous machine, then the generating system model comprises only the Equations (2.051) and (2.052).

If the flux linkage model of a synchronous machine is required. Equations (2.091) and (2.092) constitute the generating system model with the exception that $\Delta v_f = 0$, as no exciter controls is modelled and hence the field voltage v_f remains constant. With this modification Equation (2.091) and (2.092) can be rewritten as,

$$[\dot{X}_g] = [A_g] [X_g] + [W_i] [\Delta i_{DQ}] + [B_{tw}] \Delta T_m \qquad (2.119)$$

$$[\Delta i_{DQ}] = [C_g] [X_g] - [Y_d] [\Delta v_{DQ}] \qquad (2.120)$$

Substituting for $[\Delta i_{DQ}]$ from Equation (2.120) in Equation (2.119) gives,

$$[\dot{X}_g] = [A_g + W_i C_g] [X_g] - [W_i Y_d] [\Delta v_{DQ}] + [B_{tw}] \Delta T_m \qquad (2.121)$$

Equations (2.121) and (2.120) can be put in the general form of Equations (2.003) and (2.004) to result in the following state space model of the generating system.

$$[\dot{X}_d] = [A_d] [X_d] + [B_d] [\Delta V_d]$$
$$[\Delta I_d] = [C_d] [X_d] - [Y_d] [\Delta V_d]$$

where, $\quad [X_d] = [X_g];$ $\qquad [A_d] = [A_g + W_i C_g];$ $\qquad [B_d] = - [W_i Y_d];$

$\qquad\qquad [\Delta I_d] = [\Delta i_{DQ}];$ $\qquad [C_d] = [C_g];$ $\qquad\qquad\qquad [\Delta V_d] = [\Delta v_{DQ}]$

In Equation (2.121) the vector $[B_{tw}]$ is the input distribution vector for the change in mechanical torque input applied to this machine. The vector $[B_{tw}]$ is not needed in the formation of the system state matrix. It is needed only for the calculation of residues, or frequency or time responses.

2.9.2 Generating system model considering machine and exciter dynamics

The flux linkage model of the synchronous machine is considered in this case. In this model the field voltage of the synchronous machine is related to the exciter output by the following relation [15],

$$v_f = \frac{r_f}{x_{ad}} Efd \tag{2.122}$$

Linearizing Equation (2.122) gives,

$$\Delta v_f = \frac{r_f}{x_{ad}} \Delta Efd \qquad (2.123)$$

Equation (2.123) provides the interface between the machine and exciter model. For the exciter, the external inputs ($|\Delta v_t|$, Δv_{ref}) are expressed as functions of the vector [U] in the state space representation of the exciter model. In this representation only certain elements (Δv_D, Δv_Q and Δv_{ref}) of [U] are needed. Based on this, the state space equations of the exciter model (Equations (2.105) and (2.106)) are rewritten by partitioning the vector [U] and matrices [B_e] and [K_e], so that only the elements of [U], needed to represent the external inputs are considered.

$$[\dot{X}_e] = [A_e] [X_e] + [B_{e1}] [\Delta v_{DQ}] + [B_{e2}] \Delta v_{ref} \qquad (2.124)$$
$$\Delta Efd = [M_e] [X_e] + [K_{e1}] [\Delta v_{DQ}] + [K_{e2}] \Delta v_{ref} \qquad (2.125)$$

[B_{e1}], [B_{e2}] and [K_{e1}], [K_{e2}] can be easily obtained by the proper partitioning of matrices [B_e] and [K_e] respectively. It must be noted that as the PSS is not modelled, $\Delta v_{so} = 0$.

To interface the exciter and machine model, ΔEfd is substituted from Equation (2.125) in Equation (2.123). This results in Δv_f, which is expressed as a function of the exciter variables . Substituting the resulting expression in Equation (2.091) gives,

$$[\dot{X}_g] = [A_g \quad (E_x'M_e)] \begin{bmatrix} X_g \\ X_e \end{bmatrix} + [W_i] [\Delta i_{DQ}] + [B_{tw}] \Delta T_m + [(E_x'K_{e1})] [\Delta v_{DQ}]$$
$$+ [E_x'K_{e2}] \Delta v_{ref} \qquad (2.126)$$

Expressing $[\Delta i_{DQ}]$ in Equation (2.126) as a function of synchronous machine variables using Equation (2.092) gives,

$$[\dot{X}_g] = [A_{gg} \quad A_{ge}] \begin{bmatrix} X_g \\ X_e \end{bmatrix} + [B_g] [\Delta v_{DQ}] + [B_{tw}] \Delta T_m + [E_x{}'K_{e2}] \Delta v_{ref} \qquad (2.127)$$

where, $\qquad [Ex'] = \dfrac{r_{fl}}{x_{ad}} [Ex]; \qquad A_{gg} = [A_g + W_iC_g]; \qquad A_{ge} = [E_x{}'M_e];$

and $\qquad [B_g] = [-W_i\,Y_d + (E_x{}'K_{e1})]$

The machine and exciter state Equations (2.127) and (2.124) can be combined together as,

$$\begin{bmatrix} \dot{X}_g \\ \dot{X}_e \end{bmatrix} = \begin{bmatrix} A_{gg} & A_{ge} \\ 0_{ng \times nx} & A_e \end{bmatrix} \begin{bmatrix} X_g \\ X_e \end{bmatrix} + \begin{bmatrix} B_g \\ B_e \end{bmatrix} [\Delta v_{DQ}] + [B_{tw}{}'] \Delta T_m + [B_{rf}] \Delta v_{ref}$$

$$(2.128)$$

where, ng,nx is the number of states in the machine and exciter models respectively and,

$$[B_{tw}{}'] = \begin{bmatrix} B_{tw} \\ 0_{nx \times 1} \end{bmatrix} \qquad \text{and} \qquad [B_{rf}] = \begin{bmatrix} E_x{}' K_{e2} \\ B_{e2} \end{bmatrix}$$

To maintain compatibility of the overall state vector, the output current Equation (2.092) is modified as,

$$[\Delta i_{DQ}] = [C_g \quad 0_{2 \times nx}] \begin{bmatrix} X_g \\ X_e \end{bmatrix} - [Y_d] [\Delta v_{DQ}] \qquad (2.129)$$

Equations (2.128) and (2.129) can be put in the general form of Equations (2.003) and (2.004) to result in the following state space model of the generating system.

$$[\dot{X}_d] = [A_d] [X_d] + [B_d] [\Delta V_d]$$
$$[\Delta I_d] = [C_d] [X_d] - [Y_d] [\Delta V_d]$$

where,

$$[X_d] = \begin{bmatrix} X_g \\ X_e \end{bmatrix} ; \qquad [A_d] = \begin{bmatrix} A_{gg} & A_{ge} \\ 0 & A_e \end{bmatrix} ; \qquad [B_d] = \begin{bmatrix} B_g \\ B_e \end{bmatrix} ;$$

$$[\Delta I_d] = [\Delta i_{DQ}] ; \qquad [C_d] = [C_g \quad 0_{2 \times nx}] ; \qquad \text{and} \quad [\Delta V_d] = [\Delta v_{DQ}]$$

In Equation (2.128) the vectors $[B_{tw}{}']$ and $[B_{rf}]$ are the input distribution vectors for either a change in mechanical torque input applied to this machine or a change in the voltage reference input to the exciter. The vectors $[B_{tw}{}']$ and $[B_{rf}]$ are not needed in the formation of the system state matrix. They are needed only for the calculation of residues, or frequency or time responses.

2.9.3 Generating system model considering the dynamics of machine, exciter and PSS

This is the most detailed representation of the generating system. The flux linkage model of the synchronous machine is considered here. To interface the PSS and exciter models with the synchronous machine model, the PSS and exciter state space equations can be rewritten as,

$$[\dot{X}_e] = [A_e] [X_e] + [B_{e1}] [\Delta v_{DQ}] + [B_{e2}] [\Delta v_{ref}] + [B_{vso}] [\Delta v_{so}] \qquad (2.130)$$

$$\Delta Efd = [M_e] [X_e] + [K_{e1}] [\Delta v_{DQ}] + [K_{e2}] [\Delta v_{ref}] + K_{vso} [\Delta v_{so}] \qquad (2.131)$$

$$[\dot{X}_s] = [A_s] [X_s] + [B_{s1}] \Delta\omega + [B_{s2}] [\Delta v_{DQ}] + [B_{s3}] [\Delta i_{DQ}] \qquad (2.132)$$

$$\Delta v_{so} = [M_s] [X_s] + [K_{s1}] \Delta\omega + [K_{s2}] [\Delta v_{DQ}] + [K_{s3}] [\Delta i_{DQ}] \qquad (2.133)$$

Equations (2.132) and (2.133) correspond to the PSS state space Equations (2.117) and (2.118), and are derived by partitioning the vector [U] to explicitly introduce interface variables $\Delta\omega$, $[\Delta v_{DQ}]$ and $[\Delta i_{DQ}]$. Accordingly, the matrices $[B_{s1}]$, $[B_{s2}]$, $[B_{s3}]$ and $[K_{s1}]$, $[K_{s2}]$, $[K_{s3}]$ are obtained by the proper partitioning of the matrices $[B_s]$ and $[K_s]$ respectively.

On the same basis, the exciter state space Equations (2.105) and (2.106) are written in the form of Equation (2.130) and (2.131). It may be noted that Δv_{so} now appears as a variable in the exciter state Equation (2.130) as PSS is being considered and this forms a basis for interfacing the exciter and PSS models. Equations (2.130) and (2.132) are combined together, and eliminating Δv_{so} using Equation (2.133) gives,

$$[\dot{X}_{es}] = [A_{es}] [X_{es}] + [B_{esv}] [\Delta v_{DQ}] + [B_{esi}] [\Delta i_{DQ}] + [B_{sw}] \Delta \omega + [B_{esr}] [\Delta v_{ref}]$$

$$(2.134)$$

where,

$$[X_{es}] = \begin{bmatrix} X_e \\ X_s \end{bmatrix} ; \qquad\qquad [A_{es}] = \begin{bmatrix} A_e & B_{vso} M_s \\ 0_{ns \times nx} & A_s \end{bmatrix} ;$$

$$[B_{esv}] = \begin{bmatrix} B_{e1} + B_{vso} K_{s2} \\ B_{s2} \end{bmatrix} ; \qquad [B_{esi}] = \begin{bmatrix} B_{vso} K_{s3} \\ B_{s3} \end{bmatrix} ;$$

$$[B_{sw}] = \begin{bmatrix} B_{vso} K_{s1} \\ B_{s1} \end{bmatrix} ; \qquad and \qquad [B_{esr}] = \begin{bmatrix} B_{e2} \\ 0_{ns \times 1} \end{bmatrix}$$

Eliminating $[\Delta v_{so}]$ from Equation (2.131) using Equation (2.133) gives,

$$\Delta Efd = [M_{es}] [X_{es}] + [K_{esv}] [\Delta v_{DQ}] + [K_{esi}] [\Delta i_{DQ}] + [K_{esw}] \Delta \omega + [K_{e2}] [\Delta v_{ref}]$$

$$(2.135)$$

where, $\qquad [M_{es}] = [\ M_e \qquad K_{vso} M_s \ ] ; \qquad [K_{esv}] = [\ K_{e1} + K_{vso} K_{s2} \ ] ;$

$$[K_{esi}] = [\ K_{vso} \ K_{s3} \ ] \quad and \qquad [K_{esw}] = [\ K_{vso} K_{s1} \ ]$$

To interface the PSS and exciter model with the machine model, ΔEfd is substituted from Equation (2.135) in Equation (2.123). This results in Δv_f which is expressed as a function of exciter and PSS variables. This resulting expression can be combined with Equation (2.091) of synchronous machine model to result in the following equation.

$$[X_{ges}^{\cdot}] = [A_{gesv}] [X_{ges}] + [W_I] [\Delta i_{DQ}] + [B_v] [\Delta v_{DQ}] + [B_{ref}] [\Delta v_{ref}] + [B_T] \Delta T_m$$

$$(2.136)$$

where, ng, nx, ns are the number of states in the machine, exciter and PSS models and, $\quad$ nxs = nx + ns; $\quad$ ngxs = ng + nx + ns. Also,

$$[A_{gesv}] = \begin{bmatrix} A_g & E_x^{'} M_{es} \\ 0_{nxs \times ng} & A_{es} \end{bmatrix} + \begin{bmatrix} 0_{2 \times 1} & 0_{2 \times (ngxs-1)} \\ \omega_0 \dfrac{r_f}{x_{ad}} & 0_{1 \times (ngxs-1)} \\ B_{sw} & 0_{nxs \times (ngxs-1)} \end{bmatrix} ;$$

$$[W_I] = \begin{bmatrix} W_i + E_x^{'} K_{esi} \\ B_{esi} \end{bmatrix} ; \qquad [B_v] = \begin{bmatrix} E_x^{'} K_{esv} \\ B_{esv} \end{bmatrix} ;$$

$$[B_{ref}] = \begin{bmatrix} E_x^{'} K_{e2} \\ B_{esr} \end{bmatrix} \qquad and \qquad [B_T] = \begin{bmatrix} B_{tw} \\ 0_{nxs \times 1} \end{bmatrix}$$

The $[\Delta i_{DQ}]$ term in Equation (2.136) can be eliminated using Equation (2.092) to give,

$$[X_{ges}^{\cdot}] = [A_{ges}] [X_{ges}] + [B_{ges}] [\Delta v_{DQ}] + [B_{ref}] [\Delta v_{ref}] + [B_T] \Delta T_m \qquad (2.137)$$

where,

$$[A_{ges}] = [A_{gesv}] + \begin{bmatrix} W_I C_g & 0_{ng \times nxs} \\ 0_{nxs \times ng} & 0_{nxs \times nxs} \end{bmatrix} \qquad and \qquad [B_{ges}] = [B_v - W_I Y_d]$$

The output current ($[\Delta i_{DQ}]$) in Equation (2.092) can be expressed in terms of the generating system state variables as,

$$[\Delta i_{DQ}] = [C_{ges}] [X_{ges}] - [Y_d] [\Delta v_{DQ}] \qquad (2.138)$$

where, $\qquad [C_{ges}] = [C_g \ 0_{2 \times nxs}]$

Equations (2.137) and (2.138) can be put in the general form of Equations (2.003) and (2.004) to result in the following state space model of the generating system.

$$[\dot{X}_d] = [A_d] [X_d] + [B_d] [\Delta V_d]$$
$$[\Delta I_d] = [C_d] [X_d] - [Y_d] [\Delta V_d]$$

where, $\qquad [X_d] = [X_{ges}]; \qquad [A_d] = [A_{ges}] ; \qquad [B_d] = [B_{ges}] ,$

$\qquad\qquad [\Delta I_d] = [\Delta i_{DQ}] \qquad [C_d] = [C_{ges}] ; \qquad [\Delta V_d] = [\Delta v_{DQ}]$

In Equation (2.137) the vectors $[B_{tw}']$ and $[B_{rf}]$ are the input distribution vectors for either a change in mechanical torque input applied to this machine or a change in the voltage reference input to the exciter. The vectors $[B_{tw}']$ and $[B_{rf}]$ are not needed in the formation of the system state matrix. They are needed only for the calculation of residues, or frequency or time responses.

2.10 Static Var Compensator (SVC) model

The primary function of the Static Var Compensator is to provide voltage support by maintaining the voltage magnitude of a specified bus constant. With the addition of supplementary controls it can also be used to enhance the damping of the electromechanical modes. The SVC dynamics is modelled by the generalized method of control system representation as described in Section (2.4.1). The SVC model takes the form of a variable susceptance controlled by the voltage magnitude of a specified sensing bus. The control output is the value of the change in susceptance. The sign of the output is taken to be that of an inductance for sensing bus voltage magnitude higher than the reference value and of a capacitance for sensing bus voltage magnitude lower than the reference value.

The steady state current in the D-Q coordinates (i_D, i_Q) injected into the power system by the SVC is,

$$[i_{DQ}] = [Y_{SVC}]\,[v_{DQ}] \tag{2.139}$$

where, $[Y_{SVC}]$ is the steady state shunt susceptance offered by the SVC,

$$[i_{DQ}] = [i_D \quad i_Q]^T; \qquad\qquad [v_{DQ}] = [v_D \quad v_Q]^T;$$

$$[Y_{SVC}] = \begin{bmatrix} 0 & -B \\ B & 0 \end{bmatrix}; \qquad \text{and} \qquad B = \frac{Q}{|v|^2}$$

The steady state reactive power injected into the power system by the SVC is Q, which is positive if the net effect of the SVC is that of a capacitor, and is negative if the net effect of the SVC is that of a inductor. The

terminal voltage magnitude of the SVC is $|v|$ and can be expressed as a function of the D-Q components of the terminal voltage as,

$$|v| = \sqrt{v_D{}^2 + v_Q{}^2} \tag{2.140}$$

Linearizing Equation (2.140), gives,

$$[\Delta i_{DQ}] = \begin{bmatrix} -v_Q \\ v_D \end{bmatrix} \Delta B + [Y_{SVC}] [\Delta v_{DQ}] \tag{2.141}$$

2.10.1   SVC voltage regulator model

The voltage regulator of the SVC gives a control output based on the feedback of the change in the voltage magnitude of a specified bus. The control output of the SVC voltage regulator is ΔB. Figure (2.7) shows the block diagram of the transfer function of the SVC voltage regulator [1].
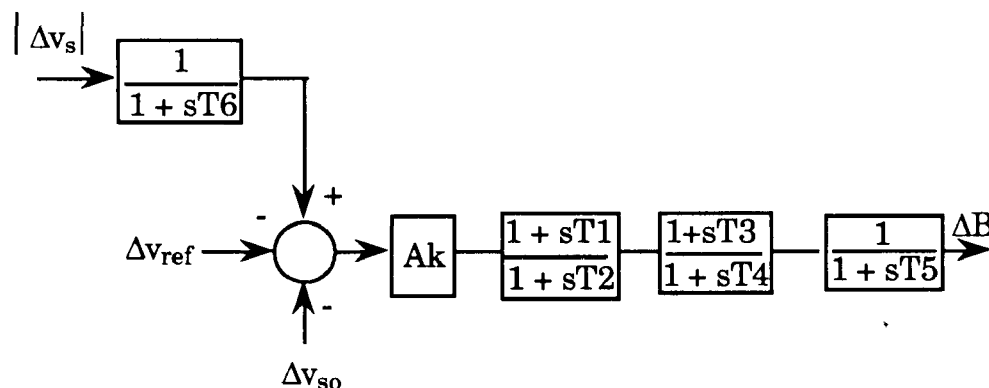
Figure (2.7): Block diagram of SVC voltage regulator

In this figure the inputs $|\Delta v_s|$, Δv_{ref} and Δv_{so} denote small changes in the sensing bus voltage magnitude, reference voltage and output of the supplementary control, all expressed in per unit.

2.10.2 Initial state space equations

Based on Equations (2.017) to (2.020) of Section (2.4.1), the initial state space equations of the SVC voltage regulator can be written as,

$$[\dot{X}_v] = [A_v] [X_v] + [B_v] [u] + [B_{ss}] \Delta v_{so} \qquad (2.142)$$

$$[y] = [C_v] [X_v] + [D_v] [u] + [D_{ss}] \Delta v_{so} \qquad (2.143)$$

$$[u] = [L_v] [y] + [G_v] [U] \qquad (2.144)$$

$$\Delta B = [M_v] [y] + [K_v] [U] \qquad (2.145)$$

$[X_v]$ is the state vector of the SVC voltage regulator. Vectors $[z]$ and $[U]$ of Equations (2.020) and (2.019) are defined in the case of the SVC voltage regulator as,

$$[z] = \Delta B$$

$$[U] = [\; \Delta v_D \;\; \Delta v_Q \;\; \Delta v_{Ds} \;\; \Delta v_{Qs} \;\; \Delta v_{Df} \;\; \Delta v_{Qf} \;\; \Delta v_{Dt} \;\; \Delta v_{Qt} \;\; \Delta v_{ref} \;\; \Delta \omega \;]^T$$

$$(2.146)$$

where, Δv_{Ds}, Δv_{Qs} are the D-Q components of the small changes in the sensing bus voltage, Δv_{Df}, Δv_{Qf} are the D-Q components of the small changes in the sending end bus voltage of the specified line, Δv_{Dt}, Δv_{Qt} are

the D-Q components of the small changes in the receiving end bus voltage of the specified line and $\Delta\omega$ is the small change in speed of a specified generating system. The vector [U] contains variables whose linear combinations defines the external inputs to the SVC voltage regulator as well as supplementary control input signal. From the block diagram of the SVC voltage regulator given in Figure (2.7), it is seen that the external inputs are $|\Delta v_s|$, Δv_{ref} and Δv_{so}.

The steady state sensing bus voltage magnitude $|v_s|$ can be expressed as a function of its D-Q components as,

$$|v_s| = \sqrt{v_{Ds}^2 + v_{Qs}^2} \tag{2.147}$$

Linearizing Equation (2.147), the expression for the small changes in the sensing bus voltage magnitude $|\Delta v_s|$ is derived as,

$$|\Delta v_s| = \left[\frac{v_{Ds}}{|v_s|} \quad \frac{v_{Qs}}{|v_s|}\right][\Delta v_{Ds} \quad \Delta v_{Qs}]^T \tag{2.148}$$

$|\Delta v_s|$ can be expressed as a function of the vector [U] using Equations (2.148) and (2.146) as,

$$|\Delta v_s| = [0 \quad 0 \quad \frac{v_{Ds}}{|v_s|} \quad \frac{v_{Qs}}{|v_s|} \quad 0 \quad 0 \quad 0 \quad 0 \quad 0 \quad 0][U] \tag{2.149}$$

Similarly the input Δv_{ref} which has a negative sign as shown in Figure (2.7) can also be expressed as a function of the vector [U] as,

$$-\Delta v_{ref} = [0 \quad 0 \quad 0 \quad 0 \quad 0 \quad 0 \quad 0 \quad 0 \quad -1 \quad 0] \, [U] \qquad (2.150)$$

The remaining input Δv_{so}, is treated separately for the ease in interfacing the SVC voltage regulator model with the supplementary control. The influence of the input Δv_{so} on the SVC voltage regulator is described by the vectors $[B_{ss}]$ and $[D_{ss}]$ in Equations (2.142) and (2.143). The formulation of these vectors is illustrated through an example in Appendix (A1.3). It must however be noted that from the block diagram of the SVC voltage regulator of Figure (2.7) that the sign of the input Δv_{so} is negative and must be taken into account while forming the vectors $[B_{ss}]$ and $[D_{ss}]$.

The matrices $[A_v]$, $[B_v]$, $[C_v]$, $[D_v]$, $[L_v]$, $[G_v]$, $[M_v]$ and $[K_v]$ in Equations (2.142) to (2.145) correspond to the matrices $[A]$, $[B]$, $[C]$, $[D]$, $[L]$, $[G]$, $[M]$ and $[K]$ of Equations (2.017) to (2.020). All these matrices except $[G_v]$ and $[K_v]$ can be determined solely based on the parameters of the various constituent regulator blocks and their interconnections. Matrices $[G_v]$ and $[K_v]$ can be formulated from the knowledge of external inputs and the constituent regulator blocks to which they are applied. In a manner identical to that describing the formulation of the matrices $[G_v]$ and $[K_v]$ for PSS Type-3 model, let the first and second block in the sequence of stacking the individual block state space equations be where the inputs $|\Delta v_s|$ and Δv_{ref} are applied respectively, then the matrices $[G_v]$ and $[K_v]$ using Equations (2.144), (2.145), (2.149) and (2.150) are,

$$[G_v] = [\quad 0_{nv \times 2} \quad G_{v1} \quad 0_{nv \times 4} \quad A_{v1} \quad 0_{nv \times 1} \quad]$$

where, nv is the number of states in the SVC voltage regulator; and

$$[G_{v1}] = \begin{bmatrix} \dfrac{v_{Ds}}{|v_s|} & \dfrac{v_{Qs}}{|v_s|} \\ 0_{(nv-1)\times 1} & 0_{(nv-1)\times 1} \end{bmatrix} ; \qquad [A_{v1}] = [0 \quad -1 \quad 0_{1\times (nv-2)}]^T$$

2.10.3 Final state space equations

Eliminating vectors [u] and [y] from Equations (2.142) to (2.145), the final state space equations of the voltage regulator are obtained as,

$$[\dot{X}_v] = [A_{stc}] [X_v] + [B_{stc}] [U] + [B_{vso}] \Delta v_{so} \qquad (2.151)$$

$$\Delta B = [M_{stc}] [X_v] + [K_{stc}] [U] + K_{vso} \Delta v_{so} \qquad (2.152)$$

where, the matrices $[A_{stc}]$, $[B_{stc}]$, $[M_{stc}]$ and $[K_{stc}]$ correspond to the matrices $[A_c]$, $[B_c]$, $[M_c]$ and $[K_c]$ of Equations (2.021) and (2.022) respectively. Also,

$$[B_{vso}] = [B_v L_v [I_v - D_v L_v]^{-1} D_{ss} + B_{ss}]; \qquad K_{vso} = M_v [I_v - D_v L_v]^{-1} D_{ss}$$

2.11 Supplementary control model

The supplementary control provides an input (Δv_{so}) to the SVC voltage regulator in order to modulate the voltage reference, thus modifying the output of the SVC voltage regulator in a manner so that the damping of electromechanical modes is increased. The supplementary control

dynamics is modelled by the generalized method of control system representation as described in Section (2.4.1). Depending on the type of feedback signals used in supplementary control, four different types of supplementary control are considered here, which are,

i)Type-1: where the feedback signal to the supplementary control is the small change in a specified line current magnitude ($|\Delta i|$) in per unit.

ii)Type-2: where the feedback signal is the small change in the sending end real power (ΔP_{line}) of a specified line in per unit.

iii)Type-3: where the feedback signal is the small change in the sending end reactive power (ΔQ_{line}) of a specified line in per unit.

iv)Type-4: where the feedback signal is the small change in the specified generating systems speed ($\Delta \omega$) in per unit.

Figure (2.8) gives the block diagram of the supplementary control transfer function. ΔSig is the input signal depending upon the type of supplementary control considered as described above. Δv_{so} is the output of the supplementary control.

Type-1: ΔSig = $|\Delta i|$
Type-2: ΔSig = ΔP_{line}
Type-3: ΔSig = ΔQ_{line}
Type-4: ΔSig = $\Delta \omega$
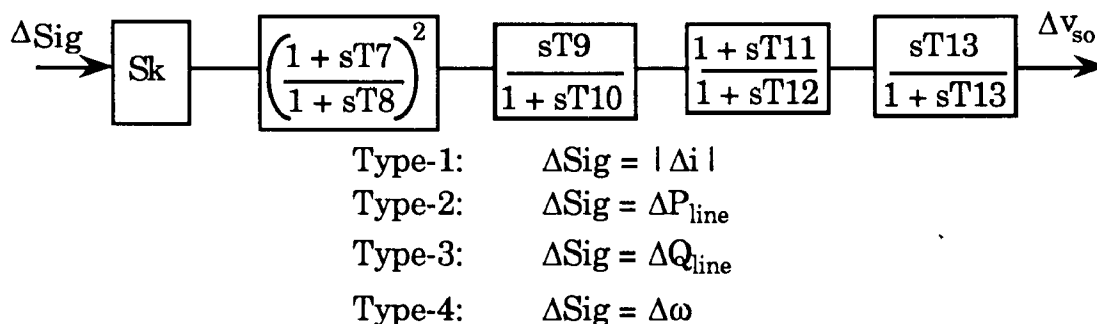
Figure (2.8): Block diagram of supplementary control

2.11.1 Initial equations for the state space formulations

Based on Equations (2.017) to (2.020) of Section (2.4.1), the initial state space equations of the supplementary control can be written as,

$$[\dot{X}_s] = [A_t][X_s] + [B_t][u] \qquad (2.153)$$

$$[y] = [C_t][X_s] + [D_t][u] \qquad (2.154)$$

$$[u] = [L_t][y] + [G_t][U] \qquad (2.155)$$

$$\Delta v_{so} = [M_t][y] + [K_t][U] \qquad (2.156)$$

$[X_s]$ is the state vector of the supplementary control. The vector $[U]$ is the same as in case of SVC voltage regulator and is given as,

$$[U] = [\ \Delta v_D \quad \Delta v_Q \quad \Delta v_{Ds} \quad \Delta v_{Qs} \quad \Delta v_{Df} \quad \Delta v_{Qf} \quad \Delta v_{Dt} \quad \Delta v_{Qt} \quad \Delta v_{ref} \quad \Delta \omega\ ]^T$$

The vector $[z]$ of Equation (2.020) is defined in the case of supplementary control as,

$$[z] = \Delta v_{so}$$

The supplementary control input (ΔSig) can be expressed in terms of the elements of vector $[U]$ as shown below:

i)<u>Type-1:</u> Here the input is the small change in the specified line current magnitude ($|\Delta i|$) in per unit. The steady state line current magnitude in a specified line can be expressed as,

$$|i| = \sqrt{i_{D1}{}^2 + i_{Q1}{}^2} \qquad (2.157)$$

where, i_{Dl}, i_{Ql} are the steady state D-Q components of the line current respectively. These can also be expressed as a function of the D-Q components of the steady state sending end (v_{Df}, v_{Qf}) and receiving end (v_{Dt}, v_{Qt}) voltages as shown below,

$$[i_{Dl} \quad i_{Ql}]^T = \begin{bmatrix} G_l & B_l \\ -B_l & G_l \end{bmatrix} \{[v_{Df} \quad v_{Qf}]^T - [v_{Dt} \quad v_{Qt}]^T\} \qquad (2.158)$$

where, $G_l = \dfrac{R_l}{R_l^2 + X_l^2}$; and $B_l = \dfrac{X_l}{R_l^2 + X_l^2}$;

R_l = Line resistance (p.u)

X_l = Line reactance (p.u). It is positive for inductive reactance and negative for capacitive reactance.

Linearizing Equations (2.157) and (2.158), the expression for the small changes in the specified line current magnitude $|\Delta i|$ can be derived as,

$$|\Delta i| = KI [v_{Df} \quad v_{Qf} \quad -v_{Dt} \quad -v_{Qt}] [\Delta v_{Df} \quad \Delta v_{Qf} \quad \Delta v_{Dt} \quad \Delta v_{Qt}]^T \qquad (2.159)$$

where, $KI = \dfrac{G_l^2 + B_l^2}{\left((v_{Df} - v_{Qf})^2 + (v_{Dt} - v_{Qt})^2\right)^{\frac{1}{2}}}$

$|\Delta i|$ can be expressed as a function of the vector $[U]$ using Equation (2.159) and (2.146) as,

$$|\Delta i| = KI \, [0 \quad 0 \quad 0 \quad 0 \quad v_{Df} \quad v_{Qf} \quad -v_{Dt} \quad -v_{Qt} \quad 0 \quad 0] \, [U] \qquad (2.160)$$

ii)Type-2: Here the input is the small changes in the specified line sending end power (ΔP_{line}) in per unit. The steady state sending end power (P_{line}) in a specified line can be expressed as,

$$P_{line} = v_{Df} i_{D1} + v_{Qf} i_{Q1} \qquad (2.161)$$

Combining the linearized form of Equations (2.161) and (2.158), the expression for the small changes in the sending end power in a specified line is given as,

$$\Delta P_{line} = [ga \quad gb \quad gc \quad gd] \, [\Delta v_{Df} \quad \Delta v_{Qf} \quad \Delta v_{Dt} \quad \Delta v_{Qt}]^T \qquad (2.162)$$

where,
$$ga = 2G_1 v_{Df} - G_1 v_{Dt} - B_1 v_{Qt};$$
$$gb = 2G_1 v_{Qf} + B_1 v_{Dt} - G_1 v_{Qt};$$
$$gc = B_1 v_{Qf} - G_1 v_{Df}; \text{ and}$$
$$gd = -B_1 v_{Df} - G_1 v_{Qf}$$

ΔP_{line} can be expressed as a function of the vector $[U]$ using Equation (2.162) and (2.146) as,

$$\Delta P_{line} = [0 \quad 0 \quad 0 \quad 0 \quad ga \quad gb \quad gc \quad gd \quad 0 \quad 0] \, [U] \qquad (2.163)$$

iii)Type-3: Here the input is the small changes in the specified line sending end reactive power (ΔQ_{line}) in per unit. The steady state sending end reactive power (Q_{line}) in a specified line can be expressed as,

$$Q_{line} = v_{Qf} i_{D1} - v_{Df} i_{Q1} \qquad (2.164)$$

Combining the linearized forms of Equations (2.164) and (2.158), the expression for the small changes in the sending end reactive power in a specified line is given as,

$$\Delta Q_{line} = [ga \quad gb \quad gc \quad gd] [\Delta v_{Df} \quad \Delta v_{Qf} \quad \Delta v_{Dt} \quad \Delta v_{Qt}]^T \qquad (2.165)$$

where,
$$ga = 2B_l v_{Df} + G_l v_{Qt} - B_l v_{Dt};$$
$$gb = 2B_l v_{Qf} - G_l v_{Dt} - B_l v_{Qt};$$
$$gc = -G_l v_{Qf} + B_l v_{Df}; \text{ and}$$
$$gd = G_l v_{Df} - B_l v_{Qf}$$

ΔQ_{line} can be expressed as a function of the vector [U] using Equation (2.165) and (2.146) as,

$$\Delta Q_{line} = [0 \quad 0 \quad 0 \quad 0 \quad ga \quad gb \quad gc \quad gd \quad 0 \quad 0] [U] \qquad (2.166)$$

iv)Type-4: Here the input is the small changes in the specified generating system speed ($\Delta \omega$). The feedback signal ($\Delta \omega$) can be expressed as a function of the vector [U] as shown below,

$$\Delta\omega = [0 \quad 0 \quad 0 \quad 0 \quad 0 \quad 0 \quad 0 \quad 0 \quad 0 \quad 1] [U] \qquad (2.167)$$

The matrices $[A_t]$, $[B_t]$, $[C_t]$, $[D_t]$, $[L_t]$, $[G_t]$, $[M_t]$ and $[K_t]$ in Equations (2.153) to (2.156) correspond to the matrices $[A]$, $[B]$, $[C]$, $[D]$, $[L]$, $[G]$, $[M]$ and $[K]$ of Equations (2.017) to (2.020). All these matrices except $[G_t]$ and $[K_t]$ can be determined solely based on the parameters of the various constituent supplementary control blocks and their interconnections. Matrices $[G_t]$ and $[K_t]$ can be formulated from the knowledge of external inputs and the constituent supplementary control blocks to which they are applied. For the block diagrams of the supplementary control shown in Figure (2.8) the matrices $[G_t]$ and $[K_t]$ are derived using Equations (2.155), (2.156), (2.160), (2.163), (2.166) and (2.167), depending on the type of feedback signal to the supplementary control.

i)Type-1: The feedback signal is $|\Delta i|$ and hence, the matrices $[G_t]$ and $[K_t]$ are derived as,

$$[G_t] = [0_{nc \times 4} \quad G_{t1} \quad 0_{nc \times 2}]$$

where, nc is the number of supplementary control states and;

$$[G_{t1}] = KI \begin{bmatrix} v_{Df} & v_{Df} & v_{Dt} & v_{Dt} \\ 0_{(nc-1) \times 1} & 0_{(nc-1) \times 1} & 0_{(nc-1) \times 1} & 0_{(nc-1) \times 1} \end{bmatrix}$$

Also,

$[K_t] = [0_{1 \times 10}]$

ii)Type-2: The feedback signal is ΔP_{line} and hence, the matrices $[G_t]$ and $[K_t]$ are derived as,

$$[G_t] = [0_{nc \times 4} \quad G_{t1} \quad 0_{nc \times 2}]$$

where, nc is the number of supplementary control states and;

$$[G_{t1}] = \begin{bmatrix} ga & gb & gc & gd \\ 0_{(nc-1) \times 1} & 0_{(nc-1) \times 1} & 0_{(nc-1) \times 1} & 0_{(nc-1) \times 1} \end{bmatrix};$$

The coefficients ga,gb,gc,gd are obtained from the Equation (2.162). Also,

$$[K_t] = [0_{1 \times 10}]$$

iii)Type-3: The feedback signal is ΔQ_{line} and hence, the matrices $[G_t]$ and $[K_t]$ are derived as,

$$[G_t] = [0_{nc \times 4} \quad G_{t1} \quad 0_{nc \times 2}]$$

where, nc is the number of supplementary control states and;

$$[G_{t1}] = \begin{bmatrix} ga & gb & gc & gd \\ 0_{(nc-1) \times 1} & 0_{(nc-1) \times 1} & 0_{(nc-1) \times 1} & 0_{(nc-1) \times 1} \end{bmatrix};$$

The coefficients ga,gb,gc,gd are obtained from the Equation (2.176). Also,

$$[K_t] = [0_{1 \times 10}]$$

iv)Type-4: The feedback signal is $\Delta \omega$ and hence, the matrices $[G_t]$ and $[K_t]$ are derived as,

$$[G_t] = [0_{nc \times 9} \quad G_{t1}]$$

where, nc is the number of supplementary control states and;

$$[G_{t1}] = [1 \quad 0_{1 \times (nc-1)}]^T$$

Also,

$$[K_t] = [0_{1 \times 10}]$$

In all the supplementary control models (Type-1, Type-2, Type-3 and Type-4) it is seen that the matrix $[K_t]$ is a null matrix. This is so, because in all these models there is no feedforward path from the external input to the output Δv_{so}.

2.11.2 Final state space equations

Eliminating vectors [u] and [y] from Equations (2.153) to (2.156), the final form of the state space equations for the supplementary control can be derived as,

$$[\dot{X}_s] = [A_s] [X_s] + [B_s] [U] \qquad (2.168)$$

$$\Delta v_{so} = [M_s] [X_s] + [K_s] [U] \qquad (2.169)$$

Matrices $[A_s]$, $[B_s]$, $[M_s]$ and $[K_s]$ correspond to the matrices $[A_c]$, $[B_c]$, $[M_c]$ and $[K_c]$ of Equations (2.021) and (2.022) respectively.

2.12 Interconnection of SVC and its associated controls

The SVC can be modelled with the following options;

i)   SVC with no supplementary control and,

ii)   SVC with supplementary control.

2.12.1   SVC model with no supplementary control

For the SVC voltage regulator, the external inputs ($|\Delta v_s|$, Δv_{ref}) are expressed as functions of the vector [U] in the state space representation of the SVC voltage regulator model. In this representation only certain elements (Δv_{Ds}, Δv_{Qs} and Δv_{ref}) of [U] are needed. Based on this, the state space equations of the SVC voltage regulator model (Equations (2.151) and (2.152)) are rewritten by partitioning the vector [U] and matrices $[B_{stc}]$ and $[K_{stc}]$, so that only the elements of [U] needed to represent the external inputs are considered.

$$[\dot{X}_v] = [A_{stc}] [X_v] + [B_{stc1}] [\Delta v_{DQs}] + [B_{rf}] [\Delta v_{ref}] \qquad (2.170)$$

$$\Delta B = [M_{stc}] [X_v] + [K_{stc1}] [\Delta v_{DQs}] + [K_{rf}] [\Delta v_{ref}] \qquad (2.171)$$

$[B_{stc1}]$, $[B_{rf}]$ and $[K_{stc1}]$, $[K_{rf}]$ can be easily obtained by the proper partitioning of matrices $[B_{stc}]$ and $[K_{stc}]$ respectively. It must be noted that as the supplementary control is not modelled, $\Delta v_{so} = 0$.

Eliminating ΔB in Equation (2.141) using Equation (2.171) gives,

$$[\Delta i_{DQ}] = \begin{bmatrix} -v_Q \\ v_D \end{bmatrix} [M_{stc}] [X_v] + [Y_s] [\Delta v_{DQs}] + [Y_{SVC}] [\Delta v_{DQ}] + [K_{ref}] \Delta v_{ref}$$

$$(2.172)$$

where, $\qquad [K_{ref}] = \begin{bmatrix} -v_Q \\ v_D \end{bmatrix} [K_{rf}] \qquad$ and $\qquad [Y_s] = \begin{bmatrix} -v_Q \\ v_D \end{bmatrix} [K_{stc1}]$

Equation (2.170) and (2.172) can be put in the general form of Equations (2.003) and (2.004) to result in the following state space model of the SVC.

$$[\dot{X}_d] = [A_d] [X_d] + [B_d] [\Delta V_d]$$
$$[\Delta I_d] = [C_d] [X_d] - [Y_d] [\Delta V_d]$$

where, $\qquad [X_d] = [X_v]; \qquad\qquad\qquad [A_d] = [A_{svc}] ;$

$\qquad\qquad [B_d] = \begin{bmatrix} 0_{nv \times 2} & B_{stc1} \end{bmatrix} ; \qquad [\Delta I_d] = [\Delta i_{DQ}] ;$

$\qquad\qquad [C_d] = \begin{bmatrix} -v_Q \\ v_D \end{bmatrix} [M_{stc}] ; \qquad\qquad [Y_d] = - [Y_{SVC}] - \begin{bmatrix} -v_Q \\ v_D \end{bmatrix} [K_{stc1}];$

and, $\qquad [\Delta V_d] = [\Delta v_D \quad \Delta v_Q \quad \Delta v_{Ds} \quad \Delta v_{Qs}]T$

In Equations (2.170) and (2.172), the vectors $[B_{rf}]$ and $[K_{ref}]$ are the input distribution vectors for a change in the voltage reference input to the SVC. The vectors $[B_{rf}]$ and $[K_{ref}]$ are not needed in the formation of the system state matrix. They are needed only for the calculation of residues, or frequency or time responses, as will be shown later.

2.12.2   SVC model with supplementary control

To interface the models of the supplementary control to the SVC voltage regulator, the SVC voltage regulator and supplementary control state space equations can be rewritten as,

Regulator:

$$[\dot{X}_v] = [A_{stc}] [X_v] + [B_{stc1}] [\Delta v_{DQs}] + [B_{rf}] \Delta v_{ref} + [B_{vso}] \Delta v_{so} \qquad (2.173)$$

$$[\Delta B] = [M_{stc}] [X_v] + [K_{stc1}] [\Delta v_{DQs}] + [K_{rf}] \Delta v_{ref} + K_{vso} \Delta v_{so} \qquad (2.174)$$

Supplementary control:

$$[\dot{X}_s] = [A_s] [X_s] + [B_{s1}] [\Delta v_c] + [B_{s2}] \Delta \omega \qquad (2.175)$$

$$\Delta v_{so} = [M_s] [X_s] + [K_{s1}] [\Delta v_c] + K_{s2} \Delta \omega \qquad (2.176)$$

Equations (2.175) and (2.176) correspond to the supplementary control state space Equations (2.168) and (2.169), and are derived by partitioning the vector [U] to explicitly introduce interface variables $[\Delta v_c]$, $\Delta \omega$, $[\Delta v_{DQs}]$ and Δv_{ref} . Accordingly the matrices $[B_{s1}]$, $[B_{s2}]$ and $[K_{s1}]$, K_{s2} (scalar), are

obtained by the proper partitioning of the matrices $[B_s]$ and $[K_s]$. In Equations (2.175) and (2.176) the vector $[\Delta v_c]$ is defined as,

$$[\Delta v_c] = [\Delta v_{Df} \quad \Delta v_{Qf} \quad \Delta v_{Dt} \quad \Delta v_{Qt}]^T$$

On the same basis, the SVC voltage regulator state space Equations (2.151) and (2.152) are written in the from of Equations (2.173) and (2.174). It may be noted that in these equations, Δv_{so} now appears as a variable, since supplementary control is being considered and thus, forms a basis for interfacing the SVC voltage regulator and its supplementary control models. Equations (2.173) and (2.175) are combined together, and eliminating Δv_{so} using Equation (2.176) gives,

$$[\dot{X}_{comp}] = [A_{comp}] [X_{comp}] + [B_{comp}] [\Delta V_{svc}] + [B_{cw}] \Delta \omega + [B_{ref}] \Delta v_{ref} \quad (2.178)$$

where,

$$[X_{comp}] = \begin{bmatrix} X_v \\ X_s \end{bmatrix}; \qquad [A_{comp}] = \begin{bmatrix} A_{stc} & B_{vso} M_s \\ 0_{nc \times nv} & A_s \end{bmatrix};$$

$$[B_{cw}] = \begin{bmatrix} B_{vso} K_{s2} \\ B_{s2} \end{bmatrix}; \qquad [B_{ref}] = \begin{bmatrix} B_{rf} \\ 0_{nc \times 1} \end{bmatrix}$$

$$[B_{comp}] = \begin{bmatrix} 0_{nv \times 2} & B_{stc} & B_{vso} K_{s1} \\ 0_{nc \times 2} & 0_{nc \times 2} & B_{s1} \end{bmatrix} \text{ and}$$

$$[\Delta V_{svc}] = [\Delta v_D \quad \Delta v_Q \quad \Delta v_{Ds} \quad \Delta v_{Qs} \quad \Delta v_{Df} \quad \Delta v_{Qf} \quad \Delta v_{Dt} \quad \Delta v_{Qt}]^T$$

Eliminating Δv_{so} from Equation (2.174) using Equation (2.176), gives,

$$\Delta B = [M_{comp}] [X_{comp}] + [K_{comp}] [\Delta V_{svc}] + K_{cw} \Delta\omega + K_{rf} \Delta v_{ref} \qquad (2.179)$$

where, $\qquad [M_{comp}] = [M_{stc} \quad K_{vso} M_s]; \qquad [K_{comp}] = [K_{stc1} \qquad K_{vso} \quad M_s]$
and $\qquad K_{cw} = K_{vso} K_{s2}$

Eliminating ΔB in Equation (2.141) using Equation (2.179), gives,

$$[\Delta i_{DQ}] = [C_{comp}] [X_{comp}] - [Y_{comp}] [\Delta V_{svc}] + [C_{cw}] \Delta\omega + [K_{ref}] \Delta vref \qquad (2.180)$$

where,

$$[C_{comp}] = \begin{bmatrix} -v_Q \\ v_D \end{bmatrix} [M_{stc} \quad K_{vso} M_s]; \qquad [C_{cw}] = \begin{bmatrix} -v_Q \\ v_D \end{bmatrix} K_{vso} \quad K_{s2};$$

$$[K_{ref}] = \begin{bmatrix} -v_Q \\ v_D \end{bmatrix} K_{rf} \qquad \text{and} \qquad [Y_{comp}] = -[Y_{SVC} \qquad \begin{bmatrix} -v_Q \\ v_D \end{bmatrix} [K_{stc} \quad K_{vso} K_{s1}]]$$

Equations (2.178) and (2.180) can be rewritten as follows,

$$[\dot{X}_d] = [A_d] [X_d] + [B_d] [\Delta V_d] + [B_{cw}] \Delta\omega \qquad (2.181)$$

$$[\Delta I_d] = [C_d] [X_d] - [Y_d] [\Delta V_d] + [C_{cw}] \Delta\omega \qquad (2.182)$$

where,

$[X_d] = [X_{comp}];\qquad [A_d] = [A_{comp}];\qquad [B_d] = [B_{comp}];\qquad [\Delta V_d] = [\Delta V_{svc}];$

$[\Delta I_d] = [\Delta i_{DQ}];\qquad [C_d] = [C_{comp}] \qquad\qquad \text{and} \qquad\qquad [Y_d] = [Y_{comp}]$

In Equations (2.178) and (2.180) the variable $\Delta\omega$ appears only when the supplementary control is of Type-4, hence for the other types of supplementary control (Type-1, Type-2 and Type-3) Equations (2.181) and (2.182) can be written in the general form of Equations (2.003) and (2.004) to result in the state space model of the SVC. Also in Equations (2.178) and (2.180) the vectors $[B_{rf}]$ and $[K_{ref}]$ are the input distribution vectors for a change in the voltage reference input to the SVC. The vectors $[B_{rf}]$ and $[K_{ref}]$ are not needed in the formation of the system state matrix. They are needed only for the calculation of residues, or frequency or time responses, as will be shown later.

For the supplementary control of Type-4 it can be noticed that $\Delta\omega$ is not included in the overall SVC state vector $[X_d]$. This is because $\Delta\omega$ is a state which corresponds to the specified generating system. Hence, inclusion of the effect of $\Delta\omega$ state on SVC is treated separately after the complete system state space equations are derived. This is illustrated through an example shown below.

The state space equations for the generating systems and SVCs with one of them having a supplementary control of Type-4, can be combined as described in Section (3.1) and expressed in the form,

$$[\dot{X}] = [A_{st}] [X] + [B_{st}] [\Delta V] + [B_{cw}'] \Delta\omega \qquad (2.183)$$

$$[\Delta I] = [C_{st}] [X] - [Y_{st}] [\Delta V] + [C_{cw}'] \Delta\omega \qquad (2.184)$$

For the SVC with supplementary control of Type-4, the individual device matrices are the same as that given in Equations (2.181) and (2.182) in the formation of matrices $[A_{st}]$, $[B_{st}]$, $[C_{st}]$ and $[Y_{st}]$. $[B_{cw}']$ and $[C_{cw}']$ are vectors of appropriate sizes and have vectors $[B_{cw}]$ and $[B_{cw}]$ of Equations (2.181) and (2.182) as their nonzero entries. Since $\Delta\omega$ is a state variable defined for the specified generating system, it is included in the overall system state vector $[X]$ and hence can be expressed in terms of the vector $[X]$. Equations (2.183) and (2.184) can now be simplified to result in the overall state space representation of the system, which is of the form

$$[\dot{X}] = [A_{st}'] [X] + [B_{st}] [\Delta V]$$
$$[\Delta I] = [C_{st}'] [X] - [Y_{st}] [\Delta V] \quad (2.184)$$

where, $[A_{st}']$ and $[C_{st}']$ are the resulting matrices formed due to the inclusion of vectors $[B_{cw}']$ and $[C_{cw}']$ in matrices $[A_{st}]$ and $[C_{st}]$ respectively. Using matrices $[A_{st}']$ and $[C_{st}']$ the overall system state matrix $[A]$ is formulated in the same way as given by Equation (2.008) and is,

$$[A] = [A_{st}'] + [B_{st}] [Y + Y_D]^{-1} [C_{st}']$$

2.13 Discussion

This chapter has given a detailed description of how the various subsystem models of the power system are modelled. The interfacing of these models to the network is also explained. Modifications on existing or

the incorporation of new models can be easily achieved by following the same framework of modelling described in this chapter.

A program called the Small Signal Stability (S^3) programme has been developed incorporating this modelling technique for the purpose of conducting small signal stability studies. It is interesting to note that the network admittance matrix may or may not be collapsed to its device buses while forming the overall system state matrix. In the S^3 programme, presently the admittance matrix is collapsed to its device buses as explained in Appendix (A1.7).

Chapter 3

Techniques for Small Signal Stability Analysis

and

Design of Damping Control

3.1   General

The small signal stability analysis of a power system deals with the study of underdamped power systems where minor disturbances can cause the machine rotor angle to oscillate around its steady state value at the natural frequency of the total electromechanical system. These oscillations called the electromechanical modes of oscillation are of very low frequency, typically in the range of 0.1 to 2.5 Hz. These modes are initiated by the interaction of the electrical and mechanical torques applied to the rotating system of the synchronous machine in the event of a disturbance in the power system. The primary objective of small signal stability analysis is to identify and damp out the poorly damped electromechanical modes of oscillation.

This chapter reviews some of the techniques currently used for the small signal stability assessment and design of damping control. The

8 6

small signal stability assessment is usually based on eigenvalue analysis. The design of damping control to improve system stability is carried out using frequency response technique, pole placement by residue calculations and time response.

3.2 Eigenvalue analysis for small signal stability investigations

The power system small signals can be described in the linearized domain by the following state equation as derived in the previous chapter.

$$[\dot{X}] = [A][X]$$

The eigenvalues of the state matrix [A] provide information about the small signal behavior of the power system. For, the power system to be stable, all the eigenvalues of [A] should have a negative real part. The imaginary part of each eigenvalue gives the natural frequency of oscillation of the power system. These oscillations can range from electromechanical modes to the control modes. The damping ratio of the corresponding eigenvalues indicate how well these oscillations are damped. The poorly damped oscillations corresponding to the control modes can be damped effectively by the proper tuning of various controls present in the system. The poorly or negatively damped oscillations (eigenvalues) corresponding to the electromechanical modes of oscillation which are a cause of concern in the small signal stability analysis of a power system, can be damped through the proper design of damping control.

An eigenvalue corresponds to the electromechanical mode of oscillation if its frequency of oscillation lies between 0.1 to 2.5 Hz. and is predominantly influenced by the speed ($\Delta\omega$) state of the synchronous machine. It is possible that some control modes might also have frequency of oscillation in this range but it will not be mainly influenced by the speed ($\Delta\omega$) state of the synchronous machine. The influence of the speed ($\Delta\omega$) state on an eigenvalue can be obtained from a sensitivity index called the state participation factor. The state participation factor of a state is the sensitivity of the eigenvalue to the change in the corresponding diagonal element in the system state matrix of the power system model. The magnitude of this factor for an eigenvalue conveys information of how the corresponding state of the system model influences the specific eigenvalue. Also, since these factors are non-dimensional, they do not have the scaling problems associated with eigenvectors and are therefore, better suited to determine which states predominantly influence the specific eigenvalue. Based on this procedure, the concerned electromechanical modes of oscillation and the synchronous machines predominantly influencing these modes can be identified. The procedure for the evaluation of state participation factors is given in Appendix (A1.8).

The state participation factors of all the states for a specific eigenvalue are useful in determining the influence of various system states on that eigenvalue. But, the state participation factor does not give information of the effect of the passive elements in the power system like tie

line impedances or loads on the small signal stability. This information is useful for a better understanding of the small signal stability problem.

Electromechanical modes of oscillation are loosely classified into local, intermachine and interarea modes of oscillation. Local modes are dominated by a single machine having a very significant state participation factor of its speed ($\Delta\omega$) and rotor angle ($\Delta\delta$) states to this mode compared to all of the other synchronous machines present in the system. The frequency range of the local mode is approximately 0.5 to 2.5 Hz.

Intermachine modes are characterized by a small group of machines having significant magnitude of state participation factors of their speed ($\Delta\omega$) and rotor angle ($\Delta\delta$) states to this mode compared to the other synchronous machines present in the system. The frequency range of the intermachine modes is roughly 0.3 to 1.0 Hz.

Interarea modes are characterized by a number of synchronous machines located in one 'area' (set of coherent machines) having a significant state participation factor of their speed ($\Delta\omega$) and rotor angle ($\Delta\delta$) states to this mode compared to the machines in other areas of the system. The frequency range of these modes is around 0.1 to 0.6 Hz.. This demarcation of the frequency ranges for the local, intermachine and interarea modes is not strict and may vary according to the system under consideration [2,17].

In a physical sense, the occurrence of electromechanical modes of oscillation can be described by machines oscillating or 'swinging' against each other. The information about which machine is swinging against the other for a mode under consideration, can be obtained by determining the mode shape of the electromechanical oscillation.

The modes shape for a particular electromechanical oscillation (eigenvalue) is described by the elements of the associated eigenvector corresponding to the speed deviation ($\Delta\omega$) of all the machines present in the system. The various synchronous machines whose speed ($\Delta\omega$) states (in the eigenvector under consideration) have a positive real part, oscillate (swings) against those synchronous machines whose speed ($\Delta\omega$) states have a negative real part. For intermachine and interarea modes, the mode shapes will similarly depict the two groups of machines or areas which are swinging against each other. Also, the mode shape provides the knowledge about the interface between the group of machines or areas, which is demarcated by the eigenvector elements corresponding to the speed ($\Delta\omega$) states of the synchronous machines having a small magnitude [5,6].

In the study of the small signal behavior of a power system, the machine rotor angle is defined with respect to a fixed reference. The formulation of the linearized synchronous machine state space model described in the previous chapter utilizes the bus angles as obtained from the load flow analysis for the calculation of the machine rotor angle (δ). In load flow calculations, the bus angles are defined with respect to a slack bus, which can also be taken as the infinite bus for small signal stability studies. Normally a bus whose voltage magnitude and phase angle is not

influenced by any disturbance in the system and remains constant is chosen as an infinite bus. An implicit assumption involved in this is that the dynamics of the synchronous machine or equivalent external system connected to this infinite bus cannot be represented in small signal stability investigations. An attempt to model the power system without an infinite bus will result in one or two zero eigenvalues [1,10]. One of the zero eigenvalues is caused as the rotor angle is now defined with respect to a floating reference. Another zero eigenvalue can appear if the inherent damping of the synchronous machine is ignored. This zero eigenvalue situation can be avoided, either by redefining the state variables corresponding to the rotor angle and speed deviation states, or considering an infinite bus in the model formulation.

3.3 Techniques for the design of damping control

The design of damping control is carried out using standard techniques like frequency response and pole placement [22]. The advantage of these techniques is that the state space representation of the system can be directly used without explicitly deriving the system transfer function as is the case in other standard techniques like root locus. The control design can also be carried out using time response with step or impulse inputs. This, however,results in a trial and error procedure for a complex system.

3.3.1 Frequency response technique

The frequency response calculation is a very powerful tool for control system design. The power system is taken to be that of a Single Input Multiple Output (SIMO) type. This enables the calculation of the frequency response of various signals simultaneously. The frequency response of the various monitored signals in the power system can be calculated with respect to one of the following inputs:

i)Voltage reference of the excitation system of a synchronous machine.

ii)Mechanical torque applied to a synchronous machine.

iii)Voltage reference of the regulator of a SVC.

The state space equation describing the dynamics of the system is,

$$[\dot{X}] = [A]\,[X] + [B_{inp}]\,u \tag{3.01}$$

where, [X] is the state vector of the system, [A] is the system state matrix, $[B_{inp}]$ is the matrix defining the distribution of the input u to the system. Transforming Equation (3.01) into the Laplace domain gives,

$$[X(s)] = [sI - A]^{-1}\,[B_{inp}]\,u(s) \tag{3.02}$$

where, [I] is the identity matrix having the same dimension as matrix [A].

For frequency response calculations the Laplace operator 's' is replaced by the imaginary frequency $j\omega$ i.e. $s = j\omega$ and the frequency 'ω' is

varied over a range of interest. $u(s=j\omega)$ is taken as unit in frequency response calculations. Thus Equation (3.02) can be rewritten as,

$$[X(j\omega)] = [j\omega I - A]^{-1} [B_{inp}] \qquad (3.03)$$

The calculation of the frequency response from Equation (3.03) would require the inversion of matrix $[j\omega I - A]^{-1}$ for each frequency point ω ; this is computationaly expensive. In order to reduce the computational effort, matrix [A] is diagonalized using standard eigenvector transformations as shown below.

$$[\Lambda] = P [A] P^{-1} \qquad (3.04)$$

where, $[\Lambda]$ is a diagonal matrix with eigenvalues of [A] as its diagonal elements. [P] is the transformation matrix whose columns are the eigenvectors corresponding to each eigenvalue of [A]. Combining this equation with Equation (3.03) gives,

$$[X(j\omega)] = [P]^{-1} [j\omega I - \Lambda]^{-1} [P] [B_{inp}] \qquad (3.05)$$

The use of Equation (3.05) for the calculation of the frequency response would require the inversion of the matrix $[j\omega I - \Lambda]$ at each frequency point which is trivial as this matrix is diagonal. Equation (3.05) gives the state vector $[X(j\omega)]$ for each frequency point i.e. the frequency response of the system state vector.

The monitored signal (y) present in the system for which the frequency response is being obtained can be expressed as a function of the system states [X] as,

$$y = [C_y] [X] \qquad (3.06)$$

Transforming the above equation into the frequency domain and substituting the value of [X(jω)] from Equation (3.05) gives,

$$y(j\omega) = [C_y] [P]^{-1} [j\omega I - \Lambda]^{-1} [P] [B_{inp}] \qquad (3.07)$$

This expression can be used directly for obtaining the frequency response of the monitored signal y.

Frequency response technique has been extensively used for the design of PSS [6,13,17]. In the design of a PSS for a particular machine in a multimachine system, each machine except the candidate machine where the PSS is being installed is replaced by a negative impedance and the inertia constant of the candidate machine is increased by a factor of 25 so that the effect of rotor angle deviation on exciter output of the candidate machine is minimized [6]. The frequency response of the generating system electrical torque with respect to the voltage reference of the exciter is obtained. In this calculation of the frequency response only the contribution to the electrical torque from the exciter is considered. Suitable compensation networks are designed so that the phase lag from the exciter is compensated over the range of frequencies of interest. The amount of

phase compensation given is generally 30° less than the total phase lag introduced by the exciter over the frequency range of interest. The gain of the compensation network is determined by varying the gain over a range and selecting the gain value where maximum damping of the mode of interest is obtained and the damping of control modes are also acceptable. The feedback signal used for the PSS is the speed or an equivalent speed signal [6,13,14]. In this design, the PSS provides a phase lead to the speed signal with appropriate amplification to compensate the phase lag introduced by the exciter. The output of the PSS will modulate the voltage reference of the exciter in a manner that the electrical torque contribution from the exciter is in phase with the machine speed and hence increases the damping of the electromechanical mode of oscillation.

The frequency response technique for the design of PSS is very effective, but this method cannot be easily extended to the design of other damping controls like supplementary control on SVC because the compensation network will have to be designed to satisfy a single input multiple output situation. Frequency response of various signals can also be used to determine the suitability of various signals as potential feedback signals to the damping control. The electromechanical mode (eigenvalue) whose damping is to be improved, is obviously near the imaginary axis in the complex s-plane. Thus, the frequency response of a potential feedback signal would show the presence of this mode as a resonant peak in the magnitude response (the bandwidth being governed by its damping) as the frequency being varied equals the frequency of oscillation of this mode. Also, the phase response would show a dip by 180° lag. Even though the

frequency response indicates as to how the monitored signal is influenced by the poorly damped eigenvalues, it does not indicate how much information the signal has on the modes that are better damped, or information of eigenvalues which lie on the real axis in the complex s-plane. This information is important for selecting the suitable feedback signal for effective design of damping control. The frequency response of various signals present in the system can also be used to detect any non-minimum phase behavior exhibited by them [18,19].

3.3.2 Pole placement technique

The design of control has also been attempted with pole placement techniques using the residue method for placing poles. In this method, the residue of the power system model is calculated at a specified location in the complex s-plane, where the mode under consideration is desired to be shifted. Appropriate controls are designed to meet the required magnitude and phase criteria.

For a system with transfer function G(s) if the pole is to be shifted from a particular location to a new location $s = s_o = \sigma_o + j\omega_o$ in the complex s-plane, the residue of the transfer function G(s) at the complex frequency s_o is given as $G(s_o)$.

The procedure for calculating the residues is the same as that of the frequency response calculations described in the previous section. In case

of residue calculation the complex frequency is used instead of the imaginary frequency only as in the case of the frequency response calculations. Therefore, from Equation (3.07) the residue of a monitored signal with respect to a specified input at a complex frequency s_o is given by the expression,

$$y(s_o) = [C_y] [P]^{-1} [s_o I - \Lambda]^{-1} [P] [B_{inp}] \qquad (3.08)$$

where, y is the desired monitored signal and the input for the power system model is one of the following,

i)Voltage reference of the excitation system of a synchronous machine.

ii)Mechanical torque applied to a synchronous machine.

iii)Voltage reference of the regulator of an SVC.

While frequency response technique is well suited for the design of PSS, the pole placement technique provides a more general method and has been used for the PSS design and design of supplementary control of SVC [8,10].

3.3.3 Time response calculation

The time response of the system to standard test signals like impulse and step can also be used for the design of controls. The time response of various monitored signals with respect to an impulse or step in one of the following inputs can be obtained.

i)Voltage reference of the excitation system of a synchronous machine.

ii)Mechanical torque applied to a synchronous machine.

iii)Voltage reference of the regulator of an SVC.

Impulse response

For a impulse response, the input u(t) in Equation (3.01) is taken as,

$$u(0) = 1 \qquad \text{and}$$
$$u(t) = 0, \qquad \forall \, t > 0 \qquad (3.09)$$

and the system is initially assumed to be at rest, i.e. $[X(0)] = 0$. Therefore, from Equations (3.01) and (3.09), the impulse response of the system states $[X(t)]$ in the time domain is,

$$[X(t)] = [P] \, [\varepsilon^{[\Lambda t]}] \, [P]^{-1} \, [B_{inp}] \qquad (3.10)$$

Step response

For a step response the input u(t) is described by

$$u(t) = 1, \qquad \forall \, t \geq 0 \qquad (3.11)$$

and the system is assumed to be initially at rest, i.e. $[X(0)] = 0$. Therefore, from Equations (3.01) and (3.11), the step response of the system states $[X(t)]$ in the time domain is,

$$[X(t)] = [P] \, [\Lambda]^{-1} \, [\varepsilon^{[\Lambda t]} - I] \, [P]^{-1} \, [B_{inp}] \qquad (3.12)$$

Since the desired monitored signal can be expressed as a function of the system states [X], the time response of the monitored signal can be determined from Equations (3.06) and one of (3.10) or (3.12) depending on whether an impulse or step input is applied respectively as,

$$y(t) = [C_y] [X(t)] \qquad\qquad (3.13)$$

As mentioned earlier, this technique for control design results in a trial and error procedure and hence is used in relatively simple situations.

From the foregoing it is evident that a proper choice of the monitored signal is important for effective damping of the power system.

3.3.4 Monitored system signals

The various signals which can be monitored in a power system for damping purposes are the bus quantities, line quantities, machine quantities, and SVC quantities. Given below are the most commonly monitored signals in a typical power system.

i)Bus quantities:

      a)Change in bus voltage magnitude.

      b)Change in bus voltage phase.

ii)Line quantities:

a)Change in line current magnitude.

b)Change in sending end line real power.

c)Change in sending end line reactive power.

iii)Quantities related to the classical model of the synchronous machine:

a)Change in output real power.

b)Change in output reactive power.

c)Change in speed.

d)Change in rotor angle.

e)Change in output current magnitude.

iv)Quantities related to the flux linkage model of the synchronous machine:

a)Change in output real power.

b)Change in output reactive power.

c)Change in electrical torque contribution from the excitation system.

d)Change in speed.

e)Change in rotor angle.

f)Change in output current magnitude.

v)Quantities related to SVC model:

a)Change in the output reactive power.

b)Change in the output current magnitude.

Any of the above signals can be expressed in the following form,

$$y = [R] [X] + [S] [\Delta V] \tag{3.14}$$

where, y is the monitored signal, [X] is the state vector of the system, [ΔV] is the vector of system bus voltage deviations and [R],[S] define the linear

combination of the system states and bus voltages forming the monitored signal respectively. The determination of matrices [R] and [S] for the various monitored signals is quite straightforward and is not given.

From the linearized network equation (Equation (2.005)), and the stacked device output current equation (Equation (2.007)) of Chapter 2., the system bus voltages can be expressed as a function of the system states as,

$$[\Delta V] = [Y_N + Y_{st}]^{-1} [C_{st}] [X] \qquad (3.15)$$

Combining Equation (3.01) and (3.02) gives,

$$y = [C_y] [X]$$

where, $[C_y] = [R] + [S] [Y_N + Y_{st}]^{-1} [C_{st}]$

3.4 Discussion

This chapter has given a review of the various analysis tools used for the small signal stability study of a power system. Also, certain design procedures for the design of damping control have been described. Eigenanalysis, state participation factor determination, frequency, residue and time response calculations can be obtained from the Small Signal Stability (S^3) programme.

Chapter 4

New Techniques for Small Signal Stability Analysis

4.1 General

This chapter describes certain innovations to enhance and overcome some of the shortcomings of the existing techniques for the small signal stability analysis of a power system and for the design of damping control. To supplement the use of state participation factor, an index called voltage participation factor has been suggested which indicates the influence of passive network elements on system stability [20]. A suitable choice of the potential feedback signal is important for the effectiveness of the damping control. This can be evaluated based on observability criteria as described here. Also, a novel method for calculating the modal torques for the mode under consideration is introduced in this chapter. The calculation of modal torques is considered useful in assessing the small signal and transient stability.

4.2 Voltage participation factors

Voltage participation factor is the sensitivity of an eigenvalue to change in the shunt admittance at a bus, or the sensitivity of the eigenvalue to the changes in the transfer admittance between two buses. The voltage

102

participation factors are ideal for analyzing the effect of network loads and variations in tie line impedances on the small signal stability of a power system. The voltage participation factors can also provide a suitable basis for the selection of the site of a SVC equipped with damping control. This is because the SVC is modelled as a voltage controlled variable shunt susceptance. The method of calculating the voltage participation factors is described below.

Using Equations (2.005) to (2.007), the state space equation for the complete power system can be expressed in the form,

$$\begin{bmatrix} \dot{X} \\ 0 \end{bmatrix} = \begin{bmatrix} A_{st} & B_{st} \\ C_{st} & -(Y_N + Y_{st}) \end{bmatrix} \begin{bmatrix} X \\ \Delta V \end{bmatrix} \tag{4.01}$$

Transforming Equation (4.01) into the Laplace (complex frequency) domain gives,

$$\begin{bmatrix} s\,X(s) \\ 0 \end{bmatrix} = \begin{bmatrix} A_{st} & B_{st} \\ C_{st} & -(Y_N + Y_{st}) \end{bmatrix} \begin{bmatrix} X(s) \\ \Delta V(s) \end{bmatrix} \tag{4.02}$$

where, $[X(s)]$ is the state vector of the system in the Laplace domain and $[\Delta V(s)]$ is the system bus voltage vector in the complex frequency domain. Let λ_1 be an eigenvalue of the system described by Equation (4.02), and $[X(\lambda_1)]$ be the corresponding right eigenvector. Also, let the corresponding left eigenvector be $[Z(\lambda_1)]$. Substituting $s = \lambda_1$ in Equation (4.02) gives,

$$\begin{bmatrix} \lambda_1\, X(\lambda_1) \\ 0 \end{bmatrix} = \begin{bmatrix} A_{st} & B_{st} \\ C_{st} & -(Y_N + Y_{st}) \end{bmatrix} \begin{bmatrix} X(\lambda_1) \\ \Delta V(\lambda_1) \end{bmatrix} \tag{4.03}$$

where, $[\Delta V(\lambda_1)]$ is the right system bus voltage vector corresponding to the eigenvalue λ_1. A similar equation for the left eigenvector $[Z(\lambda_1)]$ as Equation (4.03) can be derived as,

$$[\lambda_1\, Z(\lambda_1) \quad 0\ ] = \begin{bmatrix} A_{st} & B_{st} \\ C_{st} & -(Y_N + Y_{st}) \end{bmatrix}^T [Z(\lambda_1) \quad \Delta W(\lambda_1)] \tag{4.04}$$

where, $[\Delta W(\lambda_1)]$ is the left system bus voltage vector corresponding to the eigenvalue λ_1. Premultiplying Equation (4.03) by the row vector $[Z(\lambda_1) \quad \Delta W(\lambda_1)]$ gives,

$$\lambda_1\, Z(\lambda_1)\, X(\lambda_1) = [Z(\lambda_1) \quad \Delta W(\lambda_1)] \begin{bmatrix} A_{st} & B_{st} \\ C_{st} & -(Y_N + Y_{st}) \end{bmatrix} \begin{bmatrix} X(\lambda_1) \\ \Delta V(\lambda_1) \end{bmatrix}$$

$$\tag{4.05}$$

The product of the right and left eigenvectors for a eigenvalue is unity as described in Appendix (A1.8). i.e.

$$Z(\lambda_1)\, X(\lambda_1) = 1.0 \tag{4.06}$$

Taking the partial derivative of the eigenvalue λ_1 with respect to the shunt admittance at the jth bus (y_{jj}) in Equation (4.05), and using the relation of Equation (4.06) gives,

$$\frac{\partial \lambda_1}{\partial y_{jj}} = - \Delta W_{(j)} \, \Delta V_{(j)} \qquad (4.07)$$

where, $\Delta W_{(j)}$ is the jth element (the jth bus left voltage) in the left voltage vector $[\Delta W(\lambda_1)]$ and $\Delta V_{(j)}$ is the jth element (the jth bus right voltage) in the right voltage vector $[\Delta V(\lambda_1)]$. Equation (4.07) is the sensitivity of the eigenvalue λ_1 to the change in shunt admittance at the jth bus.

Taking the partial derivative of the eigenvalue λ_1 with respect to the series admittance between the jth bus and the kth bus (y_{jk}) in Equation (4.05), and using the relation of Equation (4.06) gives,

$$\frac{\partial \lambda_1}{\partial y_{jk}} = - \Delta W_{(j)} \, \Delta V_{(k)} \qquad (4.08)$$

The L.H.S of Equations (4.07) and (4.08) are called the voltage participation factors.

4.3   Observability of eigenvalues in system signals

An important consideration in the choice of suitable feedback signal for damping control is that it should contain adequate information about the mode being damped. Alternatively, it can be said that the mode under consideration should be 'observable' in the signal being chosen. The concept of observability as described in control theory can, therefore, be used for the selection of the appropriate feedback signal. The calculation of

observability of eigenvalues (modes) in various signals, determines in a qualitative and quantitative manner the amount of information a signal has of the system eigenvalues. The method of calculating the observability of eigenvalues in various signals is described below.

Any signal present in the system can be expressed as a function of the system states [X] as described by Equation (3.16), which is reproduced here,

$$y = \{ [R] + [S] [Y_N + Y_{st}]^{-1} [C_{st}] \} [X]$$

Transforming the above equation into the Laplace (complex frequency) domain gives,

$$y(s) = \{ [R] + [S] [Y_N + Y_{st}]^{-1} [C_{st}] \} [X(s)] \tag{4.09}$$

Let λ_1 be an eigenvalue under consideration, and $[X(\lambda_1)]$ be the corresponding eigenvector. Then, the observability of the monitored signal (y) to this eigenvalue λ_1, is given by,

$$y(\lambda_1) = \{ [R] + [S] [Y_N + Y_{st}]^{-1} [C_{st}] \} [X(\lambda_1)] \tag{4.10}$$

Similarly the observability of the monitored signal (y) to all the system eigenvalues can also be calculated using the right eigenvector matrix [P] as,

$$[Yo] = \{ [R] + [S] [Y_N + Y_{st}]^{-1} [C_{st}] \} [P] \tag{4.11}$$

where, [Yo] is a column vector and the ith element in it is the observability of the monitored signal (y) to the ith eigenvalue of the system.

4.4   Small signal stability assessment using modal torque calculations

In an effort to improve the small signal stability of the power system it is necessary to understand the mechanism by which various power system components (excitation systems of generator, voltage regulators of SVC etc.) influence the small signal stability. In the past the explanation of these mechanisms have been addressed in a qualitative manner [2,7,13,17,19]. This can help to predict the approximate behavior of a component with regard to its effect on the system small signal stability. However, a quantitative idea about the effect of various components on system small signal stability would greatly benefit the design of various controls.

The quantitative assessment of the effect of power system components on the system small signal stability can be made on the basis of determination of the torque contribution from the individual component for each mode of oscillation. This torque contribution is called the modal torque. The modal torque has two components, the damping and the synchronizing torque. The damping torque indicates the inherent damping the system has for the mode (eigenvalue) under consideration. The synchronizing torque conveys the ability (strength or 'stiffness') of the system to restore itself to a steady state operating point after a disturbance. To understand the basic concept of how the modal torque governs the

characteristics of these modes, a description of the generation of electromechanical modes of oscillation and the corresponding torques is necessary.

4.4.1 Generation of electromechanical modes and associated torques

Electromechanical oscillations are produced by the interaction between the torques applied to the rotating system of the generators. To illustrate this, consider the single machine infinite bus system shown in Figure (4.1). The synchronous machine is modelled as a voltage source (E_q') behind a transient reactance (x_d') assuming that the field flux linkages are constant. The machine is connected to an infinite bus having voltage E_o through an external reactance (x_e).
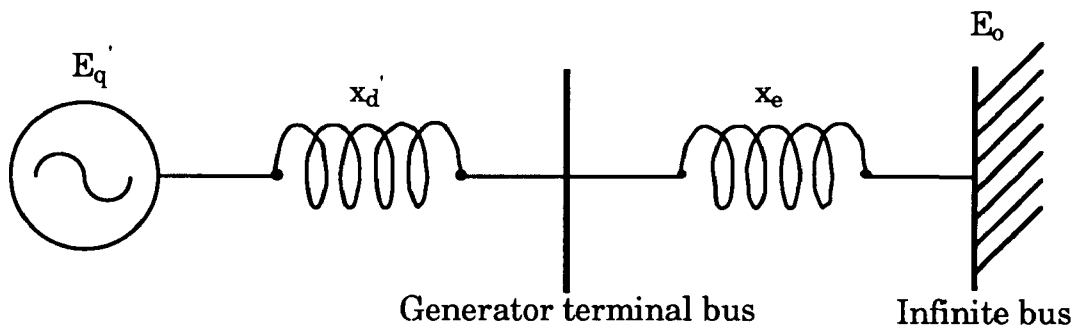
Figure (4.1): Single machine infinite bus system

The machine dynamics can be expressed as,

$$\frac{2H}{\omega_0}\frac{d\Delta\omega}{dt} + \frac{D}{\omega_0}\frac{d\Delta\delta}{dt} + K_1\Delta\delta = 0 \qquad (4.12)$$

where, D is the damping coefficient (p.u.) and the synchronizing coefficient (K_1) is given as,

$$K_1 = \frac{\partial T_e}{\partial \delta_o} = \frac{E_q' E_0}{x_d' + x_e} \cos\delta_o$$

where, δ_o is the steady state angle between E_q' and E_o in Figure (4.1) and T_e is the electrical torque. Equation (4.12) is in per unit quantities and hence; Per unit torque = Per unit power. Equation (4.12) can be transformed into the Laplace domain and can be represented in the block diagram structure as shown in Figure (4.2).
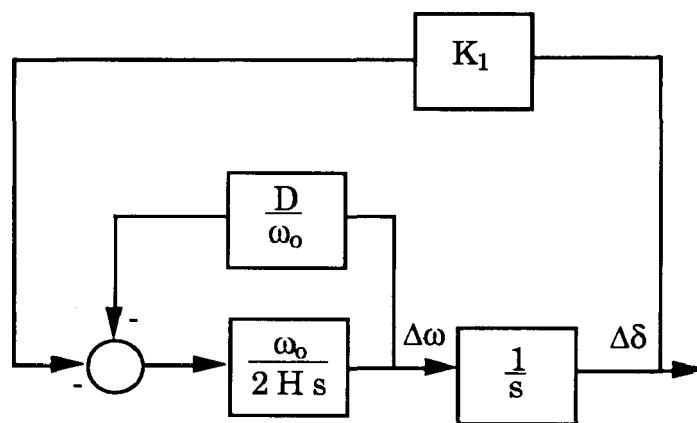
Figure (4.2): Block diagram of the single machine infinite bus system

The roots of the characteristic equation of Equation (4.12) are,

$$s_1, s_2 = -\frac{D}{4H} \pm \sqrt{\frac{D^2}{16H} - \frac{K_1 \cdot \omega_0}{2H}} \qquad (4.13)$$

Generally $\frac{D^2}{16H} << \frac{K_1 \omega_0}{2H}$, which leads to an oscillatory response. The oscillatory response of the system is attributed to the imaginary part of the roots given in Equation (4.13). This oscillation is called the electromechanical mode of the system. Examining Equation (4.12), it is evident that the torque applied to this machine is,

$$\Delta T_m = \frac{D}{\omega_0} \Delta\omega + K_1 \Delta\delta \tag{4.14}$$

This torque is also called the modal torque for the mode (eigenvalue) corresponding to the roots of the characteristic equation (Equation (4.13)). The modal torque has two components, which are,

i)Damping torque $(\frac{D}{\omega_0} \frac{d\Delta\delta}{dt} = \frac{D}{\omega_0} \Delta\omega)$: A positive value of the damping coefficient indicates that the oscillation will eventually decay, while a negative value indicates that the oscillation will rise in magnitude i.e the system is unstable. A measure of the small signal stability of the system is indicated by the amount of damping torque present in the system.

ii)Synchronizing or restoring torque $(K_1 \Delta\delta)$: This torque tends to bring the system back to the steady state operating point. A higher value of the synchronizing coefficient K_1, which is positive, indicates the strength or 'stiffness' of the system. Higher the 'stiffness', the better is the ability of the system to achieve steady state. A measure of the relative transient stability of the system is indicated by the amount of synchronizing torque present in the system.

4.4.2 Calculation of modal torques for multimachine power systems

In the case of the simple single machine infinite bus system considered above, the electromechanical oscillation can be examined through the interaction of only two states $\Delta\omega$ (small changes in speed) and $\Delta\delta$ (small changes in the rotor angle) as shown in Figure (4.1). However in a large complex system, the electromechanical oscillations would be influenced by the dynamic interaction of the other states corresponding to the various machines, SVC, HVDC etc. This calls for appropriate modelling of the various system components. The complexity of the system model would depend upon the degree of detail considered in the representation of each subsystem. A typical block diagram of such a large system is shown in Figure (4.3). Where, $\Delta\omega_m$ and $\Delta\delta_m$ are the small changes in the mth machine speed and machine angle. Figure (4.3) illustrates the dynamic interaction between the mth machine and the rest of the system which is represented by the equivalent transfer function G(s). The effect of the mth machine on the equivalent system G(s) is represented through the inputs $\Delta\omega_m$ and $\Delta\delta_m$. The output of G(s) is ΔT_m. ΔT_m is the torque contribution from the rest of the system applied to the mth machine. This torque can be split into two components; one in phase with $\Delta\omega_m$ and the other in phase with $\Delta\delta_m$. The component in phase with the small changes in speed of the mth machine ($\Delta\omega_m$) will tend to damp out the electromechanical modes of oscillation in which this machine participates, whereas the component in phase with the small changes in rotor angle for

the mth machine ($\Delta\delta_m$) will tend to restore the system to its steady state operating point.
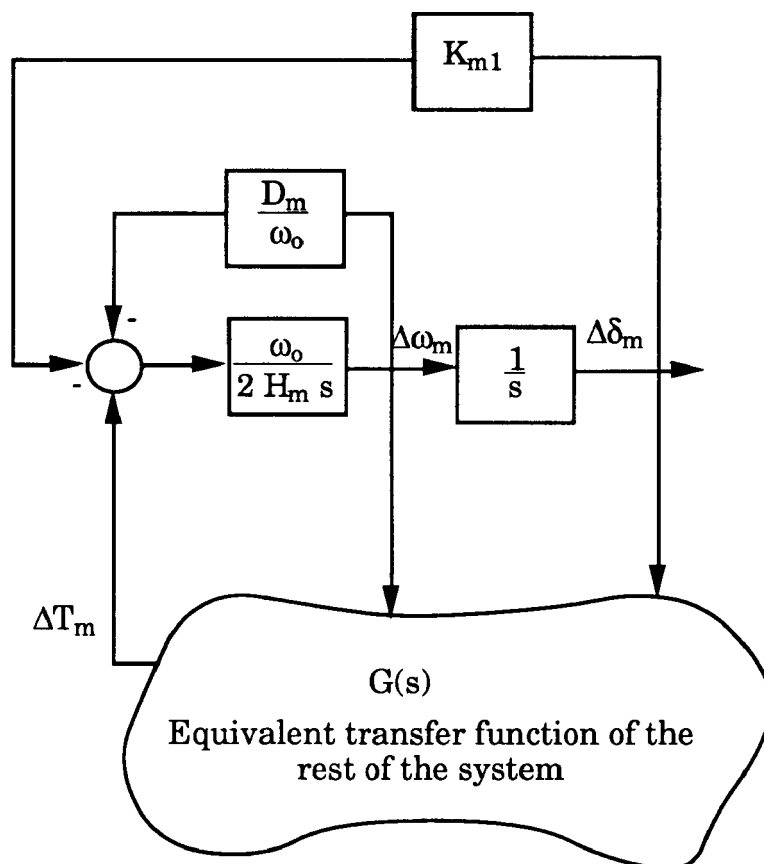
Figure (4.3): The dynamics of the mth machine in a large power system

Having identified the electromechanical mode of interest and its participating machines, the corresponding modal torque and hence the constituent damping and synchronizing torques can be calculated as illustrated below.

Consider a local mode of electromechanical oscillation as initiated from the mth generator. Let this mode of oscillation correspond to the kth eigenvalue (λ_k) of the system. Since the mode under consideration is the

local mode associated with the mth machine, only the modal torque for the mode λ_k applied to this machine need to be calculated. From the calculation of the modal torque, the damping and synchronizing torques can also be calculated.

For the mth machine, its modal acceleration corresponding to the mode λ_k is,

$$\Delta\dot{\omega}_m = \sum_1^n a_{ji}\, x_i \qquad (4.15)$$

where, n is the size of the state matrix [A], a_{ji} is the ith element in the jth row of the state matrix [A], the $\Delta\omega_m$ state of the mth machine is the jth element in the state vector and x_i is the ith element in the eigenvector of [A] corresponding to the mode λ_k.

Therefore the corresponding modal torque applied to the mth machine is,

$$\Delta T_m = -\frac{2\,H_m}{\omega_0} \sum_1^n a_{ji}\, x_i \qquad (4.16)$$

where, H_m is the inertia constant (p.u.) of the mth machine.

The modal torque ΔT_m is a complex quantity. It has a component in phase with $\Delta\omega_m$ (damping torque), and another component in phase with $\Delta\delta_m$ (synchronizing or restoring torque) as shown in Figure (4.4). Note that $\Delta\omega_m$ and $\Delta\delta_m$ are orthogonal due to the fact that

$$\Delta \omega_m = \frac{d\Delta \delta_m}{dt} \qquad\qquad (4.17)$$

The damping and synchronizing torque components of the modal torque can be determined if the angle θ (refer Figure (4.4)) is known. The eigenvector corresponding to the mode λ_k will have elements corresponding to $\Delta \omega_m$ and $\Delta \delta_m$. These elements which are complex quantities give the magnitude and angle of $\Delta \omega_m$ and $\Delta \delta_m$ with respect to a fixed reference. Also, the angle information contained in the complex quantity ΔT_m is with reference to the same fixed reference. Thus the angle θ can be obtained accordingly to calculate the modal torque components.
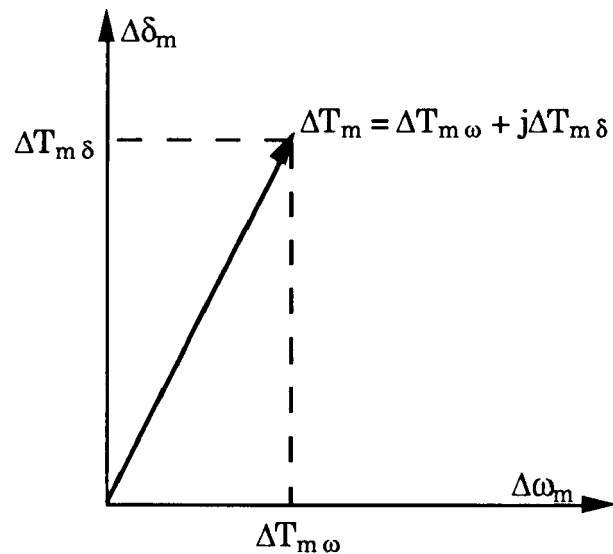
Figure (4.4) Modal torque components

In certain situations, there may be a need to determine the modal torque (and hence, the damping and synchronizing torque) contribution from a particular device (e.g. SVC or HVDC, excitation systems, voltage

regulators, etc) for a particular mode of electromechanical oscillation (eigenvalue). This can be easily obtained by modifying Equation (4.18). Suppose in the example considered above, the interest lies in determining the effect of a jth device on the local mode (λ_k). The modal torque contribution ΔT_{mj} from the jth device to m^{th} machine for the local mode (λ_k) is given as,

$$\Delta T_{mj} = -\frac{2\,H_m}{\omega_0} \sum_{j1}^{jj} a_{ji}\, x_i \qquad (4.18)$$

where, the limits j1 to jj denote the locations of the corresponding states of the jth device in the state vector.

In the above discussions we have considered a local mode and hence the modal torque contribution to only one machine was determined. For inter-area and inter-machines modes of electromechanical oscillations, the modal torques applied to more than one machine will have to be determined. This process will be a simple extension of the above method as shown below.

Let the eigenvalue λ_{k1} be an interarea mode of oscillation and the synchronous machines participating in this mode be m_1, m_2, m_3, . . . m_m. The modal torque ΔT_{kM} applied to the Mth participating machine for the interarea mode λ_{k1} is,

$$\Delta T_{k1M} = - \frac{2 H_M}{\omega_0} \sum_1^n a_{Ji} x_i \qquad (4.19)$$

where,

$M = m_1, m_2, m_3, \ldots m_m$.

H_M = Inertia constant in (p.u) of the Mth machine.

a_{Ji} = the ith element in the Jth row of the system state matrix [A].

The $\Delta\omega_M$ state of the Mth machine is the Jth element in the state vector

The modal torque contribution ΔT_{k1Mj} from the jth device to the Mth participating machine for the interarea mode λ_{k1} is

$$\Delta T_{k1Mj} = - \frac{2 H_M}{\omega_0} \sum_{j1}^{jj} a_{Ji} x_i \qquad (4.20)$$

The limits j1 to jj denote the locations of the corresponding states of the jth device in the state vector.

The analysis of the modal torque contributions for the intermachine and interarea modes is accomplished by determining the the damping and synchronizing torque contributions to each machine separately.

4.4.3 Modal torques : A discussion

The proposed method provides a systematic approach for calculating the modal torque contribution of any device for the electromechanical mode under consideration. This serves as a tool for evaluating the effect of various devices on damping electromechanical modes of oscillation. In the past this effect has been qualitatively determined for complex systems based on either extrapolation of the effect obtained in case of simple systems or through field experience. The proposed method, on the contrary, provides a mathematical basis for evaluating modal torque components which give a measure of the system small signal and transient stability. Further work needs to be done in the nondimensionalizing the torque calculations so that effective comparisons of different case studies can be accomplished. At present these torque calculations can be compared on a percentage basis of their damping and synchronizing torque contributions.

Chapter 5

Design of Damping Control

5.1   General

In this chapter the generalized procedure for the design of damping control for a power system is presented. The objective of installing damping controllers is to damp those electromechanical modes of oscillations which are otherwise poorly or negatively damped. A beneficial side effect of the use of damping controls is the possibility for the system to increase its steady state power transfer capability. This is so, because the damping control allows the system to operate at certain operating conditions which may correspond to higher levels of power transfer; which in the absence of the damping control would not have been possible. It is also important that the damping control should not adversely effect the transient stability of the system.

5.2   Generalized design procedure

The process of designing the damping control involves the following steps:

a)Identification of the least damped electromechanical mode of oscillation.

b)Determination of the damping and synchronizing torques present in the system for the least damped mode of oscillation.

c)Selection of the site for installing the damping control.

d)Selection of suitable feedback signal for the damping control.

e)Design of the compensation network i.e. determining the parameters of the damping control transfer function.

f)Validation of the design.

5.2.1 Identification of the least damped electromechanical mode of oscillation

The foremost requirement is to know whether damping control is at all needed for the power system under consideration or not. To obtain this information, the eigenvalues of the state matrix of the power system are obtained and the corresponding damping ratio for each eigenvalue associated with the electromechanical mode (0.5 to 2.5 Hz.) is evaluated. Unlike conventional control systems where one would ideally require the dominant pole to have a damping ratio of 0.707; a minimum damping ratio of 0.05 for the electromechanical mode is quite acceptable in power systems. It may however so happen that within the range of 0.5 to 2.5 Hz. there may be some modes which do not necessarily correspond to the electromechanical modes of oscillation. The eigenvalues corresponding to the electromechanical modes of oscillation of the system are identified by the determination of the state participation factors for each eigenvalue.

Those eigenvalues for which the state participation factors of the $\Delta\omega$ states of the synchronous machines are largest are taken as the electromechanical modes. The state participation factors and the mode shapes of these electromechanical oscillations are used to determine whether these modes are local, intermachine or interarea oscillations. The concept and use of the state participation factors and eigenvectors (mode shapes) is given in Chapter 3.

5.2.2 Determination of the damping and synchronizing torques present in the system

Once the least damped electromechanical mode of oscillation is identified, the damping and synchronizing torque present in the system for this electromechanical mode of oscillation is determined. The method of calculating the damping and synchronizing torques has been explained in detail in Chapter 4. The calculation of the damping and synchronizing torques helps to evaluate the effectiveness of the damping control after it is incorporated into the system.

5.2.3 Selection of the site for the location of the damping control

It is very important to choose the proper site for the location of the damping control. Improper selection of the site for damping control will require the damping control to have a large control effort in order to provide

damping for the concerned electromechanical mode of oscillation. It will lead to the damping control being overaggressive and thus detrimental to transient stability [17]. There may also arise situations where the parameters of a improperly located damping control are physically unrealizable.

The selection of a suitable location of the damping control on a device is based on the controllability of the device and the observability of the feedback signal for the electromechanical mode whose damping is to be enhanced. The controllability of a device to a particular mode is determined through the use of state and voltage participation factors. Voltage participation factors supplement the information obtained from the state participation factors for the selection of a suitable site for damping control.

The potential site of the damping control must be chosen on the basis of controllability and observability of the mode of interest, for the damping control and its feedback signal respectively. The calculation of the observability factors presented earlier is used to determine the observability of eigenvalues (modes) present in various signals under consideration. From the control system design considerations it is important that the feedback signal should not exhibit non minimum phase behavior near the frequency of the mode of interest [18].

A natural location for installing the damping control is the synchronous machine since it is itself the source of electromechanical oscillations. For local and intermachine modes the choice of location for

installing the damping control is, therefore, quite straightforward as explained below.

The criteria for selecting the device (synchronous machine) for installing the damping control is based on a sensitivity index called the state participation factor which has been described in Chapter 3. A machine which has a significantly large state participation factor of its $\Delta\omega$ state to the mode under consideration and also, a large rating is chosen for the location of the damping control which is called the Power System Stabilizer (PSS). The same procedure can be adopted for the selection of a synchronous machine for installing the damping control to damp out interarea modes. But in some situations it may be difficult to identify one machine for the installation of damping control, either, due to the fact that there might exist many machines of similar rating having significant state participation factors of their $\Delta\omega$ states making it difficult to select between them; or , some other considerations might make the installation of a PSS on a synchronous machine unattractive. In such a situation, it may be worthwhile to consider installation of the damping control on devices like SVC which may be present in the system. To know how effectively can SVC damp out interarea modes, the analysis of state participation factors will require the representation of the SVC supplementary control (damping control). But then, the problem is that the supplementary control is yet to be designed. To explore the possibility of installing a damping control on a SVC, another sensitivity index called the voltage participation factor may be used.

Voltage participation factors can be used to supplement the information obtained from the state participation factors for the selection of a suitable site for damping control. As voltage participation factor of the system bus is the sensitivity of the eigenvalue to the change in shunt admittance at the corresponding bus, it can form a basis for the selection of the SVC to be equipped with the damping control (Supplementary Control). The basic concepts of voltage participation factor is described in Chapter 4.

For electromechanical modes of oscillation the analysis of the sensitivity indices i.e. state and voltage participation factors will generally identify devices and system buses in close proximity as potential sites for the installation of damping control. In the case of local and intermachine modes as described earlier, a candidate synchronous machine is selected for the installation of the PSS. For interarea modes the analysis of the state participation factors will identify certain candidate synchronous machines as the site for the location of PSS, whereas the analysis of the voltage participation factors will identify certain candidate buses, where a SVC equipped with a damping control (supplementary control) would probably damp the interarea mode under consideration. The choice of selecting the site for installing the damping control on a synchronous machine or SVC will depend on transient stability and economic considerations. Even though interarea modes are generally adequately damped by the use of PSS, the use of damping control (Supplementary control) on SVC provides a viable option that can be used under certain conditions.

The selection of site should also take into consideration the availability of suitable feedback signals which would contain adequate information of the mode under consideration. This can be derived based on the observability criteria described in Chapter 3.

In addition to the analytical procedure outlined above, practical considerations must also be taken into account while selecting the site for damping control. For example, if the state participation factors indicate that a particular synchronous machine is suitable for the installation of a PSS and if this synchronous machine happens to be equipped with a slow acting exciter, then the control effort required by the PSS may be enormous. Under such a situation the option is either to change the exciter itself or select the next best location for installing the damping control.

5.2.4 Selection of a suitable feedback signal for the damping control

A primary requirement of a suitable feedback signal is that it should contain adequate information about the mode of oscillation which is to be damped. For this, it is necessary to calculate the observability of eigenvalues (modes) present in various signals under consideration, as described in Chapter 4. This provides the information about the presence of the mode of interest in a particular signal and its selectivity. By selectivity it means how the signal is influenced by eigenvalues other than the one that is to be damped. If the calculation of observability of system eigenvalues for the signal under consideration shows that this signal has a

high observability of not only of the mode of interest but another eigenvalue whose frequency is close to that of the mode of interest, then this signal is not a good choice for a suitable feedback signal. Based on this information, the suitable feedback signal can be chosen for damping purposes. However it is important that the output of the damping control should not strongly influence the feedback signal. Otherwise a positive feedback situation will arise which may lead to an unstable inner loop.

From the control system design considerations it is important that the feedback signal should not exhibit non minimum phase behavior near the frequency of the mode of interest [18]. In a complex power system however, this cannot be avoided, but it is possible to select a signal which does not exhibit non minimum phase behavior near the mode of interest. Whether a signal exhibits non minimum phase behavior or not can be determined by obtaining a frequency response of the signal with respect to the point where the damping control output is to be applied. If the frequency response shows a sharp dip in the magnitude response accompanied by sudden dip in phase by 180 degrees as frequency is scanned upwards, it can be concluded that there is a zero in the right half plane close to the imaginary axis of the s-plane which is the condition for a nonminimum phase behavior.

From a practical point of view the feedback signal should be easily available, i.e local signals are preferred and should exhibit good noise immunity.

5.2.5 Design of the compensation network

In this section the realization of the structure of the damping control is described. The general structure of the damping control consists of lead or lag networks in series with a gain and a washout term. The washout term is needed so that the damping control is active only when there are changes in the feedback signal applied to the damping control and thus keeping the damping control inactive under steady state conditions. The design procedure adopted here is a pole placement technique using the residue method as described below [10].

Figure (5.1) shows the interconnection between the power system G(s) and the damping control H(s). u(s) is the input to the system and y(s) is the desired feedback signal for the damping control (such as speed, line current magnitude, line real power etc.).
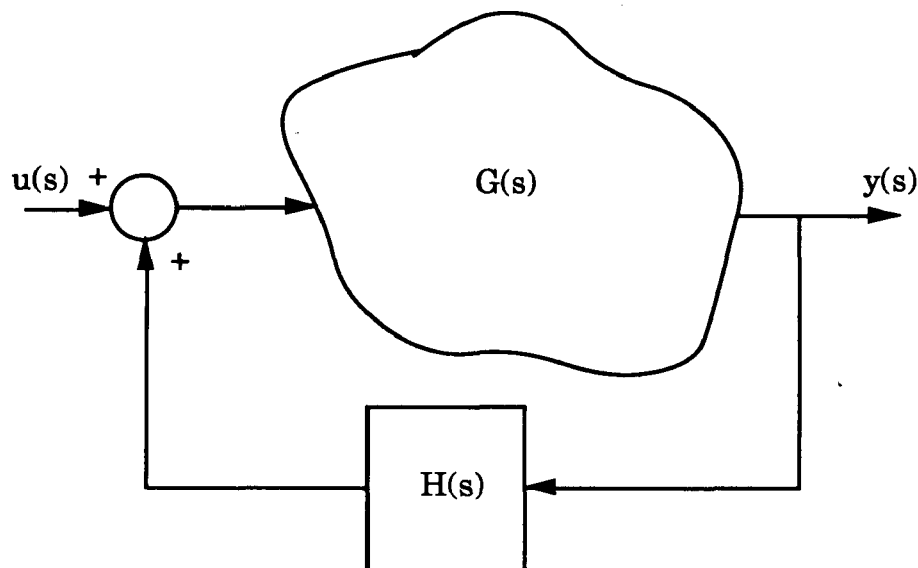
Figure (5.1): Block diagram of system G(s) and damping control H(s).

Let the electromechanical mode of oscillation (eigenvalue) whose damping is to be improved be λ_{old}. λ_{old} corresponds to one of the poles of the transfer function G(s). The requirement is to shift this eigenvalue (pole) to a new location λ_{new}. This is accomplished by the addition of the damping control H(s). The characteristic equation for the system shown in Figure (5.1) is

$$| 1 - G(s)\,H(s) | = 0 \qquad\qquad (5.01)$$

If H(s) has been properly realized then $s = \lambda_{new}$ will satisfy the above characteristic equation i.e.

$$| 1 - G(\lambda_{new})\,H(\lambda_{new}) | = 0 \qquad\qquad (5.02)$$

This implies that

$$H(\lambda_{new}) = \frac{1}{G(\lambda_{new})} \qquad\qquad (5.03)$$

and

$$| H(\lambda_{new}) | = \frac{1}{| G(\lambda_{new}) |} \qquad\qquad (5.04)$$

$$\angle H(\lambda_{new}) = -\angle G(\lambda_{new}) \qquad\qquad (5.05)$$

where, $|H(\lambda_{new})|$, $\angle H(\lambda_{new})$ and $|G(\lambda_{new})|$, $\angle G(\lambda_{new})$ are the magnitudes and phase of $H(\lambda_{new})$ and $G(\lambda_{new})$ respectively.

Equations (5.04) and (5.05) give respectively the magnitude and phase criterion. $G(\lambda_{new})$ is the residue of the transfer function $G(s)$ at $s = \lambda_{new}$. Once this is obtained then it is possible to determine the transfer function $H(s)$ satisfying the magnitude and phase criterion. This is the basic principle for the design of damping control using the residue method. The procedure for the calculation of residues is given in Chapter 3.

Certain innovations in the realization of $H(s)$ are described next to ensure that the designed damping control is robust and also enhances the 'stiffness' of the system to increase the transient stability margin of the system.

Selection of the new location of the eigenvalue (λ_{new}) :

The original eigenvalue (electromechanical mode of oscillation) λ_{old} has to be shifted to a new location to increase its damping. Defining the original eigenvalue as,

$$\lambda_{old} = \alpha_o + j\beta_o \tag{5.06}$$

The damping ratio for this eigenvalue is

$$\zeta = \frac{-\alpha_o}{\sqrt{\alpha_o^2 + \beta_o^2}} \qquad (5.07)$$

The damping ratio can be increased by:

i)Keeping α_o constant and decreasing the magnitude of β_o, or

ii)Keeping β_o constant and making α_o more negative, or

iii)Increasing the negative value of α_o and the magnitude of β_o ensuring that the resultant damping ratio is also increased.

The third option for increasing the damping ratio is considered here as it not only increases the damping of the mode of interest but also increases the 'stiffness' of the system for this mode as explained below with reference to the single machine infinite bus system shown in Figure (4.2) of Chapter 4. Neglecting the damping, the system dynamics is expressed as,

$$\frac{2H}{\omega_o} \frac{d\,\Delta\omega}{dt} + K_1\,\Delta\delta = 0 \qquad (5.08)$$

where, H is the inertia constant of the machine (p.u), K_1 is the synchronizing coefficient of the machine, $\Delta\omega$ and $\Delta\delta$ are small changes in the angular velocity of the synchronous machine (radians/sec) and small changes in the rotor angle (radians) respectively. The rotor angle is defined as the angle between the machine direct axis and the synchronously rotating reference frame of the system. The roots of the characteristic Equation of (5.08) are

$$s_1, s_2 = \pm \sqrt{\frac{-K_1 \omega_0}{2H}} \qquad (5.09)$$

It is evident that the frequency of oscillation is directly proportional to $\sqrt{K_1}$. Thus, if K_1 increases so does the frequency of the electromechanical mode of oscillation. Also, as described in Chapter 4, an increase in the value of K_1 corresponds to the increase in the 'stiffness' of the system, which increases the transient stability margin of the system. A similar observation can be made in case of large complex systems also.

The location of the old eigenvalues in the s-plane is shown in Figure (5.2). The shaded portion indicates the possible region for the new eigenvalue which would result in increased damping and 'stiffness'. The final location to which the original eigenvalue can be shifted is determined after ensuring that;

i)the damping control is not over aggressive (Gain is not too large),

ii)the damping control is physically realizable,

iii)the damping control does not deteriorate the damping of other modes or introduce new eigenvalues which are unstable, and

iv)the designed damping control provides adequate damping over a range of operating conditions.
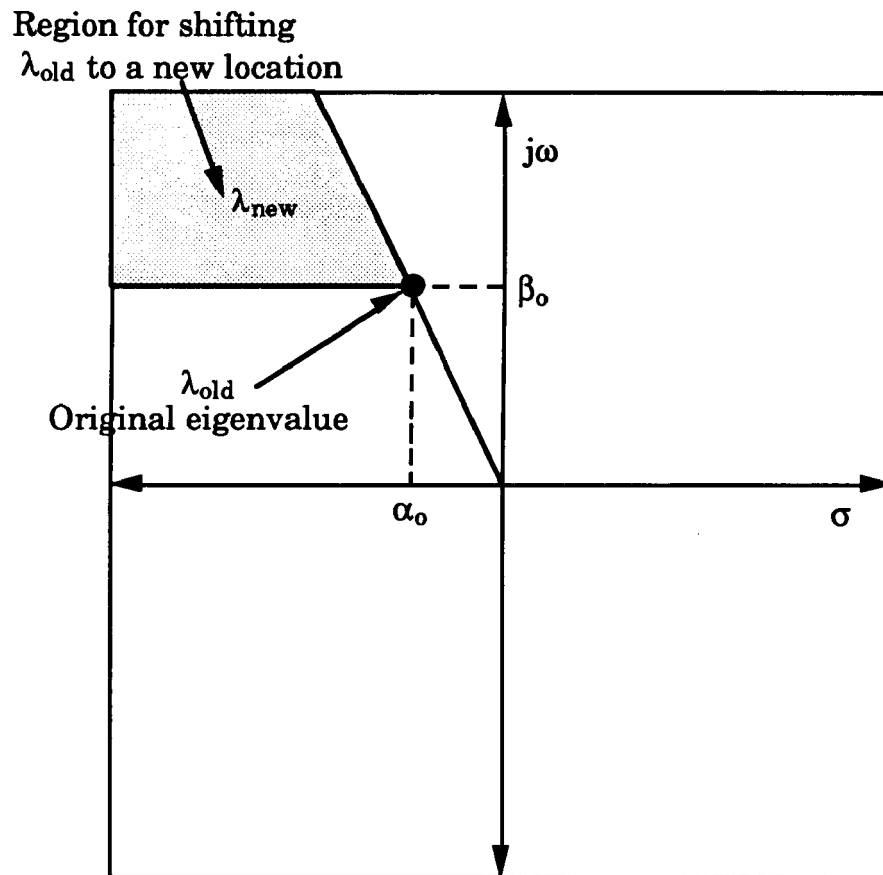
Figure (5.2): Area to shift eigenvalue

Realization of the transfer function H(s):

The general structure of the damping control consists of a series of lead, lag blocks with a washout block and a gain block as shown in Figure (5.3).

$$\Delta Sig \xrightarrow{\quad} \boxed{K} \xrightarrow{\quad} \boxed{\dfrac{1 + sT_1}{1 + sT_2}} - - \rightarrow \boxed{\dfrac{sT}{1 + sT}} \xrightarrow{\quad} \Delta v_{so}$$

Gain block   lead/lag block   Washout block
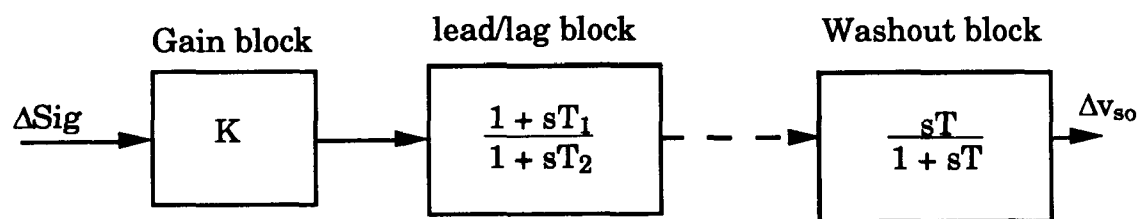
ΔSig = Feedback signal to the damping control

Δv_{so} = Damping control output

K = Gain

$T_1, T_2, \ldots T$ = Time constants.

Figure (5.3): Block diagram of damping control

The washout block must act as an all pass to signals at frequencies of interest (frequencies of the modes of interest). As electromechanical oscillations have a very low frequency, the washout time constant (T) is kept quite large (around 10 seconds). A large time constant is necessary to avoid causing phase leads at the low end of the frequency spectrum [6].

The requirement of the damping control transfer function H(s) is that it must satisfy the magnitude and phase criteria given in Equations (5.04) and (5.05) respectively. From Figure (5.3) H(s) can be rewritten as

$$H(s) = \frac{sT}{1 + sT} \, K \, h(s). \qquad\qquad (5.10)$$

where, h(s) represents the transfer function of the cascaded lead or lag blocks. The washout time constant (T) is chosen as 10 seconds for the reasons given earlier. The problem now is to realize h(s) which can be accomplished as follows:

i)From the knowledge of the total phase compensation required, $\angle G(\lambda_{new})$, the total number of lead or lag blocks can be determined. Generally the maximum phase compensation which one lead or lag block can provide is approximately 60 degrees. An attempt to achieve higher phase compensation from one block may result in undesirably large pole-zero separation. From practical considerations, a limit of say three to four blocks can be imposed on the total number of cascaded lead or lag blocks to be used. In case more blocks are required to achieve the desired phase compensation, it would be better to look for other alternative solutions to increase the damping of the mode of interest. These solutions could be in the form of a new eigenvalue location, or a different feedback signal or a different device for installing the damping control.

ii)Having determined the number of lead or lag blocks necessary to achieve the desired phase compensation, the various time constants for each lead or lag block are calculated. The requirements are:

a)The frequency at which all the lead or lag blocks together provide maximum phase compensation should be close to the frequency corresponding to the new eigenvalue location [9,10].

b)The following phase criterion obtained from Equations (5.05) and (5.10) should be satisfied.

$$\angle h(\lambda_{new}) = -\angle \frac{\lambda_{new}T}{1 + \lambda_{new}T} - \angle G(\lambda_{new}) \tag{5.11}$$

The method of determining the time constants for each lead or lag block is illustrated through an example. Figure (5.4) shows the block diagram of a hypothetical damping control. Here the washout time constant (T) is taken as 10 seconds and the number of cascaded lead or lag blocks are two.
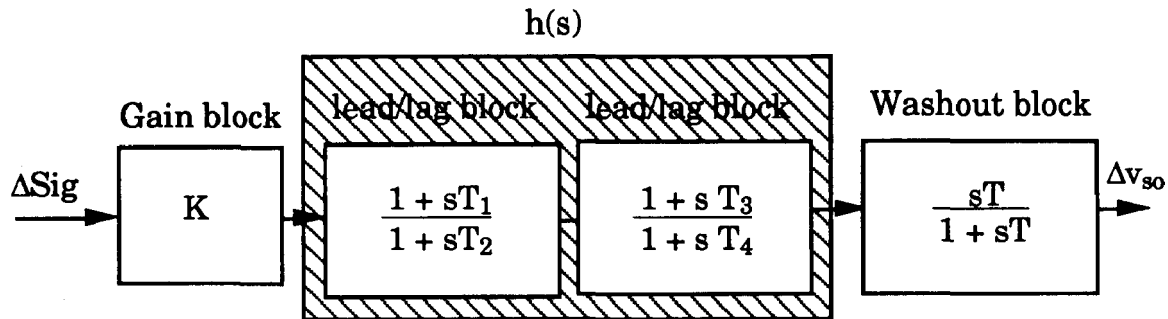
Figure (5.4): Example block diagram of damping control.

From Figure (5.4),

$$h(s) = \frac{1 + s\, T_1}{1 + s\, T_2} \frac{1 + s\, T_3}{1 + s\, T_4} \tag{5.12}$$

Generally the lead or lag blocks are taken to be identical. Hence, T_1 is the same as T_3 and T_2 is the same as T_4. Therefore,

$$h(s) = \left(\frac{1 + s\, T_1}{1 + s\, T_2}\right)^2 \tag{5.13}$$

Considering that the residue of the system transfer function G(s) at s= λ_{new} is already calculated, where, $\lambda_{new} = \alpha_n + j\beta_n$ is the new eigenvalue. The two criteria mentioned above that must be satisfied are

$$\beta_n = \frac{1}{\sqrt{T_1 \, T_2}} \tag{5.14}$$

$$\angle \left(\frac{1 + \lambda_{new} \, T_1}{1 + \lambda_{new} \, T_2} \right)^2 = - \angle \frac{\lambda_{new} T}{1 + \lambda_{new} T} - \angle G(\lambda_{new}) \tag{5.15}$$

Equations (5.14) and (5.15) are solved iteratively for T_1 and T_2. As shown earlier, the lead or lag blocks are generally taken to be identical, which leads to the determination of two unknowns from two equations. This results in a unique solution. In certain situations, where for example the damping control is being designed to satisfy the above criteria for two different operating conditions, it might be necessary to use lead or lag blocks which are not identical. In such a situation, a trial and error procedure combined with the above method will have to be used. This leads to a compromise solution where the frequency at which the damping control provides maximum phase compensation will not necessarily coincide with the frequency of the new eigenvalue or the phase criteria of Equation (5.05) may not be exactly satisfied. This results in the shifting of the mode of interest to a slightly different position than it was meant to be shifted to.

Once h(s) has been determined, it only remains to calculate the gain K of the damping control H(s). This can be calculated from the following expression which is obtained from (5.04) and (5.10).

$$K = \frac{1}{\left| \frac{\lambda_{new}T}{1 + \lambda_{new}T} \ h(\lambda_{new}) \right| \ \left| G(\lambda_{new}) \right|} \qquad (5.016)$$

In this way the entire damping control H(s) can be realized.

5.2.6 Validation of the design

The design of the damping control can be validated through small signal stability analysis. For this the damping control is introduced into the system model and the new system state matrix is obtained. The effectiveness of the damping control can be determined through:

i)Eigenvalue analysis: It must be ensured that the mode under consideration has been damped and that the damping control did not introduce any additional eigenvalue with poor damping or did not have a detrimental effect on the damping of the other modes.

ii)Determination of the damping and synchronizing torques: The damping control should result in higher damping and synchronizing torques for the mode under consideration.

5.3   Discussion

The design strategy employed here assumes that there is only one electromechanical mode of oscillation whose damping is to be increased. If there exists more than one mode whose damping is to be increased, then the design process may have to be repeated for each of the concerned electromechanical modes of oscillation. Studies to be presented later show that a proper design of the damping control will increase the damping of not only the electromechanical mode of oscillation for which it was designed, but would also increase the damping of other electromechanical modes of oscillation. Thus, enhancing the overall system small signal stability.

The design process described here explains the design strategy for one operating condition. For the design of damping control to meet the requirements of different operating conditions, the above design steps can be followed in parallel for all the operating points under consideration. This would lead to a damping control H(s) which can meet the requirements of the various operating conditions to a certain extent. In this process more weight is given to the parameters of H(s) obtained for the weakest system operating point (usually maximum loading condition).

A flow chart of the generalized design procedure formulated in this chapter is shown in Figures (5.5a) and (5.5b).

```
┌─────────────────────────┐
│  State space model of the │
│     power system          │
└─────────────────────────┘
            │
┌─────────────────────────┐
│ Eigenanalysis, state and voltage │
│ participation factor determination │
└─────────────────────────┘
            │
┌─────────────────────────┐       ┌──────────────────────────────┐
│ Any electomechanical    │  No   │ All electromechanical        │
│ modes whose damping is  │──────▶│ modes have damping           │
│ less than 0.02 ?        │       │ higher than 0.02 and hence    │
└─────────────────────────┘       │ there is no need to improve   │
            │ Yes                  │ the damping of any            │
            ▼                      │ electromechanical mode        │
┌─────────────────────────┐       └──────────────────────────────┘
│ Classify these modes into interarea, │            │
│ intermachine and local oscillations │        ┌────────┐
└─────────────────────────┘            │  Stop  │
            │                          └────────┘
┌─────────────────────────┐
│ Calculate the modal torques for │
│ these modes and on a percentage │
│ basis determine the damping and │
│ synchronizing torques for each  │
│ mode                            │
└─────────────────────────┘
            │                                    ┌────┐
            ▼                      No             │ X  │
┌─────────────────────────┐◀───────────────────◁─┘
│ Is the least damped mode │
│ an interarea oscillation ? │
└─────────────────────────┘
            │ Yes
┌─────────────────────────┐  No   ┌──────────────────────────────┐
│ Damping control is the  │──────▶│ Identify the machine         │
│ supplementary control   │       │ predominantly influencing     │
│ on a SVC                │       │ this mode                     │
└─────────────────────────┘       └──────────────────────────────┘
            │                                    │
┌─────────────────────────┐       ┌──────────────────┐
│ Shortlist the SVC's on which the │ │ Design PSS on    │
│ installation of supplementary control for │ │ this machine │
│ damping purpose shows promise, based on │ └──────────────────┘
│ the state and voltage participating factors │        │
└─────────────────────────┘                            │
            │                                           │
┌─────────────────────────┐                            │
│ Select potential feedback signals to the │          │
│ supplementary control for the shortlisted │         │
│ SVC's using the calculation of │                    │
│ observability and frequency response │              │
└─────────────────────────┘                            │
            │                                           │
┌─────────────────────────┐                            │
│ Design supplementary control │              ┌────┐  │
│ for the SVC which shows the │────────────────│ Z  │◀─┘
│ best combination of site and │             └────┘
│ feedback signal selection │
└─────────────────────────┘
```

Figure (5.5a): Flow chart for generalized design of damping control
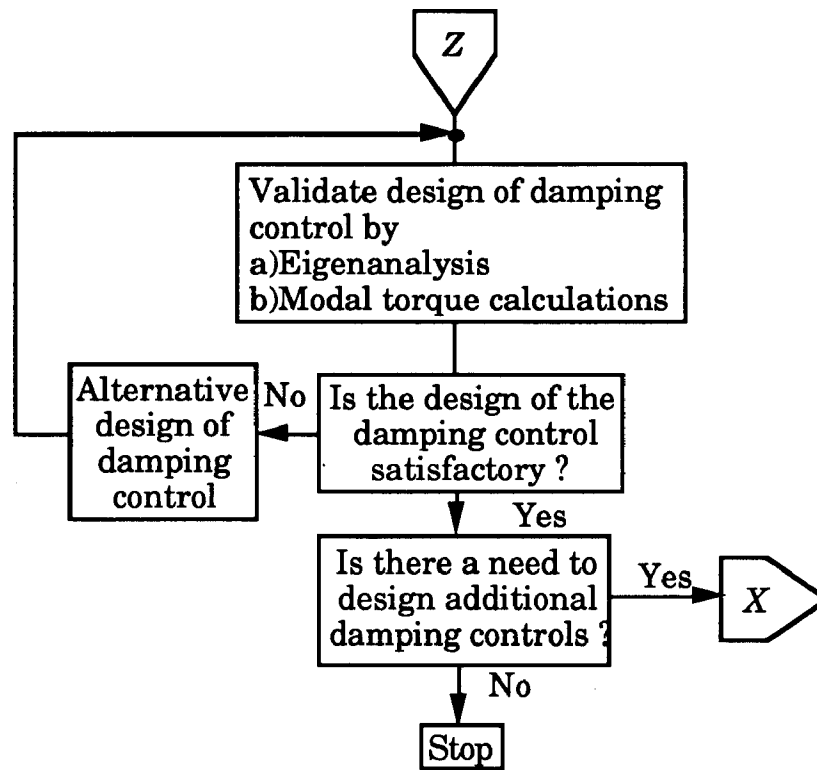
Figure (5.5b): Flow chart for generalized design of damping control (Contd).

Chapter 6

Program Development and System Studies

6.1   General

The state space representation of power system for small signal stability analysis has been described in Chapter 2. Based on this a state-of-the-art program -the Small Signal Stability (S^3) programme- has been developed incorporating the techniques for small signal stability investigations and design of damping control outlined in the earlier chapters [25]. A brief description of the structure and salient features of the S^3 program is given in this chapter. To illustrate this programs capability and to demonstrate the effectiveness of the small signal stability analysis techniques and the generalized philosophy of damping control design, a case study of a 39 bus power system is also presented. Damping control is designed for SVC (supplementary control) as well as the generating system (PSS) and their relative performances are compared.

6.2   Small Signal Stability (S^3) program

The Small Signal Stability (S^3) program has been developed with a modular structure, with each device model or subsystem described in a

separate subroutine. Based on the modelling procedure described in Chapter 2, the program proceeds systematically to formulate the linearized state space model of the individual dynamic devices which are then stacked together and interconnected through the transmission model to result in the overall system model.

The flow chart describing the structure of the S^3 program is given in Figures (6.1a) to (6.1e). The program requires two inputs, one defining the steady state operating point of the system about which the linearized system model is formulated, and the other defining the dynamic parameters of the system devices. The steady state operating point of the power system under consideration is given by its load flow solution. The dynamic parameters of the system devices which are required for the stability investigations correspond to the relevant device data including the associated control system parameters.

Using these inputs the individual device state space models are first formulated and then assembled in a systematic manner to derive the entire power system state space model as shown in Figures (6.1a) and (6.1b). The specific details of formulating the classical machine model, detailed generating system model and the SVC model are given in the flow charts shown in Figures (6.1c) to (6.1e) respectively.

```
                    ┌─────────────────┐
                    │      Start      │
                    └─────────────────┘
                            │
          ╱─────────────────────────────────╱
         ╱  Input solved load flow data defining ╱
        ╱    the system operating point       ╱
       ╱─────────────────────────────────╱
                            │
          ╱─────────────────────────────────╱
         ╱  Input device dynamic data defining ╱
        ╱   the dynamic behaviour of the system ╱
       ╱─────────────────────────────────╱
```

Process load flow and dynamic
data to identify the number and
type of devices to be modelled

| Number of generating systems to be represented by a classical machine model = NCMC | Number of SVC to be modelled = NSVC |

Number of generating systems to be represented
by a detailed model; i.e. flux linkage model of the
synchronous machine and/or exciter and PSS
dynamics also modelled = NDMC

A
Formulate the state space model
for each of the generating systems
modelled as classical machines in
the form

$$[\dot{X_d}] = [A_d] [X_d] + [B_d] [\Delta v]$$
$$[\Delta i] = [C_d] [X_d] - [Y_d] [\Delta v]$$

C
Formulate the state space model
for each SVC in the form

$$[\dot{X_d}] = [A_d] [X_d] + [B_d] [\Delta v]$$
$$[\Delta i] = [C_d] [X_d] - [Y_d] [\Delta v]$$

B
Formulate the state space model for each of
the generating systems represented by a
detailed model in the form

$$[\dot{X_d}] = [A_d] [X_d] + [B_d] [\Delta v]$$
$$[\Delta i] = [C_d] [X_d] - [Y_d] [\Delta v]$$

```
                    ┌─────┐
                    │  Z  │
                    └──┬──┘
                       ▽
```

Figure (6.1a): Flow chart of S³
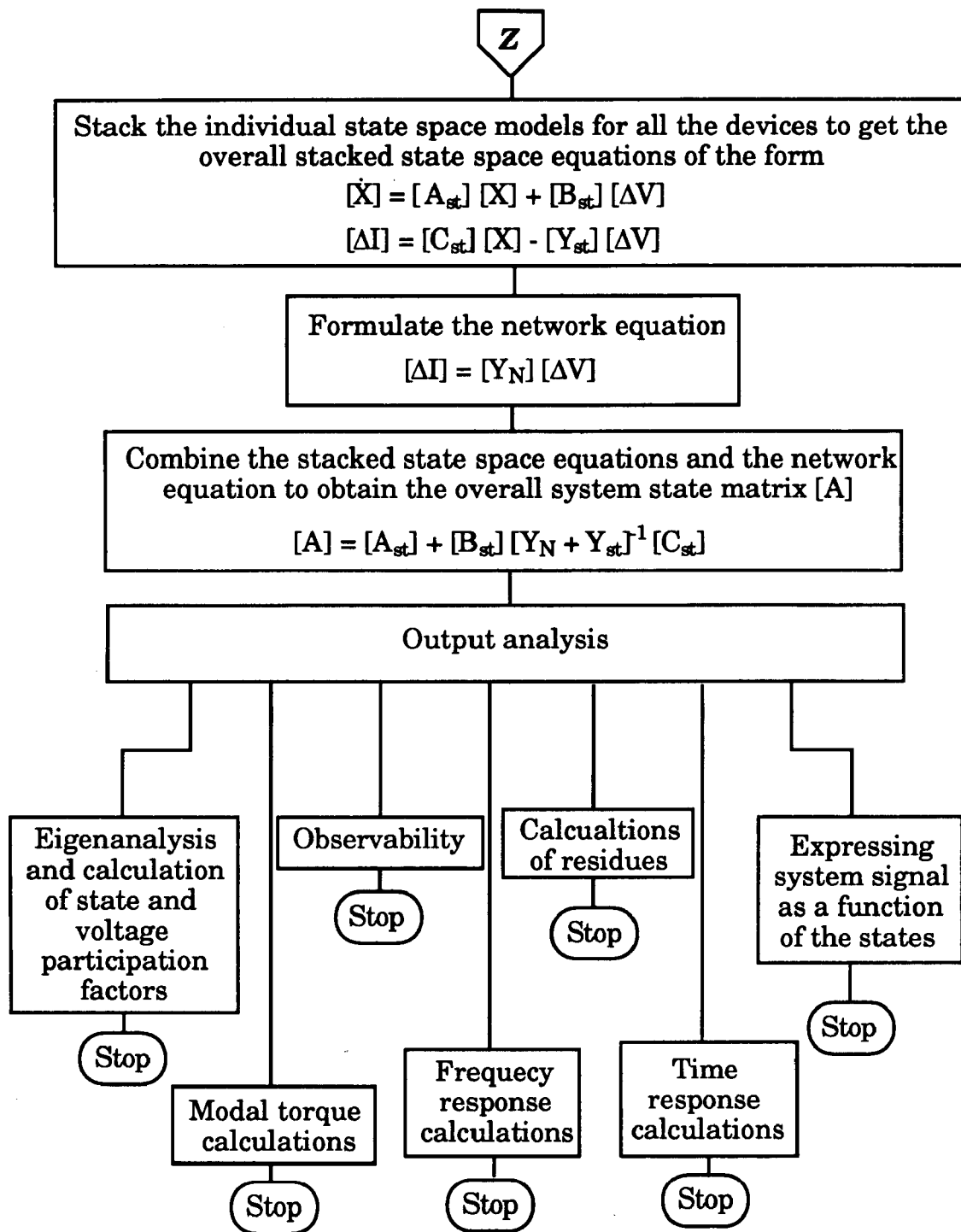
Figure (6.1b): Flow chart of S^3 (contd)
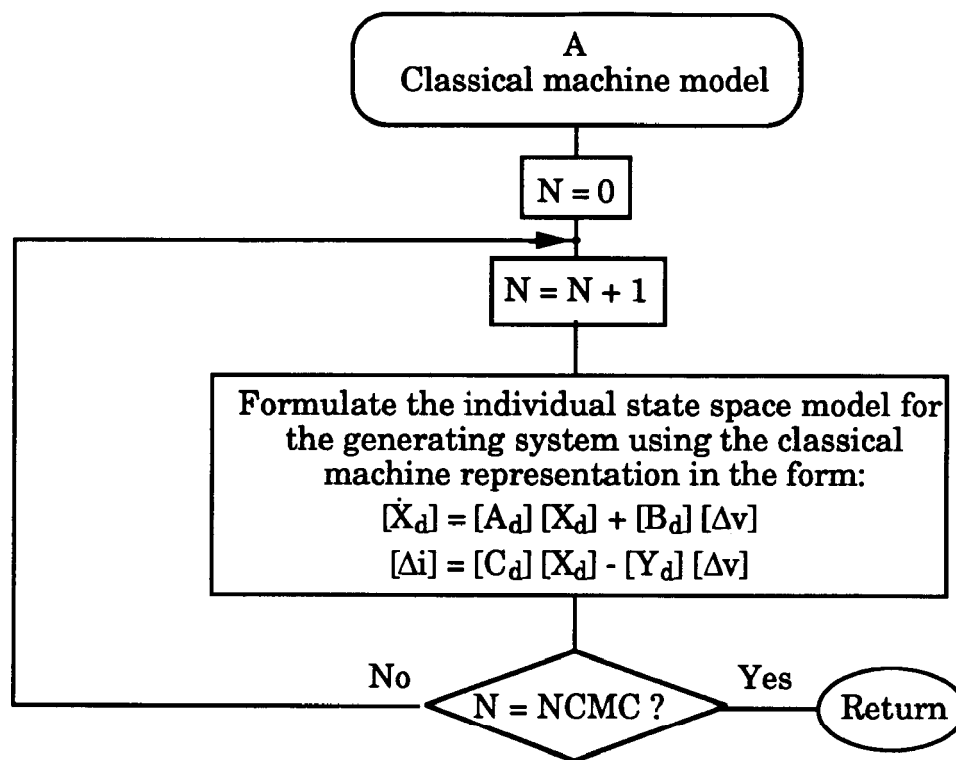
Figure (6.1c):Flow chart for formulating the state space model of the
classical machine

B
Detailed model of the generating system

$N = 0$

$N = N + 1$

Formulate the intermediate state space model of the synchronous machine in the form

$$[\dot{X}_g] = [A_g][X_g] + [B_g][\Delta i] + [E_x]\Delta v_f$$

$$[\Delta i] = [C_g][X_g] - [Y_d][\Delta v]$$

Is the exciter to be modelled ?

Yes

No

State space model of the exciter in the form

$$[\dot{X}_e] = [A_e][X_e] + [B_e][U] + [B_{vso}]\Delta v_{vso}$$

$$\Delta Efd = [M_e][X_e] + [K_e][U] + [D_{vso}]\Delta v_{vso}$$

Is PSS to be modelled ?

No

Yes

State space model of the PSS in the form

$$[\dot{X}_s] = [A_s][X_s] + [B_s][U]$$

$$\Delta v_{vso} = [M_s][X_s] + [K_s][U]$$

Interconnection of the generating system component models to formulate the state space model of the generating system of the form

$$[\dot{X}_d] = [A_d][X_d] + [B_d][\Delta v]$$

$$[\Delta i] = [C_d][X_d] - [Y_d][\Delta v]$$

No $N = NDMC ?$ Yes   Return

Figure (6.1d): Flow chart for formulating the detailed generating sys. state space model
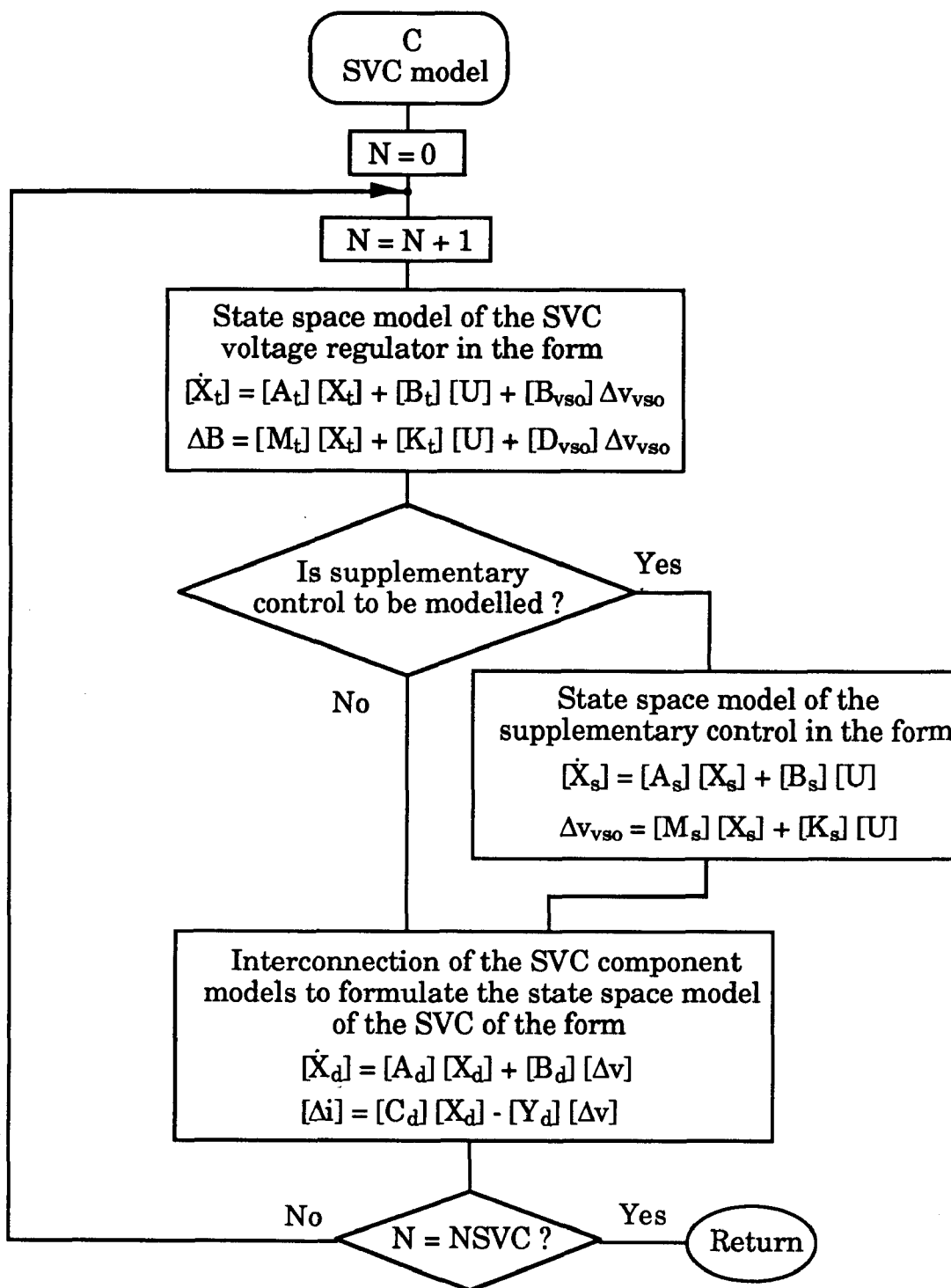
Figure (6.1e): Flow chart for formulating the SVC state space model

The Call Tree, i.e. the actual sequence of the subroutine calls in the S^3 program is shown in Figures (6.2a) and (6.2b). The subroutines in square boxes, shown in Figure (6.2b), correspond to the various analysis options available in S^3 program. In any execution of the S^3 program one of these subroutines is used depending on the study being conducted. For example, if the program is being executed to carry out the calculation of frequency response, the subroutine FRQOUT will be used. The type of analysis/calculation required is specified by the user as an input data. The matrix operations and eigenvalue\eigenvector calculations are performed by subroutines MATUTY and EISPS3 respectively [21].

S3 (Main program)

→ **INFLO** (Read load flow data)

→ **INDYNA** (Read dynamic device data)

→ **RUNIN** (Read user specified data pertaining to the mode of execution)

    → **INIRES** (Initialization of user specified data)

→ **MACLAS** (State space model for the classical representation of generating system)

→ **MACDET** (Flux linkage model of the generator)

    → **EXC1** (Exciter model)

    → **GSTAB1** (PSS model)

    → **DGCON** (State space model for the detailed representation of the generating system)

→ **SVC1** (Voltage regulator model)

    → **SVST1** (Supplementary control model)

    → **SVCON** (State space model of the SVC)

→ **REBUS** (Renumber the network buses)

→ **YNET** (Form the network admittance matrix)

Figure (6.2a): **S³** Call Tree

Figure (6.2b): S³ Call Tree (contd)

6.2.1 Salient features of the S³ program

One of the salient features of the S³ program is its modular structure which permits future extensions and modifications with relative ease and without the need for modifying the entire program. Changes to the program can be conveniently handled for modifications in any of the existing device models or analysis techniques (eg. different algorithm for calculating eigenvalues or frequency response). These modifications would only involve changes in the corresponding subroutines. Also, the program has the flexibility to include representation of other power system components like HVDC transmission systems, governor or Flexible AC Transmission System (FACTS) devices, etc. This would require describing these components in separate subroutines which can then be easily incorporated in the Call Tree. Similarly, alternative numerical techniques like sparse vector approach for storing the admittance matrix etc, can be easily implemented for better computational efficiency and increasing the capacity of the program to model larger power systems.

Another salient feature of the program is the appropriate choice of the interface variables between the devices and the transmission network. In the modelling approach discussed in Chapter 2, it was shown that the device model is interfaced with the external world through the device terminal voltage and current. Thus, the dynamic interaction between the system devices is defined through the network interconnection. This allows the modification and implementation of new models with relative ease.

The S^3 program is versatile enough and has the option to carry out small signal stability investigations and design of damping control using various analysis techniques as given below [25]:

i)   Eigenvalue analysis of the power system state matrix.

ii)   Calculation of the state and voltage participation factors of the power system state matrix.

iii)   Modal torque calculations for the modes of interest.

iv)   Calculation of observability factors in various user specified line signals.

v)   Frequency response over the range of user specified frequencies for various system signals with respect to a input. Both, the system signals and the input are user specified.

vi)   Calculations of the residues at user specified complex frequencies, for various system signals with respect to a input which are specified by the user.

vii)   Time response over the range of user specified time interval for various system signals with respect to a input. Both, the system signals and the input are user specified.

viii)   Expressing a user specified system signal as a function of the system states.

These studies give an in-depth knowledge of the dynamic behavior of the power system under consideration and also provide the information

needed to improve the existing controls or to design new controls for enhancing the small signal stability of the power system.

The S^3 program is suitable to carry out small signal stability analysis of a moderately sized power system. In its present form, the program can handle 400 system states corresponding to 20 individual power system devices and a transmission network of up to 100 buses. A large power system can also be represented in the S^3 program but it will require sparsity based storage technique for efficient computation. The features of S^3 program are comparable to that of MASS (Multi-Area Small Signal) stability program of Ontario Hydro [1].

6.3   Small Signal Stability Analysis-A Case Study

The effectiveness of the analysis techniques and the generalized philosophy of damping control design proposed in the previous chapters is demonstrated through a case study of a test system. The objective of these studies is to improve the small signal stability of the test system for two different operating conditions by the proper design of damping control to damp out the poorly damped electromechanical modes of oscillation in the system.

The two operating conditions of the test system are defined below.

i)   The operating condition under nominal system loading which is referred to as the nominal operating condition.

ii)   The operating condition that is defined by the same nominal system loading but with the heaviest loaded tie line out of service. This operating condition is referred to as the weakened operating condition. This is because of the fact that to supply the same load as that of the nominal loading condition, it has to re-route the power transfer over the in-service tie lines. This causes additional stress on the in-service tie lines as they now have to share the burden of transferring power of the out of service tie line also.

The case study of the test system can be subdivide as follows:

i)   Load flow studies to establish the operating point for representing the test system in the linearized domain. This is obtained from the load flow solution using any standard load flow package [23].

ii)   Preliminary study is carried out to first determine if any damping improvement is required due to the presence of inadequately damped electromechanical modes at both the operating points. If damping improvement is sought then the preliminary study is extended to identify the worst case condition between the two operating points and a detailed analysis of the inadequately damped electromechanical modes is carried out. This involves the determination of the modes shapes and calculations of state and voltage participation factors of system states and buses respectively for the electromechanical modes under consideration.

The identification of the worst case situation is needed because the design of damping control would have to satisfy the stability requirements for the two operating conditions. As described in Chapter 5 more weight is given to the parameters of the damping control designed for the worst case situation. In the present study, the strategy is to first design the damping control for the worst case situation and test the design at the other operating condition to check if any modifications are necessary. If not, then the design for the worst case situation stands as the final choice of damping control to meet the requirements for both the operating conditions.

iii) Design and validation of the damping control to improve the small signal stability of the test system.

6.3.1 The Test System-Modified 39 bus New England Area system

The test system is derived from the New England Area system of the United States after certain modifications [1]. The modifications include replacement of IEEE DC1 type exciters on generating systems at buses 30 and 34 by ST1 type exciters. Also, in the test system 3 SVCs have been included. The schematic of the test system is shown in Figure (6.3). The system comprises 39 buses, 48 tie lines, 9 generating systems and 3 SVCs. The system buses are numbered such that the generating systems (G30 to G38) are respectively connected to each bus from 30 to 38. SVCs S1, S16 & S23 are connected to each of the buses 1, 16 and 23 respectively, to provide

the necessary voltage support. It is interesting to note that bus 39 represents the interface between the United States and Canada. Under most operating conditions the United States imports power from Canadian utilities. In most small signal stability studies for the New England Area, bus 39 is taken to be a very strong source and is treated as a infinite bus. With this it is implicitly assumed that any disturbance occuring within the New England Area will not be transmitted to the Canadian power system.

The nine generating systems and the three SVCs are the dynamic devices in the test system and hence, are described by differential equations in the state space framework as discussed in Chapter 2. The transmission system (tie lines) and the loads form the network model which is described by a set of algebraic equations as its dynamics are ignored for the purpose of small signal stability investigations. In the case study the generating system is represented in detail considering flux linkage model of the synchronous machine and IEEE type DC1 or ST1 exciters. The voltage regulators of all three SVCs are assumed to have identical parameters for the sake of simplicity. The network and dynamic device data are given in Appendix (A2.1) and (A2.2), respectively. Bus 39 is taken as the infinite bus.

Modified 39-Bus New England Area system
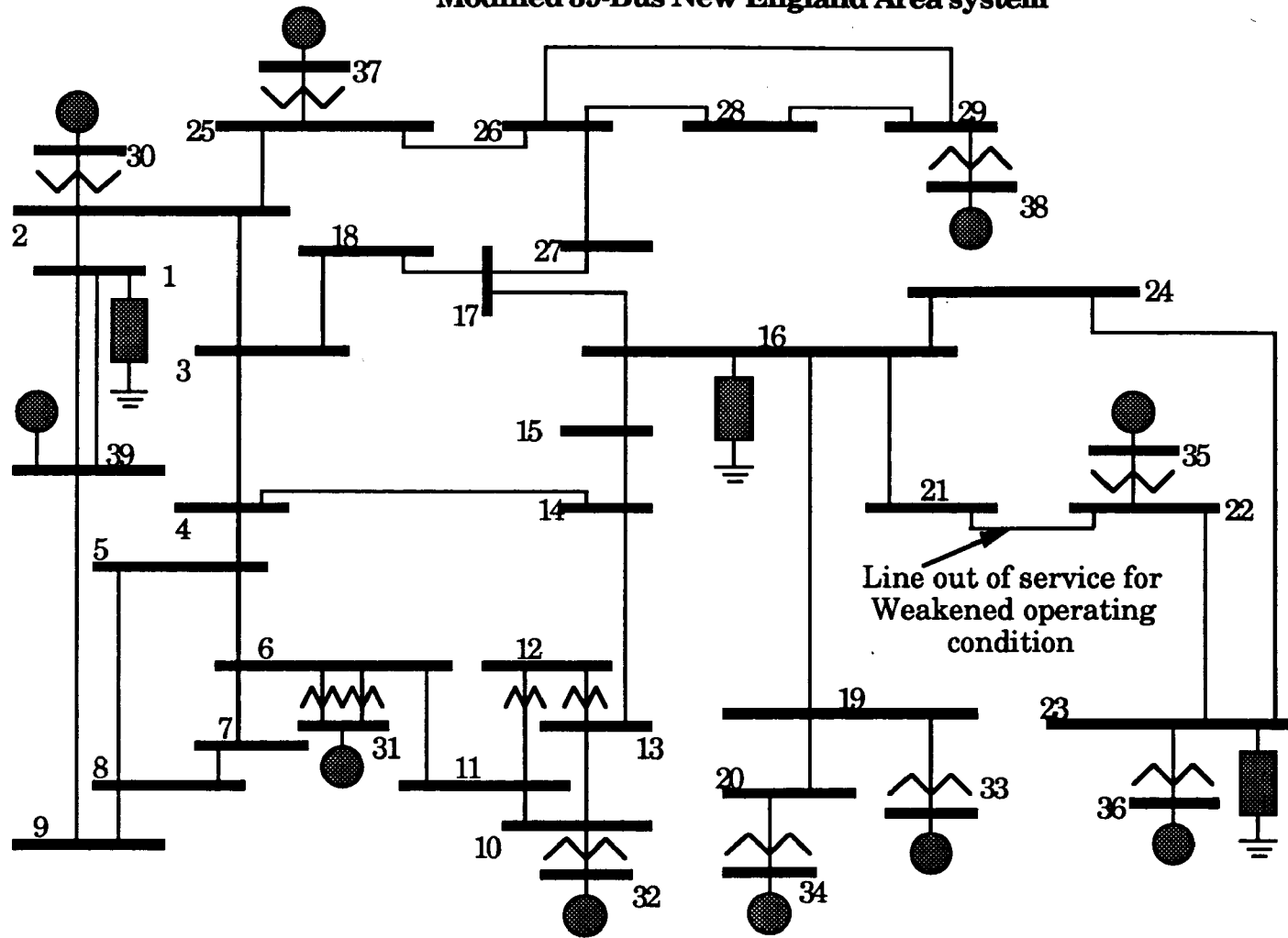
Figure (6.3)

6.3.2 Load flow studies

The load flow solution of the test system for the nominal operating condition is given in Appendix (A2.3). The heaviest loaded line in this case is the tie line between buses 21 and 22. For the weakened operating condition the load flow solution is obtained for the same loading condition but with the tie line between buses 21 and 22 out of service. The load flow result for this case is given in Appendix (A2.4). It can be seen that for both the operating conditions, the maximum generation and load is at bus 39, followed by the generating system G38. The fact that bus 39 is the strongest bus is consistent with the fact that this bus represents the strong Canadian system connected to it. In both load flow solutions it is assumed that the SVC's are floating i.e. they are neither generating nor absorbing reactive power.

The operating points thus established by the load flow solutions is given as a input to the S^3 program for all further small signal stability investigations.

6.3.3 Preliminary studies

The complete eigenvalue and the state participation factor analysis for both the nominal and weakened operating conditions shows that the least damped eigenvalues, as expected, are the electromechanical modes of oscillations. All eigenvalues except for the electromechanical modes have a damping ratio of greater than 0.1 and hence are not a cause of concern. Tables (6.1a) and (6.1b) give eigenvalues corresponding to the

electromechanical modes and the devices participating in these modes for both the nominal and weakened operating conditions respectively. In Tables (6.1a) and (6.1b) the symbol <-> in the right hand column indicates the various generating systems swinging against one another. Also, from Tables (6.1a) and (6.1b), it is seen that there are certain electromechanical modes whose damping ratio is less than the cutoff level of 0.02 (established in Chapter 5). This indicates that the damping of these modes must be improved by the suitable design of damping control(s).

Identification of the worst case situation:

Having determined the existence of inadequately damped electromechanical modes, the next step is to identify the worst case situation. From Table (6.1a) it can be seen that there are two electromechanical modes (No. 5 & 9) which are of concern as these have damping ratio less than 0.02. Also, from Table (6.1b) which corresponds to the weakened operating condition of the system, it is evident that modes 5, 6 & 9 are inadequately damped and have damping ratios less than the corresponding damping ratios obtained under the nominal operating condition. Thus the weakened operating condition of the system can be treated as the worst case situation.

Figure (6.4) graphically displays the electromechanical modes in the complex s-plane for both the weakened and nominal operating conditions. It can be seen that for the weakened operating condition the

electromechanical modes tend to be closer to the imaginary axis. For better system stability these modes need to be shifted further into the left half plane through proper design of damping control.

Before initiating the design procedure it is necessary to obtain more information about the modes (No.5, 6 & 9) whose damping needs to be improved. The mode shapes of these electromechanical modes are given in Figures (6.5a) to (6.5c) for the weakened operating condition. The ordinate in Figures (6.5a) to (6.5c) is a quantity equivalent to the speed state ($\Delta\omega$) obtained as $|\Delta\omega|\cos(\angle\Delta\omega)$ from the corresponding eigenvector of the mode under consideration. The state participation factors of each of the dominant device states ($\Delta\omega$ for generating system and control system states of SVC) to these modes (No. 5, 6 & 9) is given in Tables (6.2a) to (6.2c). An examination of the state participation factors and the modes shapes reveals that:

i)Mode No.9 is an interarea mode in which all the generating systems swing in near unison against the infinite bus '∞bus(39)'.

ii)Mode No.5 is the local mode of the generating system G30.

iii)Mode No.6 is the local mode of the generating system G34.

Based on the above preliminary investigation, the following conclusions can be drawn:

i)   There are three electromechanical modes whose damping needs improvement. The least damped mode is an interarea mode in which all the machines are swinging against the infinite bus

∞bus(39).   The other two modes are local modes of generating systems G30 and G34.

ii)   The worst case situation corresponds to the weakened operating condition.

iii)   There is a need to provide damping control to improve system damping.
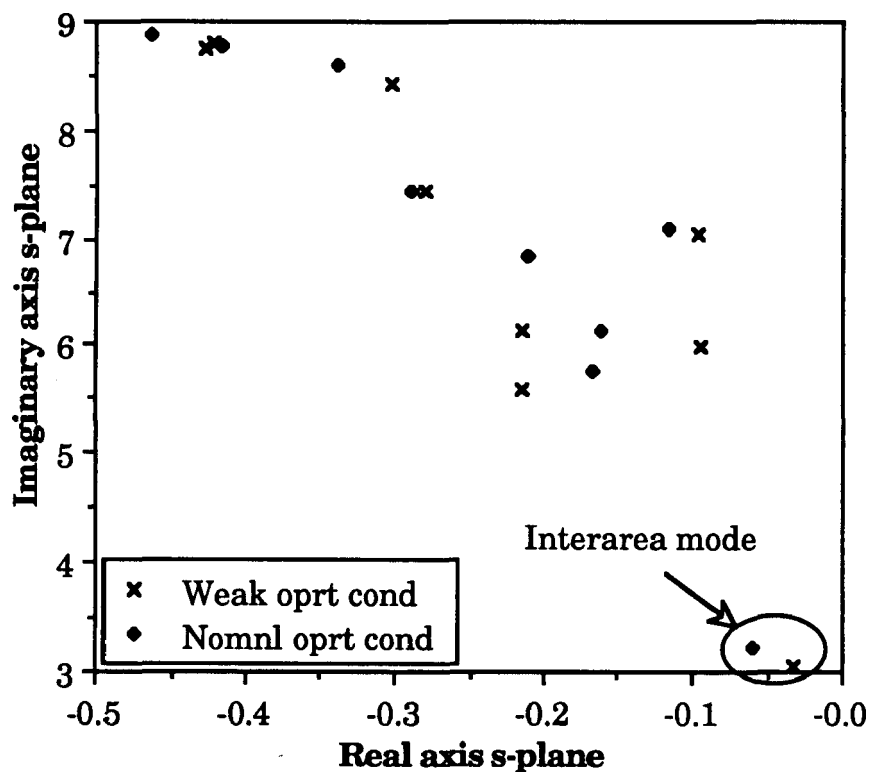
Figure (6.4): Electromechanical modes of the original system for the two operating conditions.

Table (6.1a): Electromechanical modes and participating devices for the nominal operating condition

No.	Electromechanical mode	Damping ratio	Participating devices
1	-0.3373 + j8.5928	0.03922	G33 <-> G34
2	-0.4171 + j8.7676	0.04752	G37 <-> G30
3	-0.4638 + j8.8628	0.05226	G36 <-> G35
4	-0.2887 + j7.4341	0.03880	G32 <-> G31
5	-0.1155 + j7.0859	0.01629	G30, G37 <-> Rest of the system
6	-0.2117 + j6.8445	0.03092	G35, G36 <-> G31, G34, G30
7	-0.1620 + j6.1449	0.02635	G31, G32 <-> G34, G38
8	-0.1675 + j5.7611	0.02907	G38 <-> G34
9	-0.0596 + j3.2242	0.01848	∞bus (39) <-> Rest of the system

<-> indicate the generating systems swinging against one another for a particular mode.

Table (6.1b): Electromechanical modes and participating devices for the weakened operating condition

No.	Electromechanical mode	Damping ratio	Participating devices
1	-0.3027 + j8.4137	0.03595	G33 <-> G34
2	-0.4276 + j8.7577	0.04877	G37 <-> G30
3	-0.4214 + j8.8007	0.04783	G36 <-> G35
4	-0.2799 + j7.4500	0.03755	G32 <-> G31
5	-0.0962 + j7.0307	0.01368	G30,G37 <-> Rest of the system
6	-0.0947 + j5.9863	0.01582	G34, G33 <-> G35, G36, G38
7	-0.2146 + j6.1424	0.03491	G31, G32 <-> G34, G38
8	-0.2150 + j5.5846	0.03847	G38 <-> G35
9	-0.0321 + j3.0508	0.01053	∞ bus (39) <-> Rest of the system

Mode shape of the interarea mode
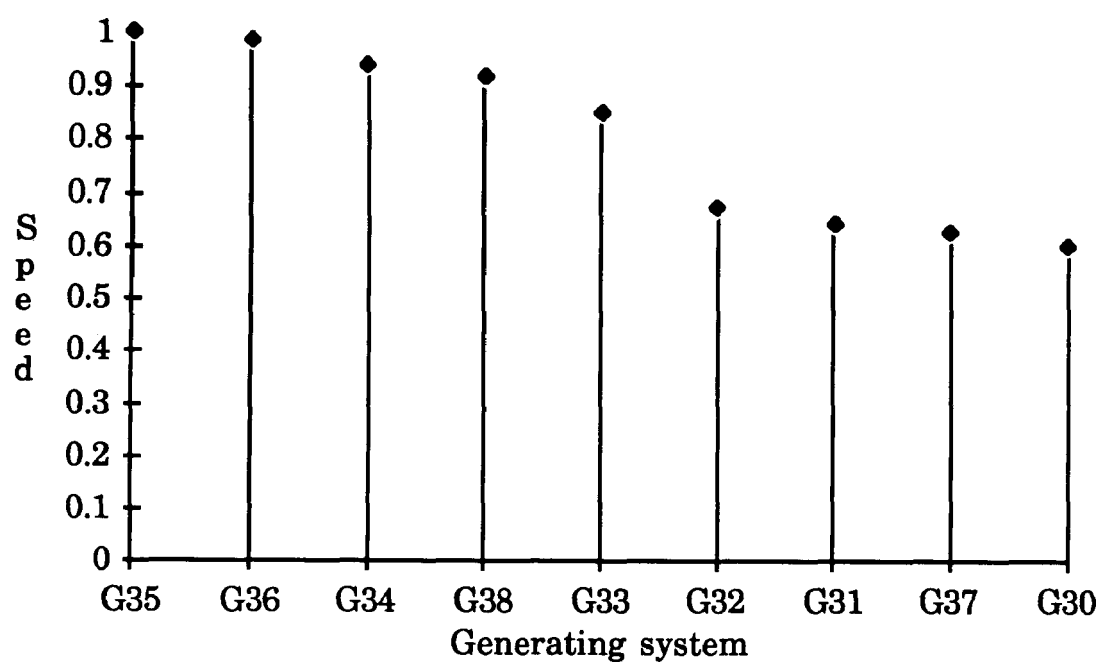
Figure (6.5a) Interarea mode shape

Mode shape for the local mode of G30
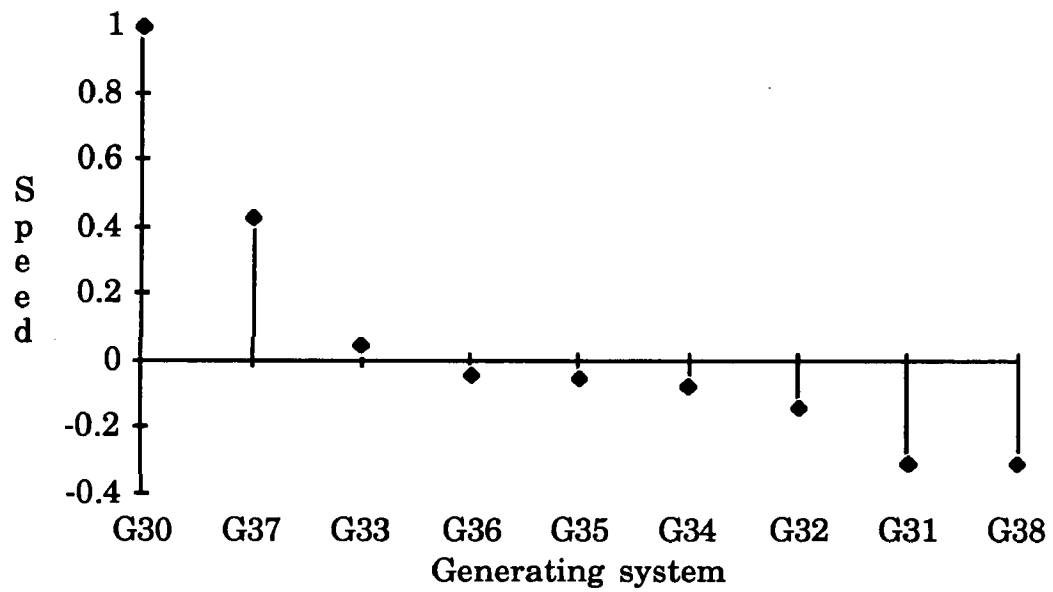
Figure (6.5b)Mode shape-local mode of G30

Mode shape for the local mode of G34
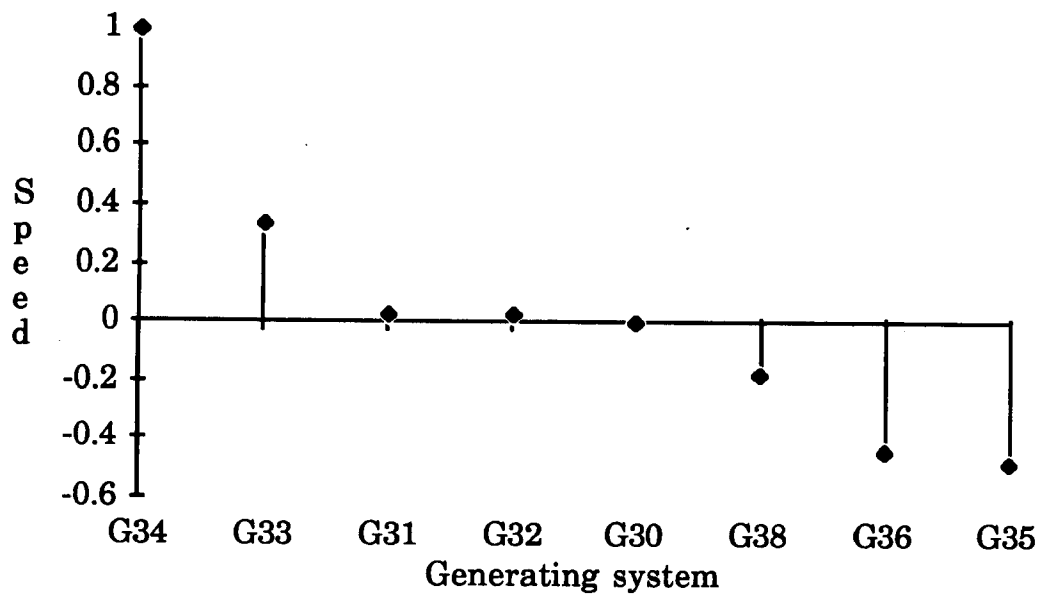
Figure (6.5c)Mode shape-local mode of G34

Table (6.2a): State participation factors for Mode No.9

Device	Device state	State participation factor
G30	$\Delta\omega$	0.0330
G31	$\Delta\omega$	0.0333
G32	$\Delta\omega$	0.0435
G33	$\Delta\omega$	0.0482
G34	$\Delta\omega$	0.0679
G35	$\Delta\omega$	0.0918
G36	$\Delta\omega$	0.0710
G37	$\Delta\omega$	0.0203
G38	$\Delta\omega$	0.1070
S1	1	0.0003
S16	1	0.0040
	2	0.0007
	3	0.0020
S23	1	0.0020
	3	0.0010

Device states 1,2 & 3 correspond to the control system states of SVC

Table (6.2b): State participation factors for Mode No.5

Device	Device state	State participation factor
G30	$\Delta\omega$	0.3784
G31	$\Delta\omega$	0.0333
G32	$\Delta\omega$	0.0097
G33	$\Delta\omega$	0.0004
G34	$\Delta\omega$	0.0037
G35	$\Delta\omega$	0.0011
G36	$\Delta\omega$	0.0006
G37	$\Delta\omega$	0.0420
G38	$\Delta\omega$	0.0421

Table (6.2c): State participation factors for Mode No.6

Device	Device state	State participation factor
G30	$\Delta\omega$	0.0019
G31	$\Delta\omega$	0.0181
G32	$\Delta\omega$	0.156
G33	$\Delta\omega$	0.0364
G34	$\Delta\omega$	0.3523
G35	$\Delta\omega$	0.0891
G36	$\Delta\omega$	0.0574
G37	$\Delta\omega$	0.0
G38	$\Delta\omega$	0.0342

6.3.4 Design of Damping control

Based on the foregoing preliminary studies, as the interarea mode is the least damped mode the damping control is first designed to improve its damping before considering the other local modes of concern. The process of designing damping control for a particular electromechanical mode can be outlined by the following steps.

i)   Selection of the type of damping control (PSS on generating system or supplementary control on SVC).

ii)   Selection of site for installing damping control.

iii)   Design of damping control compensation network.

iv)   Validation.

In Chapter 5 it is stated that for the local and intermachine modes the obvious choice for the type of damping control would be the PSS on a generating system. But for an interarea mode, which spreads over the entire system, there are two possibilities for installing the damping control.

i)   Using a PSS on a generating system

ii)   Using a supplementary control on an existing SVC.

The design of PSS to damp an interarea mode must take into account the local mode of the generating system on which the PSS is being installed. This is done because the local mode is much more strongly coupled to the generating system than the interarea mode and hence is likely to be most affected by the introduction of PSS. Thus, if the local mode is ignored in the design, the PSS could adversely effect the damping of the local mode.

The second option of using supplementary control on SVC can be applied only under special circumstances which depends on a myriad of practical considerations as described in Chapter 5.

In the present study both PSS and supplementary control on SVC are designed and their relative performance compared.

6.3.4.1   Design of Power System Stabilizer (PSS)

The first step in the design process is to identify a suitable site for the installation of PSS. This selection is relatively simple and can be based on the state participation factors of the generating system speed states for the mode under consideration.

<u>Selection of site</u>

From Table (6.2a) it is evident that the speed state of generating system G38 is the best choice for installing PSS as this machine has the largest participation to the interarea mode. Also, G38 has the largest generation after the infinite bus. But a closer look at the excitation system of G38 reveals that it is a IEEE DC1 type exciter (Appendix A2.2). This type of exciter is slow acting and hence is not a good choice for installing a PSS. In a practical situation, the utility would probably change the excitation system altogether, but in the present study an attempt is made to choose an alternative candidate location for installing PSS.

From Table (6.2a) it can be noticed that the state participation factors of the speed states of all the other generating systems are relatively close and keeping in mind that the next least damped mode is the local mode of

G30, the logical choice for installing PSS is taken as the generating system G30.

Selection of feedback signal

It is a standard practice to select the speed signal of the generator or an equivalent signal as the feedback signal for PSS. The speed signal is chosen as the feedback signal in the present study.

Design of PSS compensation network

The PSS compensation network for the generating system G30 is designed based on the following two methods to damp out the local mode as well as the interarea mode.
i)Frequency response method used by Ontario Hydro [6].
ii)Generalized damping control design using residues presented in Chapter 5.

i)Frequency response method used by Ontario Hydro [6].

In this design method the concerned generating system G30 is modelled in detail and the rest of the system devices are represented by negative impedances i.e, their dynamics are ignored. Also, the inertia

constant of the modelled generating system G30 is increased by a factor of 10-25 to minimize the effect of the influence of rotor angle variation on the excitation system output.

A frequency response of the electrical torque contribution of the excitation system with respect to the exciter voltage reference is obtained over the frequency range of interest. The phase of the frequency response indicates the phase lag introduced by the excitation system. The damping can be improved if the electrical torque applied to the machine is in phase with the speed of the generating system. The compensation network is, therefore, designed to compensate the phase lag introduced by the excitation system over the frequency range of interest (frequency range of modes whose damping needs improvement). Total phase compensation is, however, avoided as there may be a chance of overcompensation due to a variety of reasons which may lead to reduction in synchronizing torques, and thus transient stability [13]. The PSS compensation network consists of phase lead blocks. Once the lead block time constants are determined the PSS gain is determined by a trial and error procedure till acceptable damping of the modes of interest are achieved without deteriorating other modes (electromechanical and control modes) for the full system representation.

The frequency response of the electrical torque contributions from the exciter of G30 (DGET 30) is shown in Figure (6.6). It can be seen that near the frequency of the local mode (≈ 1.1 Hz.) the phase lag is approximately 100° and approximately 70° for the interarea mode (≈ 0.47 Hz.). A lead

network shown in Figure (6.7) is chosen as the phase compensation network.
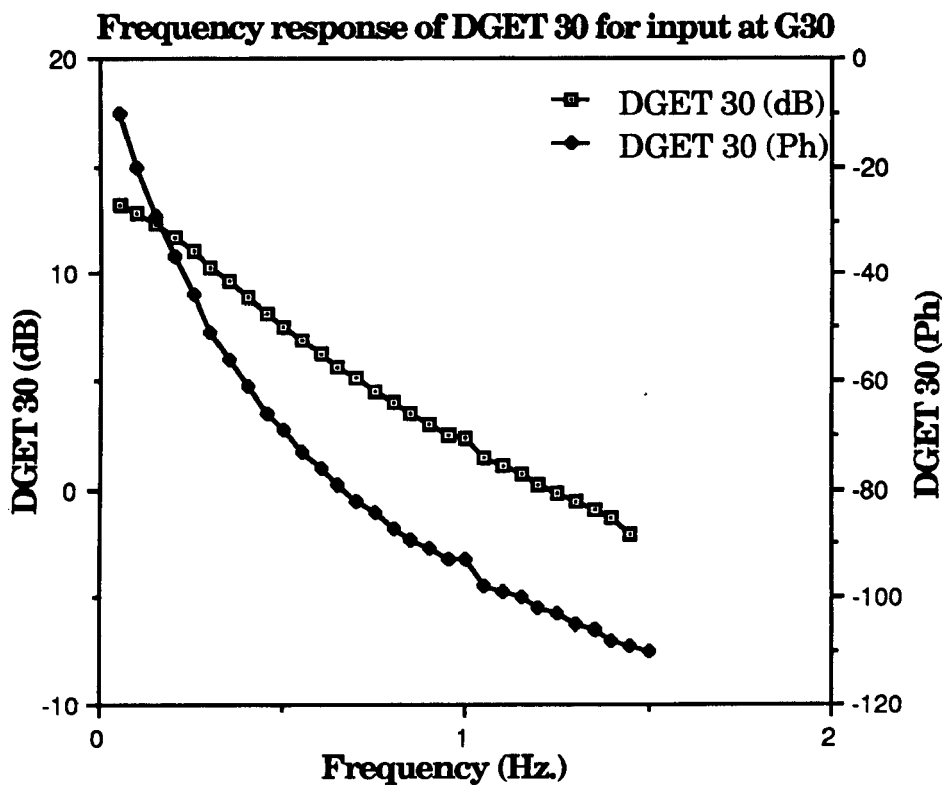
Figure (6.6)Frequency response of DGET
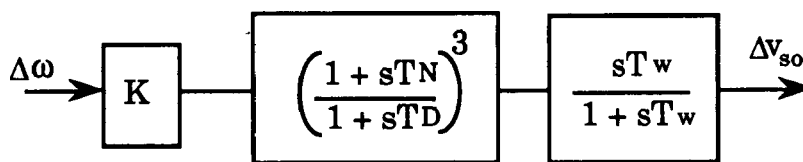
$\Delta\omega$ = speed signal

Δv_{so} = Supplementary control output

Figure (6.7): PSS block diagram

The time constants, T_N and T_D are determined so that they give a maximum phase lead of approximately 85° at the frequency of the local

mode of G30 and a phase lead of approximately 60° at the frequency of the interarea mode. The various time constants of the phase compensation network are determined as:

$$T_N = 0.225, T_D = 0.0907 \text{ and } T_W = 10.0.$$

The gain (K) is determined by a trial and error approach and is found to be 60.0

ii)Generalized damping control method

The generalized design of damping control uses a pole placement technique for shifting the eigenvalue (mode) under consideration to a suitable location. When the PSS is being designed to damp out a interarea mode, still the mode under consideration for design purposes will be the local mode. The shifting of this local mode to a suitable location should result in the improved damping of the interarea mode also. The first step in this design procedure is to select the new location of the local mode. Referring to the criteria developed in Chapter 5 the new location must be of higher frequency and should have the desired damping. Based on this a value of (-2.47 + j7.5) is chosen as the new location for the local mode of G30.

The next step is to determine the residue of the feedback signal at this new eigenvalue location in the complex s-plane. The feedback signal considered here is the speed signal and its residue at (-2.47 + j7.5) has a magnitude of 1.194 and an angle of -102.49°.

The compensation network can be designed based on the procedure described in Chapter 5. The compensation network having the same structure as that of Figure (6.7) is chosen for the PSS. The various time constants and gain of the compensation network are obtained as

$$T_N = 0.19, T_D = 0.0802, T_W = 10.0 \text{ and } K = 88.95$$

Validation of the PSS design

The PSS designs are validated by incorporating the designed PSS into the generating system (G30) model and determining the eigenvalues for both the weakened and nominal operating conditions. Tables (6.3a,b) and (6.4a,b) give the electromechanical modes with PSS designed by the frequency response method (PSS(OH)), and the generalized design method (PSS(GD)) respectively. The locations in the complex s-plane of the electromechanical modes with and without damping control for both the operating conditions is shown in Figures (6.8a) and (6.8b).

Table (6.3a): Electromechanical modes and participating devices for PSS
(OH) at G30 for the weakened operating condition

No.	Electromechanical mode	Damping ratio	Participating devices	
1	-0.3318 + j8.4046	0.03945	G33	<-> G34
2	-0.6663 + j8.7123	0.07626	G37	<-> G30
3	-0.4215 + j8.8005	0.04784	G36	<-> G35
4	-0.2812 + j7.4459	0.03774	G32	<-> G31
5	-2.0138 + j7.5175	0.25876	G30,G37	<-> Rest of the system
6	-0.0984 + j5.9827	0.01645	G34	<-> G35
7	-0.2216 + j6.1620	0.03594	G31,G32	<-> G34,G35
8	-0.3170 + j5.6356	0.05617	G38	<-> G36
9	-0.3906 + j3.1744	0.12214	∞bus(39)	<-> Rest of the system

Table (6.3b): Electromechanical modes and participating devices for PSS (OH) at G30 for the nominal operating condition

| No.	Electromechanical mode	Damping ratio	Participating devices
1	-0.3532 + j8.5973	0.04101	G33 <-> G34
2	-0.6246 + j8.7160	0.07148	G37 <-> G30
3	-0.4639 + j8.8633	0.05226	G36 <-> G35
4	-0.2891 + j7.4336	0.03886	G32 <-> G31
5	-2.1232 + j7.585	0.26956	G30,G37 <-> Rest of the system
6	-0.2320 + j6.864	0.03377	G34 <-> G35
7	-0.1623 + j6.1682	0.02631	G31,G32 <-> G34,G35
8	-0.2275 + j5.767	0.03942	G38 <-> G36
9	-0.4445 + j3.3629	0.13104	∞bus(39) <-> Rest of the system

Table (6.4a): Electromechanical modes and participating devices for PSS (GD) at G30 for the weakened operating condition

No.	Electromechanical mode	Damping ratio	Participating devices
1	-0.3343 + j8,4010	0.03977	G33 <-> G34
2	-0.6683 + j8.6558	0.07698	G37 <-> G30
3	-0.4215 + j8.8005	0.04784	G36 <-> G35
4	-0.2809 + j7.4459	0.03770	G32 <-> G31
5	-2.4137 + j7.8853	0.2927	G30,G37 <-> Rest of the system
6	-0.0990 + j5.9828	0.01654	G34 <-> G36
7	-0.2198 + j6.1635	0.03564	G31, G32 <-> G34, G38
8	-0.3135 + j5.6534	0.05537	G38 <-> G35
9	-0.4251 + j3.2972	0.12787	∞bus(39) <-> Rest of the system

Table (6.4b): Electromechanical modes and participating devices for PSS (GD) at G30 for the nominal operating condition

No.	Electromechanical mode	Damping ratio	Participating devices
1	-0.3550 + j8.5972	0.04126	G33 <-> G34
2	-0.6248 + j8.6690	0.07189	G37 <-> G30
3	-0.4639 + j8.8632	0.05227	G36 <-> G35
4	-0.2891 + j7.4336	0.03886	G32 <-> G31
5	-2.5247 + j7.9483	0.30273	G30,G37 <-> Rest of the system
6	-0.2312 + j6.8641	0.03366	G34 <-> G36
7	-0.1602 + j6.1691	0.02595	G31, G32 <-> G34, G38
8	-0.2294 + j5.7749	0.03968	G38 <-> G35
9	-0.4756 + j3.4928	0.13493	∞bus(39) <-> Rest of the system

Electromechanical modes for weakened operating condition
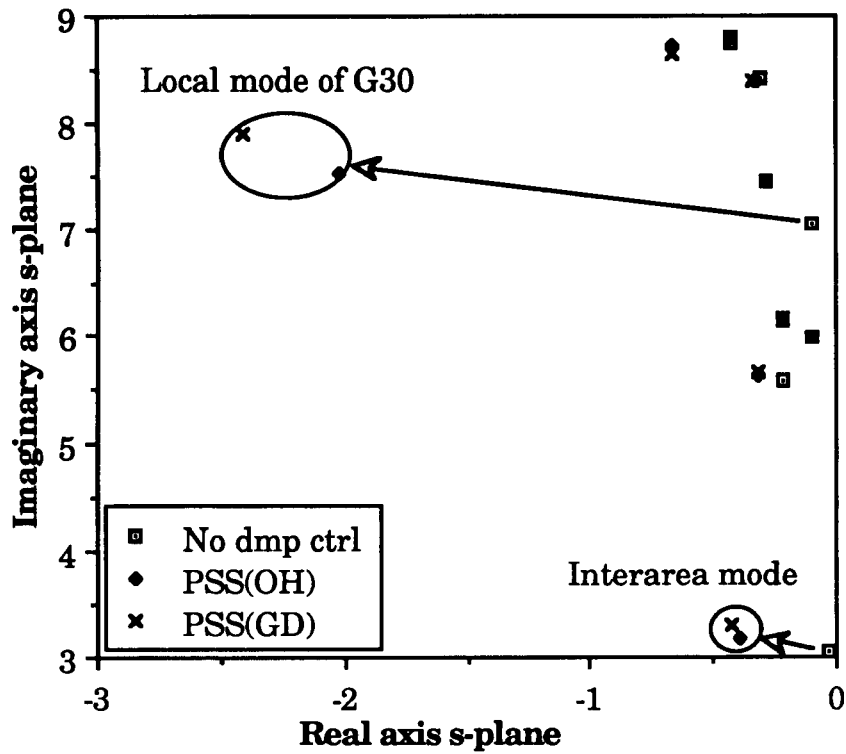
Figure (6.8a)Electromechanical modes-weakened operating condition-PSS
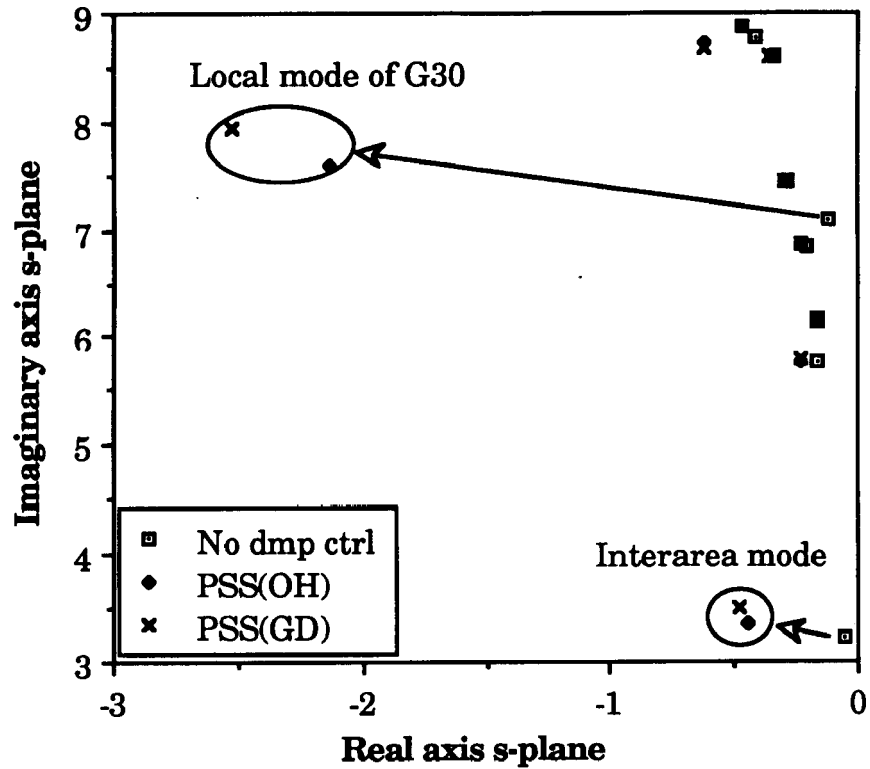
Figure (6.8b)Electromechanical modes-nominal operating condition-PSS

It is seen from Tables (6.3a,b) and (6.4a,b) that adequate damping of the interarea mode and the local mode of G30 is achieved,but the local mode of G34 is still less than the cutoff level of 0.02. Hence additional damping control by using PSS on G34 is required to increase the damping of this mode. The design of PSS at G34 is not carried out as it is trivial.

It can be noted that the parameters of the compensation network of the PSS with both the design methods (frequencies response and the generalized design method) are quite close. The frequency response method has been proven to be quite robust [6] and thus, a similar claim can be made for the generalized design method for damping control.

The PSS designs are further validated by calculating the damping and synchronizing torques for the modes under consideration to see if any beneficial changes have been brought about by the introduction of damping control. The damping component (M-ω) and the synchronizing component (M-δ) as a percentage of the total modal torque for the local mode of G30 and the interarea mode is given for the case with and without damping control in Table (6.5).

It can be seen that in the absence of any damping control the modal torque for the local mode of G30 and the interarea mode is primarily made up of the synchronizing torque. Also, for the interarea mode the damping torque is negative. With the introduction of the PSS, the damping torque component of the two modes increases significantly. The synchronizing

torque component however, shows a slight reduction. It may be pointed out that the synchronizing torque is expressed as a % and not in actual quantity. In fact to determine the change in synchronizing torque component, it is necessary to compare actual magnitude of the modal torque to make a comparison between the cases with and without damping control. This is not possible at present because of the scaling problem associated with the eigenvectors of state matrices having different sizes.

Table (6.5): Modal torque components for the weakened operating condition

Case	Local mode of G30		Interarea mode	
	M-ω	M-δ	M-ω	M-δ
No damping control	1.368%	99.96%	-1.1%	98.9%
PSS(OH)	24.89%	86.6%	12.22%	97.019%
PSS(GD)	29.3%	82.93%	12.78%	96.73%

6.3.4.2   Design of supplementary control on SVC

The supplementary control on SVC is used for damping the interarea mode. A critical part of the supplementary control design is the selection of the SVC for placing this control.

Selection of SVC for installing supplementary control

The criteria for selecting the site for installing damping control has been described in Chapter 5. The selection process involves two aspects

i)   Controllability i.e. how well the existing SVC will be able to control the interarea mode under consideration.

ii)   Observability i.e. how well the information about the interarea mode is observable in the candidate feedback signal.

For selecting a SVC the ability to 'control' the mode under consideration can be determined by the state and voltage participation factors. The use of voltage participation factor for selecting the site (SVC) for installing supplementary control is a new concept introduced in this thesis and is described in detail in Chapters 4 & 5.

The observability of the mode under consideration in the potential feedback signals can be determined by the calculation of the observability factors, described in Chapter 4.

The state participation factors of the dominant device states participating to the interarea mode is given in Table (6.2a). The voltage participation factors of all the device buses for the interarea mode is given in Table (6.6).

The potential feedback signals considered are the line current magnitude (LCUR) and sending end line real power (LMWF). These signals are chosen because these are locally available at the SVC bus in any practical installation. The observability of the interarea mode in these signals is calculated as given in Table (6.7).

On examination of the state and voltage participation factors and also the observability factors a relative ranking of the three SVCs, in accordance to their suitability for installation of supplementary control, is determined as given in Table (6.8).

From Table (6.2a) it can be seen that relative to SVCs S1 & S23, the state participation factors of the states of SVC S16 is higher. the voltage participation factors given in Table (6.6) indicate maximum controllability at SVC S23 followed by SVC S16. Thus from the controllability point of view the state and voltage participating factors indicate S16 to be the best choice for placing supplementary control followed by S23 and then S1.

From the observability point of view the local signals near S1 exhibit a very high observability to the interarea mode compared to the local signals near the other SVCs. Thus the ranking of the SVCs based on the observability criteria is S1 followed by S16 and then S23.

For the potential feedback signals chosen for the three SVCs (LMWF 2-1 for S1, LMWF 16-17 for S16, LCUR 23-22 for S23), a frequency response is obtained to detect any non-minimum phase behavior. These frequency responses are shown in Figures (6.9a,b & c). The frequency response of all the three feedback signals clearly indicate the presence of the interarea mode shown by the high peak at the frequency of the interarea mode. The phase response of LMWF 2-1 does not exhibit any non-minimum phase behavior. The phase response of LMWF 16-17 indicates the presence of a RHP zero near 1 Hz. which is not very close to the frequency of the interarea

mode. The phase response of LMWF 23-24 indicates a LHP zero which is very close to the frequency of the interarea mode. This signal therefore would not be a good choice as a feedback signal.

Based on the above discussion it can be concluded that S16 with feedback signal LMWF 16-17 and S1 with feedback signal LMWF 2-1 are both suitable choices for the location of the supplementary control. The SVC S23 with feedback signal LCUR 23-24 does not appear to be a promising location for supplementary control. However, to validate these conclusions further, supplementary control is designed for all the three SVCs and their relative performance is compared.

Table (6.6): Voltage participation factors for the interarea mode

Bus No	Device	Sensitivity of eigenvalue to shunt conductance $\frac{d\lambda}{dG}$	Sensitivity of eigenvalue to shunt susceptance $\frac{d\lambda}{dB}$
1	S1	0.0018	0.0051
16	S16	0.0376	0.0532
23	S23	0.0256	0.1247
30	G30	0.0159	0.0425
31	G31	0.0251	0.0468
32	G32	0.0264	0.0543
33	G33	0.0453	0.0910
34	G34	0.0598	0.0982
35	G35	0.0215	0.1576
36	G36	0.0269	0.1607
37	G37	0.0301	0.0491
38	G38	0.0892	0.1253

Table (6.7): Observability of the interarea mode in various signals

Signal	Observability
LMWF 16-19	-0.09 + j0.98056
LCUR 16-19	0.09266 - j1.04333
LMWF 16-21	-0.00994 + j0.08137
LCUR 16-21	-0.00570 + j0.04678
LMWF 16-24	0.01213 + j1.04345
LCUR 16-24	-0.00091 - j1.19291
LMWF 16-17	0.05656 - j1.21123
LCUR 16-17	0.06706 - j1.03185
LMWF 16-15	0.04361 - j0.96239
LCUR 16-15	0.02747 - j0.96545
LMWF 23-22	0.02002 + j0.51927
LCUR 23-22	-0.00696 - j0.56341
LMWF 23-24	-0.02275 - j0.93866
LCUR 23-24	-0.00839 - j1.18512
LMWF 2 - 1	0.05292 + j2.64926
LCUR 2 - 1	0.05834 - j2.47710

Table (6.8): Relative ranking of SVCs for supplementary control

	S1	S16	S23
State participation factors	Poor	Best	Moderate
Voltage participation factors	Poor	Good	Best
Observability of potential feedback signal	LMWF 2-1 Best	LMWF 16-17 Good	LCUR 23-22 Poor

Figure (6.9a)Frequency response LMWF 2-1

190

Frequency response of LMWF 16-17 for input at S16
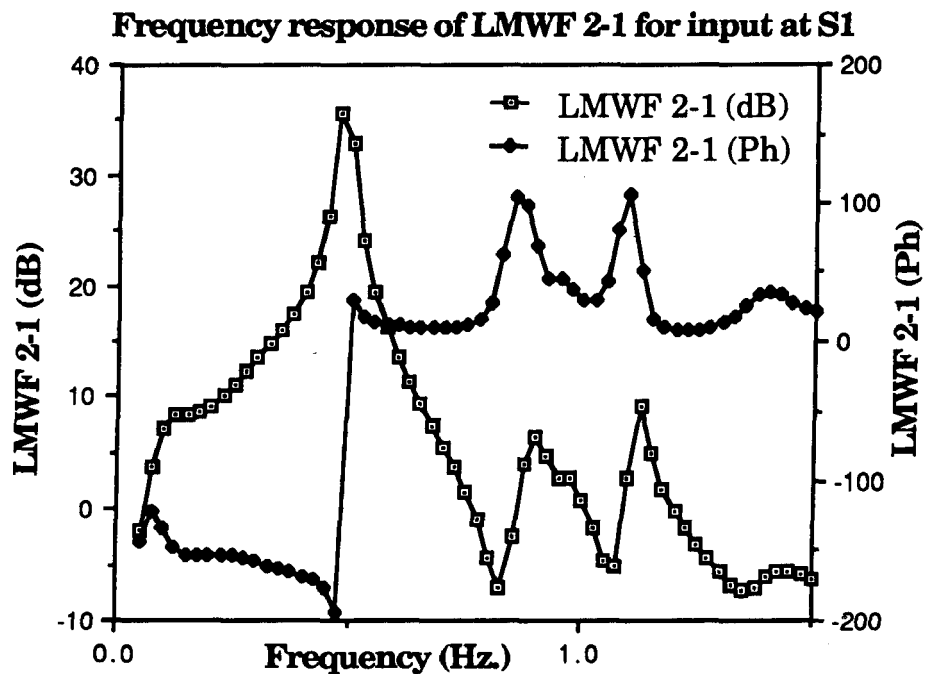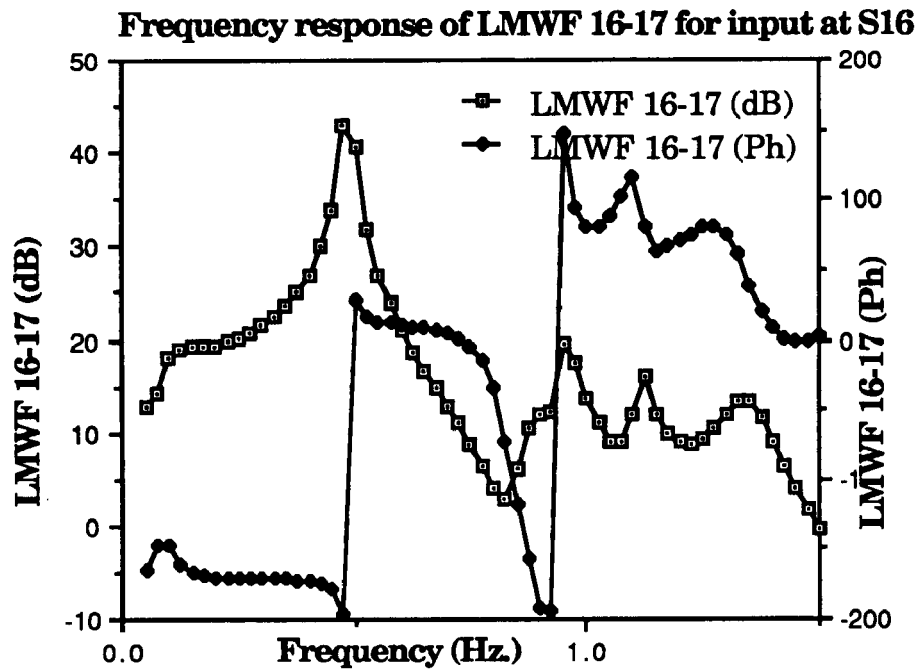
Figure (6.9b)Frequency response LMWF 16-17

Frequency response of LMWF 23-24 for input at S23
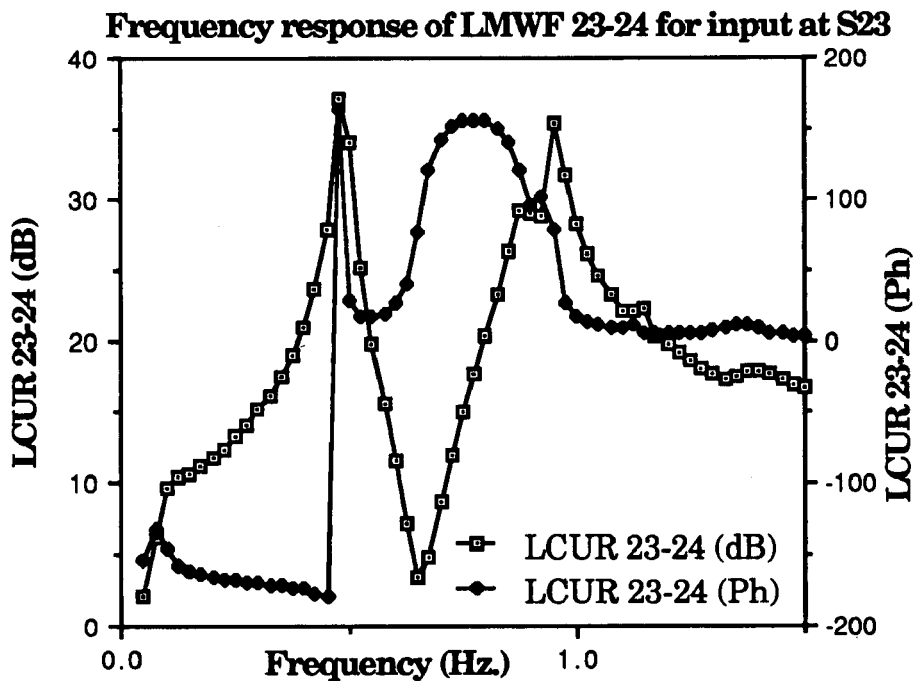
Figure (6.9c)Frequency response LMWF 23-24

Design of supplementary control compensation network

The generalized design method is used to obtain the parameters of the compensation network. The first step is to select the new eigenvalue location to which the interarea mode is to be shifted. The new location is chosen to be (-0.83 + j4.0), satisfying the criteria for selecting new eigenvalue locations described in Chapter 5. The residues of the feedback signals LMWF 2-1, LMWF 16-17 and LCUR 23-24 are obtained at the new eigenvalue location as given in Table (6.9).

Table (6.9): Residue of feedback signals at the location (-0.83 + j4.0)

	Input at S1	Input at S16	Input at S23
LMWF 2-1	2.724 $\angle$-51.92°	-	-
LMWF 16-17	-	6.82 $\angle$-50.38°	-
LCUR 23-24	-	-	5.814 $\angle$-125°

The compensation network has the structure as shown in Figure (6.10). The parameters for each of the three supplementary controls are obtained by satisfying the magnitude, phase criteria and also the criteria for providing maximum phase lead at the frequency of the new eigenvalue location as described in Chapter 5. In all the three designs the washout time constant is chosen to be 10 seconds. The design parameters are given in Table (6.10).
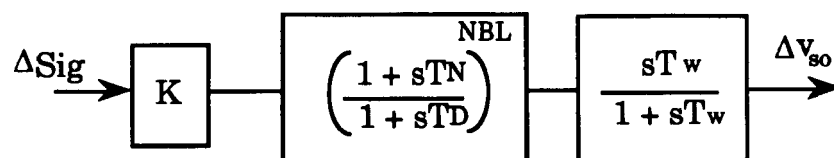
ΔSig = Feedback signal

ΔV_{so} = Supplementary control output

Figure (6.10): Block diagram of supplementary control H(s)

Table (6.10): Supplementary control parameters

	H(-0.83 + j4.0)	NBL	TN	TD	K
S1	0.3671 $\angle$51.92°	2	0.365	0.171	0.1681
S16	0.14655 $\angle$50.38°	2	0.3613	0.173	0.0686
S23	0.17199 $\angle$125°	3	0.473	0.132	0.0242

maximum phase compensation at f_m = 0.637 Hz.
washout time constant T_w = 10.0 seconds

Validation of the SVC supplementary control design

The three supplementary control designs are validated by incorporating the supplementary control into the system model one at a time and determining the eigenvalues for the two operating conditions. Tables (6.11a) to (6.11c) give the electromechanical modes of the weakened operating condition for the three designs. Tables (6.1b) gives the corresponding modes without the damping control. From comparison of the damping ratios given in Table (6.1b) and Tables (6.11a) to (6.11c), it is evident that the supplementary control at S23 has a disastrous effect on the system stability as it introduces unstable eigenvalues (Table (6.11c)). This

design is rejected and the failure of the design can be attributed to the non-minimum phase behavior of the feedback signal used and the fact that the supplementary control at S23 interacts to the local mode of the nearby generating system G36. On the other hand the supplementary control at S1 and S16 provide adequate damping and have shifted the interarea mode to the desired location. The performance of the supplementary control at S16 is marginally better than that of the supplementary control at S1 because all the electromechanical modes (Table (6.11b)) have a damping ratio greater than the cutoff level of 0.02.

Table (6.11a): Electromechanical modes and participating devices
Weakened operating condition with damping control at S1

No.	Electromechanical mode	Damping ratio	Participating devices
1	-0.3064 + j8.4206	0.03636	G33 <-> G34
2	-0.5055 + j8.7741	0.05752	G30 <-> G37
3	-0.4214 + j8.8006	0.04782	G36 <-> G35
4	-0.2791 + j7.4491	0.03744	G32 <-> G31
5	-0.2201 + j7.1418	0.03080	G30 <-> Rest of the system
6	-0.1006 + j5.9776	0.01682	G35 <-> G35, G36
7	-0.2279 + j6.1693	0.03691	G31, G32 <-> G34, G38
8	-0.4433 + j5.6763	0.07785	G38 <-> G35, G36, S16
9	-0.8556 + j3.9866	0.20983	∞ bus(39) <-> Rest of the system

Table (6.11b): Electromechanical modes and participating devices
Weakened operating condition with damping control at S16

No.	Electromechanical mode	Damping	Participating devices
1	-0.4149 + j8.6258	0.04804	G33 <-> G37
2	-0.2901 + j8.7817	0.03302	G33 <-> G37
3	-0.418 + j8.8021	0.04743	G36 <-> G35
4	-0.2843 + j7.455	0.03811	G32 <-> G31
5	-0.1613 + j7.0553	0.02285	G30 <-> Rest of the system
6	-0.1702 + j5.9303	0.02869	G34 <-> G35, G36
7	-0.2406 + j6.1563	0.03906	G31, G32 <-> G38
8	-0.3820 + j5.4438	0.07000	G38, G35, G34 <-> S16
9	-0.8596 + j3.9793	0.21115	∞ Bus(39) <-> Rest of the system

Table (6.11c): Electromechanical modes and participating devices
Weakened operating condition with damping control at S23

No.	Electromechanical mode	Damping
1	-0.4274 + j8.7581	0.04875
2	-0.4567 + j8.8067	0.05179
3	-0.2816 + j8.3627	0.03365
4	-0.2791 + j7.4492	0.03744
5	-0.1013 +j7.0178	0.01444
6	-0.1794 + j6.1398	0.02921
7	-0.1754 + j5.7973	0.03024
8	-0.8226 + j4.0144	0.20074
9	-0.7570 + j2.8379	0.25772
Unstable eigenvalues from supplementary control at S23		
	+290.5447	
	+48.0662	

The locations of the electromechanical modes for the weakened operating condition without the damping control, with the supplementary control at S16 and at S1 is given in Figure (6.12a). The arrow indicates the shift of the interarea mode from its original location to the new assigned location.

Electromechanical modes for weakened operating condition
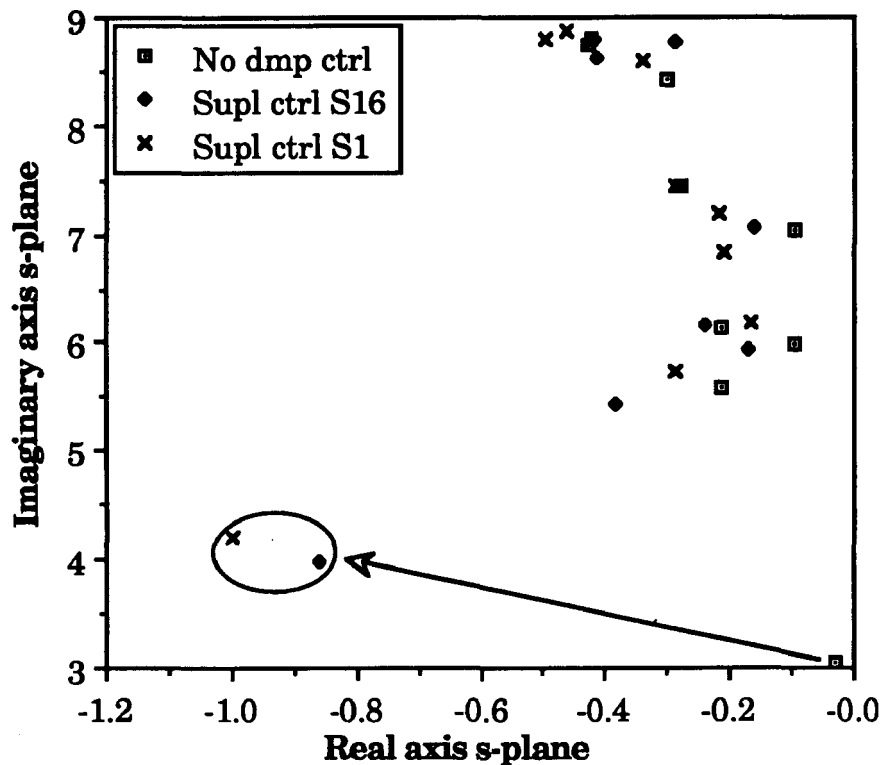
Figure (6.12a)Electromechanical modes-weakened operating condition-
S1&S16

The performance of the supplementary control at S1 and S16 is also examined under the nominal operating condition. Tables (6.12a) and (6.12b) give the electromechanical modes for the two supplementary control designs. It is seen that for both the designs there is no mode with damping ratio less than 0.02 and that the interarea mode is well damped. Thus there is no need for any modification in the supplementary control based on the system performance under the nominal operating condition.

Table (6.12a): Electromechanical modes under nominal operating condition
with supplementary control at S1

No.	Electromechanical mode	Damping	Participating devices
1	-0.3394 + j8.6012	0.03943	G33 <-> G34, G36
2	-0.4973 + j8.7898	0.05648	G37 <-> G30
3	-0.4640 + j8.8626	0.05228	G36 <-> G35
4	-0.2881 + j7.4332	0.03873	G32 <-> G31
5	-0.2197 + j7.1833	0.03057	G30 <-> Rest of the system
6	-0.2080 + j6.8423	0.03039	G36, G35 <-> G34
7	-0.1657 + j6.1867	0.02678	G31, G32 <-> G34
8	-0.2872 + j5.7461	0.04992	G38 <-> G34
9	-1.0012 + j4.2021	0.23178	∞ BUS(39) <-> Rest of the system

Table (6.12b): Electromechanical modes under nominal operating condition
with supplementary control at S16

No.	Electromechanical mode	Damping	Participating devices
1	-0.3055 + j8.8451	0.03452	G33 <-> G37
2	-0.4074 + j8.6643	0.04696	G37 <-> G33
3	-0.4590 + j8.8568	0.05176	G36 <-> G35
4	-0.2867 + j7.4383	0.03851	G32 <-> G31
5	-0.1573 + j6.9000	0.02279	G30 <-> rest of the system
6	-0.4522 + j7.2967	0.06185	G35, G36 <-> G30
7	-0.2156 + j6.1788	0.03487	G31,G32 <->G34,G38
8	-0.5102 + j5.6248	0.09034	G34, G38 <-> S16
9	-0.7234 + j4.0656	0.17518	∞ bus(39) <-> rest of the system

The location of the electromechanical modes in the complex s-plane for the nominal operating condition with and without supplementary control on S1 and S16 is shown in Figure (6.12b). The arrow indicates the shift in the interarea mode from its original location due to the supplementary control.

Electromechanical modes for nominal operating condition
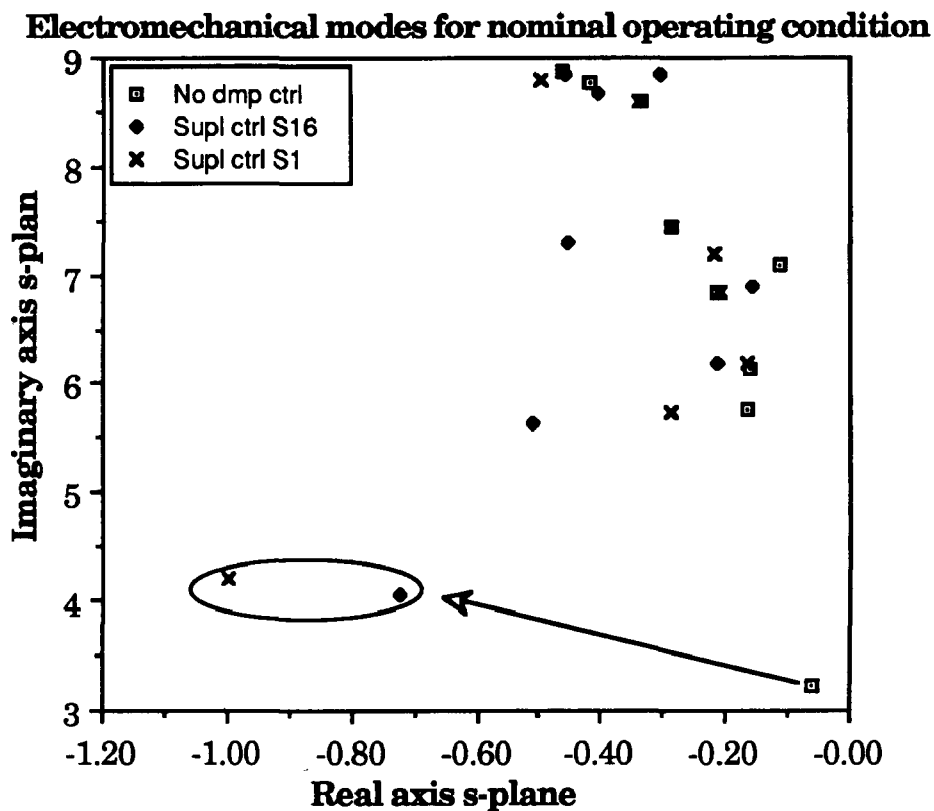
Figure (6.12b)Electromechanical modes-nominal operating condition-S1&S16

A final check of the design is made through the calculation of the damping and synchronizing torque components for the interarea mode to see if any beneficial changes have been brought about by the introduction of the damping (supplementary) control. The damping component (M-ω) and

the synchronizing component (M-δ) as a percentage of the total modal torque applied to each generating system for the interarea mode is given for the case with and without damping control in Tables (6.13a,b,c). It can be seen that the damping torque component significantly increases for the interarea mode with the introduction of supplementary control.

Table (6.13a): Modal torque components for the interarea mode with no damping control

Generating system	M-ω	M-δ
G30	-1.1%	98.9%
G31	1.0%	99.0%
G32	1.1%	98.9%
G33	1.1%	98.9%
G34	1.1%	98.9%
G35	1.1%	98.9%
G36	1.1%	98.9%
G37	1.0%	99.0%
G38	1.1%	98.9%

Table (6.13b): Modal torque components for the interarea mode with damping control at S1

Generating system	M-ω	M-δ
G30	21.021%	91.347%
G31	20.932%	91.207%
G32	20.957%	91.252%
G33	20.997%	91.214%
G34	20.985%	91.194%
G35	20.982%	91.165%
G36	20.989%	91.209%
G37	20.993%	91.046%
G38	20.969%	91.149%

Table (6.13c): Modal torque components for the interarea mode with damping control at S16

Generating system	M-ω	M-δ
G30	21.200%	91.100%
G31	21.100%	91.100%
G32	21.100%	91.100%
G33	21.100%	91.400%
G34	21.100%	91.000%
G35	21.100%	91.100%
G36	21.100%	91.100%
G37	21.100%	91.100%
G38	21.100%	91.100%

The damping torque (S-ω) and synchronizing torque (S-δ) contributed by the three SVCs individually for the cases with and without damping control is given in Tables (6.14a,b,c). It can be seen that SVC has a negative damping effect on the interarea modes in the absence of any supplementary control. Introduction of supplementary control increases the damping torque contribution of the corresponding SVC significantly.

Table (6.14a): Modal torque contributions from SVCs with no damping control

	S23-ω	S23-δ	S16-ω	S16-δ	S1-ω	S1-δ
G30	-0.342%	3.087%	-0.723%	8.332%	-0.105%	1.707%
G31	-0.314%	5.051%	-0.454%	11.837%	-0.017%	1.306%
G32	-0.314%	5.752%	-0.422%	13.568%	-0.008%	1.413%
G33	-0.581%	7.211%	-1.069%	18.654%	-0.040%	1.258%
G34	-1.300%	7.092%	-2.624%	15.911%	-0.135%	0.965%
G35	-1.500%	21.148%	-6.557%	14.656%	-0.018%	0.889%
G36	-1.600%	18.067%	-0.913%	14.327%	-0.033%	0.883%
G37	-0.469%	6.513%	-0.770%	15.780%	-0.071%	3.089%
G38	-0.412%	5.107%	-0.646%	11.239%	-0.054%	1.643%

Table (6.14b): Modal torque contributions from SVCs with damping control at S1

	S23-ω	S23-δ	S16-ω	S16-δ	S1-ω	S1-δ
G30	0.194%	1.59%	-0.509%	-0.535%	57.431%	47.222%
G31	-0.136%	2.730%	-6.759%	-1.995%	35.958%	44.554%
G32	-0.113%	3.115%	-7.867%	-2.190%	39.962%	47.829%
G33	-0.738%	3.678%	-9.045%	-4.545%	24.689%	45.916%
G34	-1.065%	2.969%	-5.569%	-4.316%	10.094%	32.266%
G35	-3.076%	0.957%	-5.737%	-4.048%	11.404%	31.503%
G36	-2.700%	0.835%	-5.751%	-4.066%	11.608%	32.157%
G37	-0.873%	3.604%	-11.136%	0.073%	128.894%	80.361%
G38	-1.218%	2.629%	-8.272%	1.454%	79.031%	29.399%

Table (6.14c): Modal torque contributions from SVCs with damping control at S16

	S23-ω	S23-δ	S16-ω	S16-δ	S1-ω	S1-δ
G30	-1.267%	-0.311%	11.231%	32.087%	-0.631%	0.196%
G31	-2.254%	-0.333%	21.132%	45.238%	-0.501%	0.200%
G32	-2.631%	-0.288%	26.769%	51.692%	-0.548%	0.237%
G33	-3.395%	-0.228%	40.494%	69.840%	-0.490%	0.232%
G34	-2.366%	-0.208%	23.566%	42.960%	-0.278%	0.122%
G35	-8.993%	-1.408%	24.633%	54.154%	-0.327%	0.127%
G36	-7.953%	-1.136%	25.486%	54.043%	-0.335%	0.135%
G37	-2.927%	-0.364%	29.522%	59.512%	-1.175%	0.491%
G38	-2.412%	-0.231%	23.424%	43.580%	-0.648%	0.288%

In the study presented above it has been shown that the supplementary control on SVC can be used to improve the damping of the interarea mode. From the study of the test system presented the following interesting observations are also made:

i)   If any mode is significantly observable in the feedback signal of the SVC supplementary control then this mode will also be affected by the supplementary control. Comparison of Tables (6.1b) & (6.11b) shows that the local mode of G34 (mode No.6) is better damped after the supplementary control is installed on S16.

ii)   Supplementary control on SVC can also change the devices participating in a particular mode. This may lead to change in the mode shape. For example in Table (6.1b) the generating system G38 which was swinging against G35 for mode No. 8 ; starts swinging against SVC S16 after supplementary control was put on S16.

6.3.5   Comparison of PSS and supplementary control performance

The performance is compared for the effect on the interarea mode, and it can be seen that both are equally effective in achieving the desired damping of the interarea mode.. Thus, the choice of damping control between PSS and supplementary control on SVC to increase the damping of interarea modes depends mostly on practical considerations. However, there are certain differences on the basis of application which are pointed out. The PSS is installed on a generating system which is the source of the electromechanical oscillations, thus, it has an inherently better

controllability than the supplementary control on SVC. The PSS is used to damp local, intermachine and interarea modes, whereas the supplementary control on SVC is recommended only for increasing the damping of interarea modes as the interarea mode spreads throughout the system and is not primarily localized to one generating system. Also, even for different operating conditions the characteristics of the interarea mode will not drastically change and a properly designed supplementary control on SVC will be capable of handling the requirements of different operating conditions. If the supplementary control on a SVC is used to damp local or intermachine modes then the performance of this damping control will depend on whether the mode under consideration exists under different operating conditions (i.e. if for a particular operating condition the concerned generating system is out of service, thus eliminating the local mode to be damped).

6.4   Conclusions

This chapter presents the development of a versatile Small Signal Stability (S^3) program based on the models and analysis techniques outlined in the previous chapters. the program has the capability and features which are comparable to the MASS program of Ontario Hydro. Utilizing this program a case study of the Modified 39-bus New England Area system is carried out to improve the system small signal stability. The damping control is implemented through PSS on generating system and supplementary control on SVC. Both the frequency response method and

the generalized design method have been used for the systematic design of the PSS, while the generalized design method is used for the design of supplementary control. Both these design methods involve the selection of suitable site, selection of suitable feedback signal and design of the compensation network. The selection of the suitable SVC for installing the damping control is based on a new concept of the use of voltage participation factor introduced in this thesis. The results obtained form the case study can be summarized as follows.

i)   The design of PSS using the frequency response and the generalized design method yield similar parameters of the compensation network and hence the generalized design method can be claimed to be equally robust as the frequency response method.

ii)   The PSS increases the damping of the modes in which the corresponding generating system participates.

iii)   The design of supplementary control on SVC using generalized design method is quite effective in improving the damping of the interarea mode.

iv)   The effectiveness of the supplementary control on a suitable SVC validates the new criteria introduced in this thesis involving the use of voltage participation factors and observability factors for the selection of a suitable site for installing the damping control.

v)   The modal torque calculations provide a clear understanding about the variations in the damping and synchronizing torque components for a particular mode. This helps in obtaining a better understanding of the dynamic behavior of the power system.

Chapter 7

Conclusions

7.1 General

This thesis establishes guidelines to aid a system planning engineer in designing damping control to enhance the small signal stability of power systems. In this context this thesis primarily deals with the following two aspects:

i) Development of a generalized procedure for the design of damping control to improve the small signal stability of a power system.

ii) Certain innovations in the techniques for better understanding of the small signal stability problem and effective design of damping control.

The proposed design procedure begins with a comprehensive investigation to get an in-depth understanding of the nature of the small signal stability problem existing in the power system using appropriate representation of the power system in the linearized domain. This is followed by the suitable design of damping control which involves the following steps:

i) selection of the type of damping control.

ii) selection of site for installing damping control

206

iii)   selection of the feedback signal

iv)   determination of the parameters of the damping control compensation network

v)   validation of the design.

The types of damping control considered here are the Power System Stabilizer (PSS) on the generating system and the supplementary control on SVC. The design procedure is general enough and can be extended for the design of damping control on other devices like HVDC transmission and Flexible AC Transmission System (FACTS) elements.

To examine the small signal stability problem and design the damping control, the power system is represented in the linearized state space framework as described in Chapter 2. The development of the power system model proceeds in a systematic manner by first deriving the constituent component models of the power system (devices and transmission network) which are then interfaced to result in the overall state space model. This modular approach of developing system model permits flexibility in representing any device or component to any desired degree of detail. Also, new models for various devices can be conveniently incorporated.

The small signal stability problem of power system can be examined using various techniques described in Chapter 3. These techniques, some of which are used for the design of damping control are,

i)   Eigenvalue/eigenvector analysis to identify the poorly damped electromechanical modes and their mode shapes. This analysis

technique is also used for final validation of the damping control design.

ii)   Application of state participation factors to identify the devices having the largest participation to the mode under consideration.

iii)   Application of the frequency response method for the selection of suitable feedback signal to the damping control. This method is also used for damping control design.

iv)   Application of time response methods for damping control design

v)   Application of residue calculations for the design of damping control.

The above techniques have been supplemented by three new techniques proposed in this thesis. These proposed techniques are:

i)   Application of modal torque calculations to get an in-depth understanding of the interactions between various devices and for damping control design validation.

ii)   Application of voltage participation factors for the selection of site for supplementary control on SVC.

iii)   Application of observability factors for the selection of the most suitable feedback signal to the damping control.

The concept of modal torques is an entirely new concept introduced in this thesis. For a particular electromechanical mode the modal torque gives the torque applied to the rotating parts of the generating system. This torque can be split into the damping and synhronizing torque components which, respectively, determine the damping and the ability of the system to restore itself to a steady state operating point. These torque components can also be used to determine in a quantitative and qualitative manner the

dynamic interaction between the various constituent system devices. The method of calculating the modal torque and its components is given in Chapter 4.

Voltage participation factor is a new sensitivity index developed by Ontario Hydro which gives the sensitivity of the mode under consideration to changes in the shunt and series admittance. The procedure to derive this factor is given in Chapter 4. This sensitivity index can be used to study the effect of static or dynamic shunt and series admittance i.e. loads, SVCs etc. on system small signal stability. Based on this, a criteria for the selection of site for installing damping control (specifically supplementary control on SVC) is proposed in this thesis.

Observability factors determine, in control system terminology, the 'observability' of a signal to a particular mode. The criteria for the selection of a suitable feedback signal to the damping control is based on the use of this observability factor. This is a well known concept in control theory and has been applied to the complex power system model through a novel method, described in Chapter 4, for calculating the observability factor of any system signal described as a function of the system states.

A generalized procedure for the design of damping control as described in Chapter 5, therefore, involves the selection of site based on the controllability of a device and the observability of the feedback signal to the mode under consideration; and the determination of the parameters of the compensation network of the damping control based on a pole placement technique. The robustness of the standard pole placement technique for the

design of damping control is achieved by certain innovations in selecting the location of the mode to be shifted and the phase characteristics of the compensation network of the damping control.

Based on the above design procedure and incorporating the system model derived in Chapter 2, a Small Signal Stability (S^3) program has been developed for small signal stability studies and design of damping control as described in Chapter 6. The modular structure of the program and certain features make the program extremely flexible. The capability and features of the (S^3) program are comparable to the MASS program developed at Ontario Hydro [1]. This program has been utilized to demonstrate the effectiveness of various analysis techniques and validate the generalized design procedure proposed in this thesis through an extensive case study of a 39-bus test system.

From the results of the case study the following general conclusions are drawn.

i) The generalized design procedure proposed in this thesis is as effective as the robust frequency response method for the design of PSS.

ii) The use of voltage participation factors and observability factors for the selection of suitable site and feedback signal for the damping control increases the effectiveness of the supplementary control on SVC in damping interarea modes.

iii) Modal torque calculations which can be used to validate a proposed design provides a better understanding about the dynamic behavior of the power system.

7.2 Major contributions of the thesis

The major contributions of this thesis are summarized below.

i) The development of a procedure for a quantitative and qualitative assessment of the dynamic interaction between the various constituent system devices through the calculation of the damping and synchronizing torque components for the mode under consideration. These modal torque components reveal the effect of various system devices on the small signal and transient stability of the power system.

ii) The development of a procedure to select a suitable site for the location of the damping control on a device. This is based on the controllability of the device and the observability of the feedback signal to the the mode under consideration. The controllability of a device to a particular mode is determined through the use of its state and voltage participation factors. The observability of any feedback signal to the mode under consideration is determined through the calculation of the observability factor for the feedback signal described as a function of the system states. The use of voltage participation factors and the method of calculating the observability factors are new contributions of this thesis.

iii) Certain innovations introduced in the standard pole placement technique have resulted in the robust design of damping control using the generalized design procedure proposed in this thesis.

iv) The development of the state-of the-art Small Signal Stability (S^3) program for small signal stability studies and design of damping

control. The capability and features of this program are comparable to that of MASS program developed at Ontario Hydro. The program is structured in a manner so that modifications can be easily accommodated without tedious and extensive changes.

7.3 Future scope of work

This thesis establishes certain guidelines for detailed investigation of the small signal stability problem and robust design of damping control. These guidelines should be further validated on systems having other dynamic devices not considered here like nonlinear loads, HVDC transmission, Flexible AC Transmission System (FACTS) elements. This will require augmenting the power system model developed in this thesis with appropriate representation of these elements.

Based on the case studies presented in this thesis the proposed generalized design procedure for damping control design has been shown to be robust. Further improvements in the design philosophy to ensure robustness can be obtained by the use of advanced techniques such as the $H\infty$ control concept.

The Small Signal Stability (S^3) program developed in this thesis is well suited to handle moderately sized power systems. To study large power systems the program efficiency should be enhanced by using alternative numerical techniques like sparse vector method for storing the network admittance matrix. Also, use of other algorithms for the

calculation of eigenvalues and eigenvectors which would take advantage of the sparsity of the network admittance matrix and would not need to formulate the huge system state matrix can be explored.

Appendix 1 - Miscellaneous Topics

A1.1 Example of the formulation of the system state matrix

The formulation of the system state matrix from the individual state space equations is described in this section. The general form all the individual device state space equations must take is;

$$[\dot{X}_d] = [A_d] [X_d] + [B_d] [\Delta V_d] \qquad (A1.01)$$

$$[\Delta I_d] = [C_d] [X_d] - [Y_d] [\Delta V_d] \qquad (A1.02)$$

where,

$[A_d]$ = Device state matrix.

$[B_d]$ = Device input distribution matrix.

$[C_d]$ = Device output distribution matrix for the device states.

$[Y_d]$ = Device admittance matrix.

$[X_d]$ = Device state matrix.

$[\Delta V_d]$ = Vector of all bus voltage changes which are inputted to this device, in the D, Q coordinates.

$[\Delta I_d]$ = Vector of all changes in current injections in the D, Q coordinates, from this device.

214

Figure (A1.1) shows a sample 5-Bus system. This system contains four devices A,B,C and D. Devices A and B are connected to the same bus i.e. Bus-2. Devices B and C have remote sensing buses. The remote sensing bus for device B is Bus-1. The remote sensing bus for device C is Bus-4. Bus-1,Bus-2 and Bus-3 are therefore device buses , Bus-4 is a remote sensing bus and Bus-5 is the load bus.
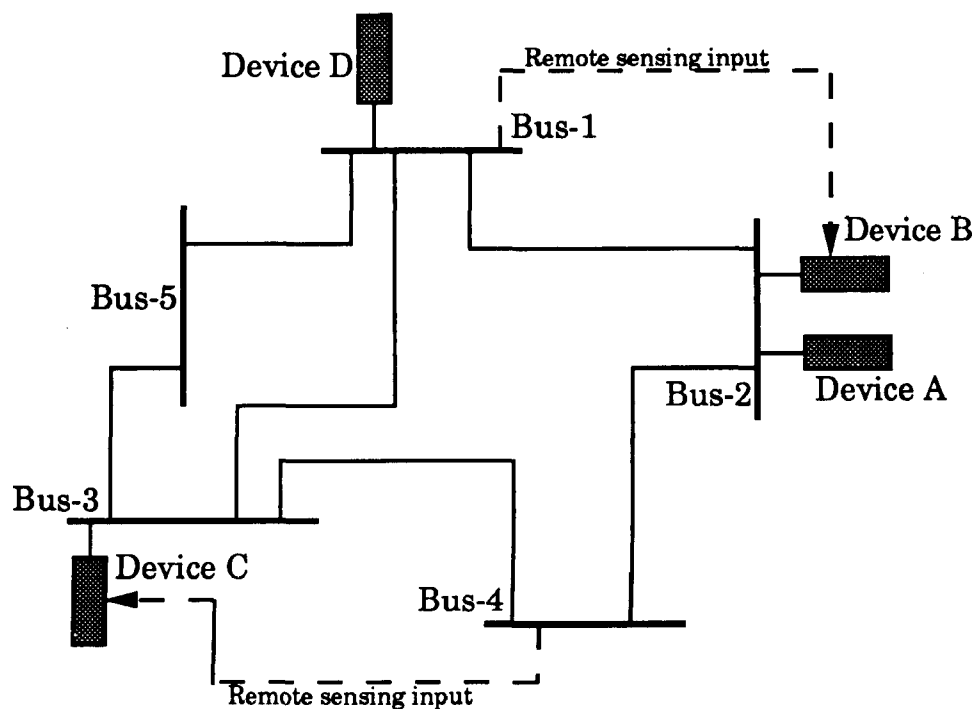

Figure (A1.1) Sample 5-bus system.

The individual device state space equations are:

Device A:

$$[\dot{X}_a] = [A_a] [X_a] + [B_{a2}] [\Delta v_2] \qquad (A1.03)$$

$$[\Delta i_a] = [C_a] [X_a] - [Y_{ad2}] [\Delta v_2] \qquad (A1.04)$$

Device B:

$$[\dot{X}_b] = [A_b] [X_b] + [B_{b2}] [\Delta v_2] + [B_{b1}] [\Delta v_1] \qquad (A1.05)$$

$$[\Delta i_b] = [C_b] [X_b] - [Y_{bd2}] [\Delta v_2] - [Y_{bd1}] [\Delta v_1] \qquad (A1.06)$$

Device C:

$$[\dot{X}_c] = [A_c] [X_c] + [B_{c3}] [\Delta v_3] + [B_{c4}] [\Delta v_4] \qquad (A1.07)$$

$$[\Delta i_c] = [C_c] [X_c] - [Y_{cd3}] [\Delta v_3] - [Y_{cd4}] [\Delta v_4] \qquad (A1.08)$$

Device D:

$$[\dot{X}_d] = [A_d] [X_d] + [B_{d1}] [\Delta v_1] \qquad (A1.09)$$

$$[\Delta i_d] = [C_d] [X_d] - [Y_{dd1}] [\Delta v_1] \qquad (A1.10)$$

where;

$[X_a]$, $[X_b]$, $[X_c]$, $[X_d]$ = State vectors of the devices A, B, C and D.

$[A_a]$, $[A_b]$, $[A_c]$, $[A_d]$ = State matrices of devices A, B, C and D.

$[B_{a2}]$, $[B_{b2}]$, $[B_{b1}]$, $[B_{c3}]$, $[B_{c4}]$, $[B_{d1}]$ = Input distribution matrices for the individual device buses and remote sensing buses.

$[C_a]$, $[C_b]$, $[C_c]$, $[C_d]$ = Individual device output distribution matrix for the device states.

$[Y_{ad2}]$, $[Y_{bd2}]$, $[Y_{bd1}]$, $[Y_{cd3}]$, $[Y_{cd4}]$, $[Y_{dd1}]$ = Individual device admittance matrix.

$[\Delta v_1]$, $[\Delta v_2]$, $[\Delta v_3]$, $[\Delta v_4]$ = Bus-1, Bus-2, Bus-3 and Bus-4 voltage changes respectively

$[\Delta i_a]$, $[\Delta i_b]$, $[\Delta i_c]$, $[\Delta i_d]$ = Device A, B, C and current injection changes into the power system respectively.

The linearized algebraic equation describing the passive interconnecting network is

$$[\Delta I] = [Y_N] [\Delta V] \tag{A1.11}$$

where;

$$[\Delta I] = \begin{bmatrix} \Delta i_1 \\ \Delta i_2 \\ \Delta i_3 \\ \Delta i_4 \\ \Delta i_5 \end{bmatrix} = \text{Changes in the current injections into the individual buses.}$$

$[Y_N]$ = Linearized admittance matrix of the interconnecting power system.

$$[\Delta V] = \begin{bmatrix} \Delta v_1 \\ \Delta v_2 \\ \Delta v_3 \\ \Delta v_4 \\ \Delta v_5 \end{bmatrix} = \text{Changes in the individual bus voltages.}$$

From Equation (A1.04), (A1.06), (A1.08), (A1.10), (A1.11), one can get;

$$[\Delta i_1] = [\Delta i_d] \tag{A1.12}$$

$$[\Delta i_2] = [\Delta i_a] + [\Delta i_b] \tag{A1.13}$$

$$[\Delta i_3] = [\Delta i_c] \tag{A1.14}$$

$$[\Delta i_4] = 0 \tag{A1.15}$$

$$[\Delta i_5] = 0 \tag{A1.16}$$

From Equation (A1.12) to (A1.16) and Equation (A1.11) one can get;

$$[\Delta I] = [C_{st}] \ [X] - [Y_{st}] \ [\Delta V] \tag{A1.17}$$

where,

$$[X] = \begin{bmatrix} X_a \\ X_b \\ X_c \\ X_d \end{bmatrix} ; [C_{st}] = \begin{bmatrix} C_d & 0 & 0 & 0 \\ 0 & C_a & C_b & 0 \\ 0 & 0 & C_c & 0 \\ 0 & 0 & 0 & 0 \\ 0 & 0 & 0 & 0 \end{bmatrix}$$

$$[Y_{st}] = \begin{bmatrix} Y_{dd1} & 0 & 0 & 0 & 0 \\ Y_{bd1} & Y_{ad2} + Y_{bd2} & 0 & 0 & 0 \\ 0 & 0 & Y_{cd3} & Y_{cd4} & 0 \\ 0 & 0 & 0 & 0 & 0 \\ 0 & 0 & 0 & 0 & 0 \end{bmatrix}$$

Stacking Equations (A1.03), (A1.05), (A1.07) and (A1.09) together gives,

$$[\dot{X}] = [A_{st}] \ [X] + [B_{st}] \ [\Delta V] \tag{A1.18}$$

where,

$$[A_{st}] = \begin{bmatrix} A_d & 0 & 0 & 0 \\ 0 & A_a & 0 & 0 \\ 0 & 0 & A_b & 0 \\ 0 & 0 & 0 & A_c \end{bmatrix} ; [B_{st}] = \begin{bmatrix} 0 & B_{a2} & 0 & 0 & 0 \\ B_{b1} & B_{b2} & 0 & 0 & 0 \\ 0 & 0 & B_{c3} & B_{c4} & 0 \\ B_{d1} & 0 & 0 & 0 & 0 \end{bmatrix}$$

From Equation (A1.17), (A1.18) and (A1.11) the state matrix [A] of the system is,

$$[A] = [A_{st}] + [B_{st}] [Y_N + Y_{st}]^{-1} [C_{st}] \qquad \text{(A1.19)}$$

A1.2 State space equations of elementary control blocks

The elementary state space equations for the following elementary blocks are given.

i)Lag block: $\qquad \dfrac{1}{1 + sT}$

The block diagram of this transfer function is shown in Figure (A1.2).
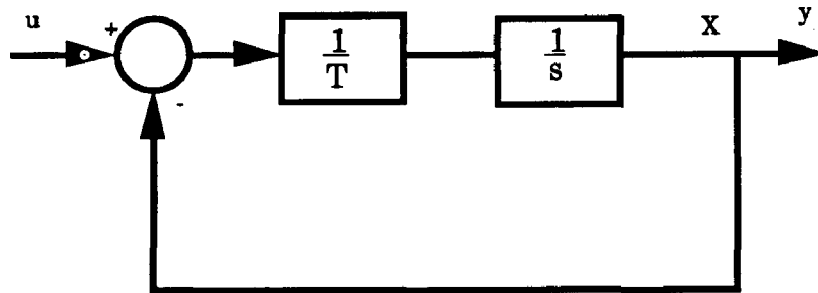
Figure (A1.2) Lag block transfer function

The elementary state space equation for this block is

$$\dot{X} = -\frac{1}{T} X + \frac{1}{T} u \qquad \text{(A1.20)}$$

$$y = X \qquad \text{(A1.21)}$$

In this case the output of the block is the state.

ii) Lead/Lag block: $\qquad \dfrac{1 + sT_1}{1 + sT_2}$

The block diagram of this transfer function is shown in Figure (A1.3).
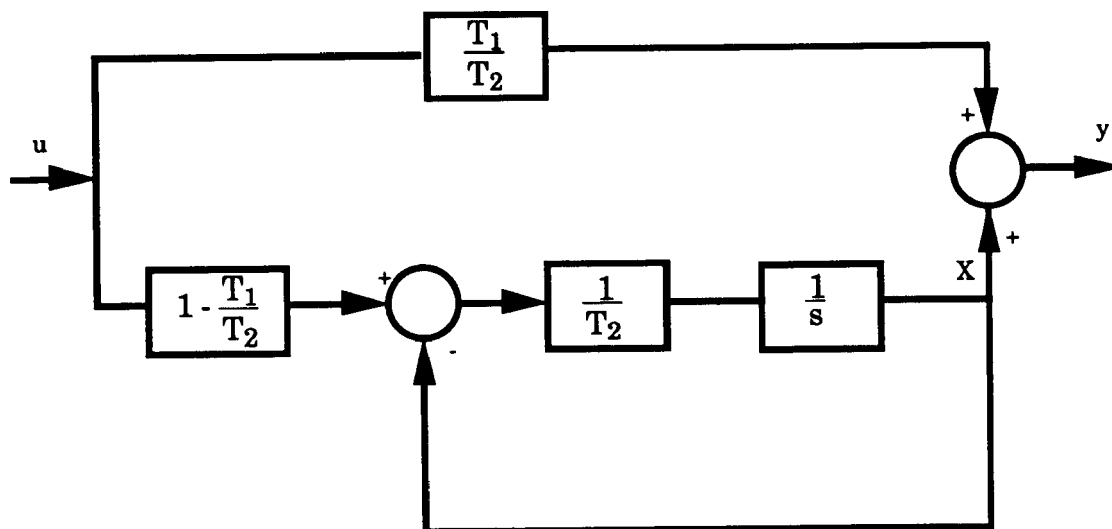
Figure (A1.3) Lead/Lag block transfer function

The elementary state space equation for this block is

$$\dot{X} = -\frac{1}{T_2} X + \frac{T_2 - T_1}{T_2{}^2} u \qquad\qquad (A1.22)$$

$$y = X + \frac{T_1}{T_2} u \qquad\qquad (A1.23)$$

ii) Washout block: $\qquad \dfrac{sT}{1 + sT}$

The block diagram of this transfer function is shown in Figure (A1.4).
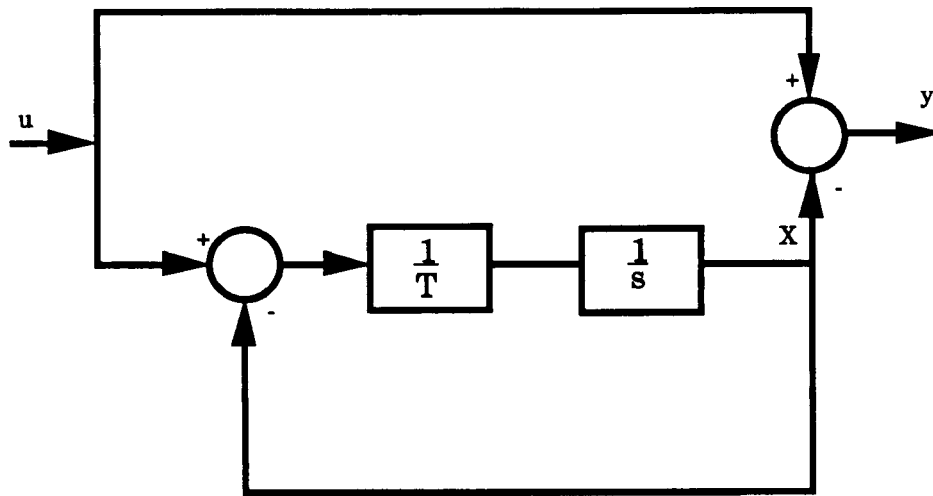
Figure (A1.4) Washout block transfer function

The elementary state space equation for this block is

$$\dot{X} = -\frac{1}{T} X + \frac{1}{T} u \qquad \text{(A1.24)}$$

$$y = -X + u \qquad \text{(A1.25)}$$

A1.3 State space equations of a sample control system

The elementary state space equations for a control system are:

$$[\dot{X}] = [A] [X] + [B] [u] \qquad \text{(A1.26)}$$

$$[y] = [C] [X] + [D] [u] \qquad \text{(A1.27)}$$

$$[u] = [L] [y] + [G] [i] \qquad \text{(A1.28)}$$

$$[z] = [M] [y] + [K] [i] \qquad \text{(A1.29)}$$

where,

[X] = State vector of the control system.

$$[\dot{X}] = \frac{d}{dt} [X]$$

[u] = Vector of the inputs to all the individual blocks.

[y] = Vector of the outputs from all the individual blocks.

[i] = Vector of the actual external inputs to the control system.

[z] = Vector of the actual outputs from the control system.

[A], [B], [C], [D] = Matrices assembled from the stacking of the state space equations of each individual control block.

[L] = Matrix describing the interconnections between the various elementary blocks present in the control system.

[G] = Matrix describing the distribution of the external inputs to the control system.

[M] = Matrix describing the contributions of the outputs of the various internal elementary blocks to each of the final outputs to the external world from the control system.

[K] = Feedforward matrix describing the contributions of the external inputs to the final output of the control system.

The method developing the matrices [A], [B], [C], [D], [L], [G], [M] and [K] are illustrated by an example. Figure (A1.5) shows the block diagram of the transfer function of the excitation system of the synchronous machine.
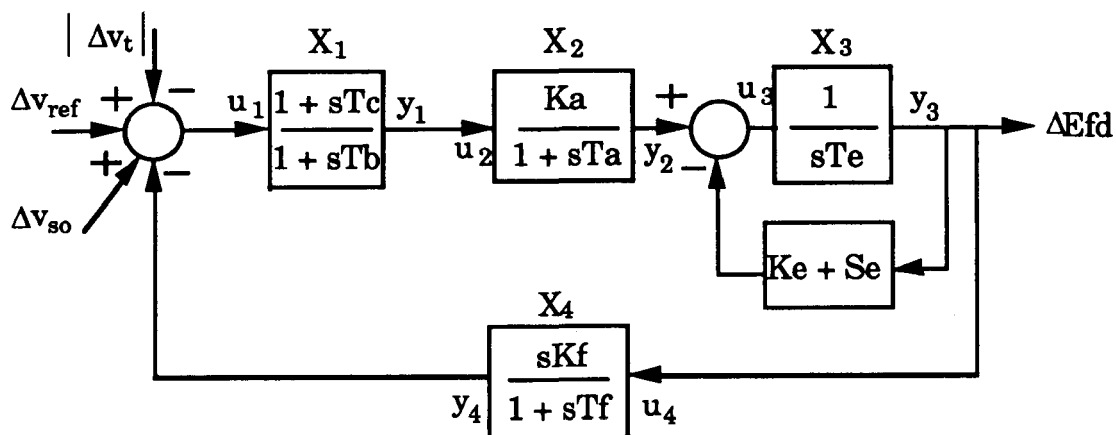
Figure (A1.5) Exciter block diagram.

The state space equations describing this system are

$$[\dot{X}] = [A] [X] + [B] [u] + [B_{ss}] [\Delta v_{so}] \qquad (A1.30)$$

$$[y] = [C] [X] + [D] [u] + [D_{ss}] [\Delta v_{so}] \qquad (A1.31)$$

$$[u] = [L] [y] + [G] [i] \qquad (A1.32)$$

$$\Delta Efd = [M] [y] + [K] [i] \qquad (A1.33)$$

where,

$$[X] = \begin{bmatrix} X_1 \\ X_2 \\ X_3 \\ X_4 \end{bmatrix} ; [u] = \begin{bmatrix} u_1 \\ u_2 \\ u_3 \\ u_4 \end{bmatrix} ; [y] = \begin{bmatrix} y_1 \\ y_2 \\ y_3 \\ y_4 \end{bmatrix} ; [i] = \begin{bmatrix} \Delta \omega \\ \Delta v_D \\ \Delta v_Q \\ \Delta i_D \\ \Delta i_Q \\ \Delta v_{ref} \end{bmatrix}$$

$$[A] = \begin{bmatrix} \dfrac{-1}{T_b} & 0 & 0 & 0 \\ 0 & \dfrac{-1}{T_a} & 0 & 0 \\ 0 & 0 & \dfrac{-K_e}{T_e} & 0 \\ 0 & 0 & 0 & \dfrac{-1}{T_f} \end{bmatrix} ; [B] = \begin{bmatrix} \dfrac{T_b - T_c}{T_b{}^2} & 0 & 0 & 0 \\ 0 & \dfrac{K_a}{T_a} & 0 & 0 \\ 0 & 0 & \dfrac{1}{T_e} & 0 \\ 0 & 0 & 0 & \dfrac{K_f}{T_f} \end{bmatrix}$$

$$[B_{ss}] = \begin{bmatrix} \dfrac{T_b - T_c}{T_b{}^2} \\ 0 \\ 0 \\ 0 \end{bmatrix} ; [C] = \begin{bmatrix} 1 & 0 & 0 & 0 \\ 0 & 1 & 0 & 0 \\ 0 & 0 & 1 & 0 \\ 0 & 0 & 0 & -1 \end{bmatrix} ; [D] = \begin{bmatrix} \dfrac{T_c}{T_b} & 0 & 0 & 0 \\ 0 & 0 & 0 & 0 \\ 0 & 0 & 0 & 0 \\ 0 & 0 & 0 & \dfrac{K_f}{T_f} \end{bmatrix} ;$$

$$[D_{ss}] = \begin{bmatrix} \dfrac{T_c}{T_b} \\ 0 \\ 0 \\ 0 \end{bmatrix} ; [L] = \begin{bmatrix} 0 & 0 & 0 & -1 \\ 1 & 0 & 0 & 0 \\ 0 & 1 & 0 & 0 \\ 0 & 0 & 1 & 0 \end{bmatrix} ; [M] = [\ 0\ \ 0\ \ 1\ \ 0\ ] ; [K] = [\ 0\ \ 0\ \ 0\ \ 0\ \ 0\ \ 0\ ]$$

$$[G] = \begin{bmatrix} 0 & \dfrac{-v_D}{|v_t|} & \dfrac{-v_Q}{|v_t|} & 0 & 0 & 0 \\ 0 & 0 & 0 & 0 & 0 & 0 \\ 0 & 0 & 0 & 0 & 0 & 0 \\ 0 & 0 & 0 & 0 & 0 & 0 \end{bmatrix}$$

A1.4 Derivation of the state space equation describing the rotating system of a synchronous machine

The steady state kinetic energy or the kinetic energy at the rated synchronous speed of the machine is

$$W_{kin}{}^o = \frac{1}{2} I \omega_0{}^2 \tag{A1.34}$$

Where,

$W_{kin}{}^o$ = Rated kinetic energy of the rotating system of the synchronous machine.

I = Moment of Inertia of the rotating system..

ω_0 = Rated synchronous speed of the system.

The rate of change of kinetic energy is the power input to the rotating system. The rate of change of kinetic energy about the synchronous speed of the system (ω_0) in per unit is

$$\frac{I \, \omega_o}{P_{base}} \frac{d}{dt} \omega \qquad (A1.35)$$

where,

P_{base} = Base power of the system.

ω = Instantaneous speed of the machine (p.u.).

The power input to the rotating system is the difference between the mechanical power input and the electrical power output of the rotating system. Now,

$$T_m = \text{Mechanical power input (p.u.).} \qquad (A1.36)$$

$$\psi_d \, i_q - \psi_q \, i_d = \text{Electrical power output (p.u).} \qquad (A1.37)$$

where,

ψ_d = d-axis stator flux linkages in per unit voltage.

ψ_q = q-axis stator flux linkages in per unit voltage.

i_d = d-axis component of the machine terminal current (p.u.).

i_q = q-axis component of the machine terminal current (p.u.).

From Equation (A1.35) to (A1.37) the following relation can be obtained,

$$\frac{I \, \omega_o}{P_{base}} \frac{d}{dt} \omega = T_m - \psi_d \, i_q - \psi_q \, i_d \qquad (A1.38)$$

Linearizing Equation (A1.38) gives,

$$\frac{2H}{\omega_0} \frac{d}{dt}\Delta\omega = \Delta T_m + \Delta\Psi_q \, i_d - \Delta\Psi_d \, i_q + \Psi_q \, \Delta i_d - \Psi_d \, \Delta i_q \qquad (A1.39)$$

where,

$$H = \frac{W_{kin}^o}{P_{base}} = \text{Inertia constant of the machine (p.u.)}.$$

## A1.5 Calculation of the synchronous machine saturation factors

The synchronous machines magnetic circuit is subject to saturation depending on the operating point. This saturation effects the value of the mutual reactance x_{ad}, x_{aq} of the equivalent circuits shown in Figure 2.3(a) and (b) in Chapter 2. In the program S^3 two types of saturation can be modelled.

i)Saturation in the d-axis represented. The q-axis is assumed to be unaffected by saturation.(ISAT = 1)

ii)Saturation in both the d and q-axis is represented. The q-axis saturation factors are the same as that of the d-axis saturation factors.(ISAT=2)

Figure (A1.6) gives the saturation characteristics. The vertical axis is the flux linkages across the mutual reactance branch x_{ad} in per unit voltage. The horizontal axis is the field current (p.u.) required to produce the required flux linkages.
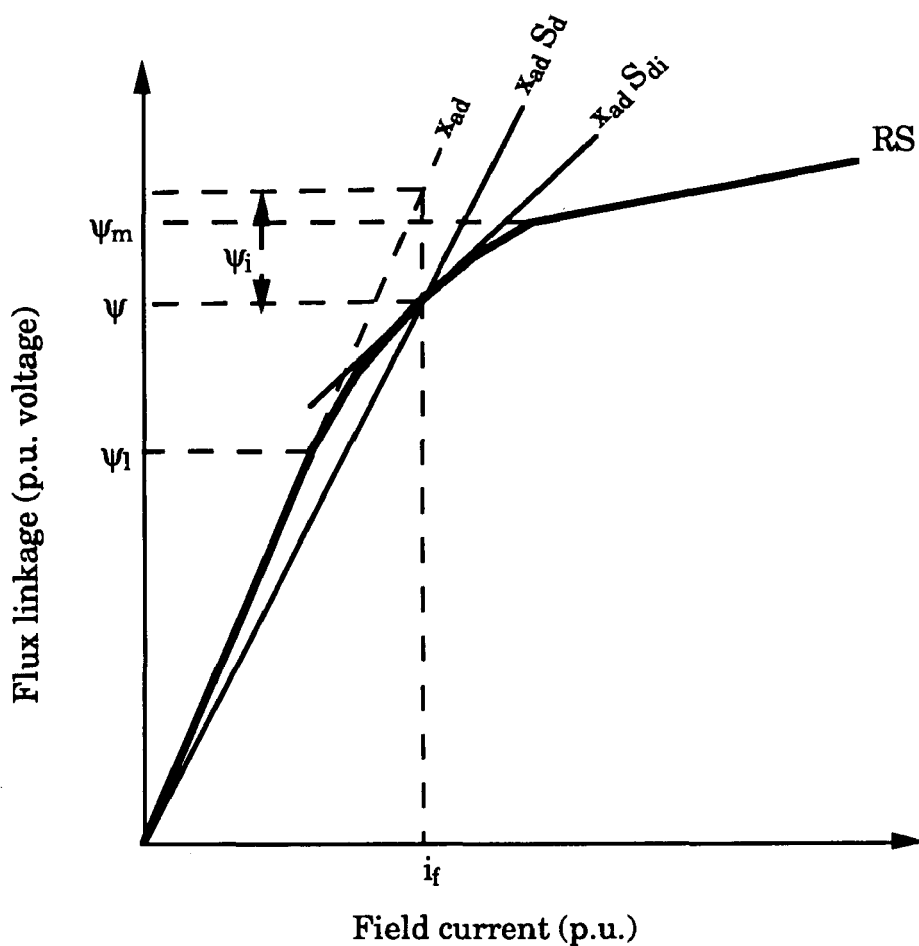
Figure (A1.6) Machine saturation curve.

The curve of flux linkages (ψ) versus the field current (i_f) is split into three regions; Region 1, Region 2 and Region 3.

Region 1: Here the relationship between the flux linkage (ψ) in per unit voltage and the field current (i_f) is linear i.e.

$$\psi = x_{ad}\, i_f \qquad\qquad\qquad (A1.40)$$

where,

x_{ad} = Unsaturated mutual reactance (p.u.).

Region 2: Here the relationship between the flux linkage (ψ) in per unit voltage and the field current (i_f) is nonlinear and is given by

$$\psi = x_{ad}\, i_f - \psi_i \qquad\qquad (A1.41)$$

where, $\psi_i = A_{ex}\, \varepsilon^{\,B_{ex}(\psi - \psi_1)} \qquad\qquad (A1.42)$

ψ_1 = The level of flux linkages beyond which the saturation characteristics become nonlinear.

A_{ex} , B_{ex} = Constant coefficients of the saturation function defining ψ_i in Region 2.

Region 3: Here the relationship between the flux linkage (ψ) in per unit voltage and the filed current (i_f) is linear but the slope of the characteristic is different than in Region 1. The relation between the flux linkage in per unit voltage and the field current is given by

$$\psi = x_{ad}\, i_f - \psi_i \qquad\qquad (A1.43)$$

where, $\psi_i = A_{ex}\, \varepsilon^{\,B_{ex}(\psi_m - \psi_1)} + RS\,(\psi - \psi_m) \qquad\qquad (A1.44)$

and

ψ_m = The level of flux linkages defining the transition between Region 2 and Region3.

A_{ex} , B_{ex} = Constant coefficients of the saturation function defining ψ_i in Region 2.

RS = Ratio of the slopes of the saturation characteristics in Region1 to that of Region 3.

A1.5.1 Determination of ψ from the terminal quantities

Figure (A1.7) gives the phasor diagram of the synchronous machine under steady state operation. ψ is the voltage behind the stator resistance (r_a) and stator leakage reactance (x_l). Therefore,
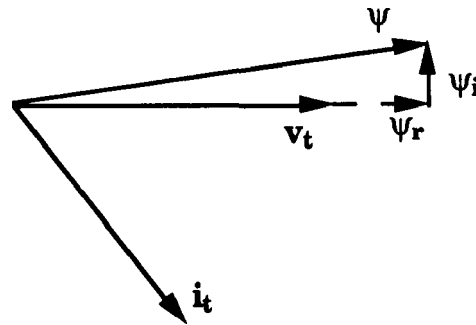

Figure (A1.7): Phasor diagram of terminal quantities

$$\psi = \sqrt{{\psi_r}^2 + {\psi_i}^2} \qquad (A1.45)$$

where,

$\psi_r = v_t + r_a (i_t \cos\phi) + x_l (i_t \sin\phi)$

$\psi_i = -r_a (i_t \sin\phi) + x_l (i_t \cos\phi)$

ϕ = Power factor of the machine

v_t = Terminal voltage magnitude (p.u.).

i_t = Terminal current magnitude (p.u.).

A1.5.2   Calculation of the saturation factors S_d and S_q

In representing machine saturation, the unsaturated mutual reactances cannot be used. The saturated reactances x_{ads}, x_{aqs}, give the slope of the line passing through the origin which intersects the saturation characteristics at the corresponding operating point. Therefore,

$$x_{ads} = x_{ad} S_d \qquad (A1.46)$$

$$x_{aqs} = x_{aq} S_q \qquad (A1.47)$$

Region 1: Here as the saturation characteristic is linear the saturated mutual reactances and the unsaturated reactances are the same. Therefore,

$$x_{ads} = x_{ad} \qquad (A1.48)$$

$$x_{aqs} = x_{aq} \qquad (A1.49)$$

For ISAT = 1 or 2

$$S_d = 1 \qquad (A1.50)$$

$$S_q = 1 \qquad (A1.51)$$

Region 2 & Region 3: The flus linkages in per unit voltage in terms of the saturated reactance is

$$\psi = x_{ads} \, i_f \tag{A1.52}$$

From Equations (A1.41), (A1.42), (A1.45) and (A1.51) one gets,

$$S_d = \frac{\psi}{\psi + \psi_i} \tag{A1.53}$$

For ISAT = 1

$$S_d = \frac{\psi}{\psi + \psi_i} \tag{A1.54}$$

$$S_q = 1 \tag{A1.55}$$

For ISAT = 2

$$S_d = S_q = \frac{\psi}{\psi + \psi_i} \tag{A1.56}$$

It must be noted that the calculation of ψ_i is different in Region 2 and Region 3.

A1.5.3 Calculation of the incremental saturation factors S_{di} and S_{qi}

In the small signal analysis of power system the machine incremental saturation factors are used. The incremental saturated

reactances x_{adsi}, x_{aqsi}, give the slope of the line tangent to the saturation characteristic at the operating point. Therefore,

$$x_{adsi} = x_{ad} S_{di} \qquad \text{(A1.57)}$$

$$x_{aqsi} = x_{aq} S_{qi} \qquad \text{(A1.58)}$$

<u>Region 1:</u> Here as the saturation characteristic is linear the incremental saturated mutual reactances and the unsaturated reactances are the same i.e. the machine is operating in the linear range. Therefore,

$$x_{adsi} = x_{ad} \qquad \text{(A1.59)}$$

$$x_{aqsi} = x_{aq} \qquad \text{(A1.60)}$$

For ISAT = 1 or 2

$$S_{di} = 1 \qquad \text{(A1.61)}$$

$$S_{qi} = 1 \qquad \text{(A1.62)}$$

<u>Region 2 & Region 3:</u> From Equation (A1.41) and (A1.43) one gets for Regions 2 and 3,

$$\psi = x_{ad} i_f - \psi_i \qquad \text{(A1.63)}$$

The first derivative with respect to the field current of Equation (A1.63) gives the slope of the tangent to the saturation characteristic at the operating point. therefore,

$$\frac{\Delta\psi}{\Delta i_f} = \frac{x_{ad}}{1 + \psi_i\, B_{sat}} = x_{adsi} = \text{incremental saturated reactance.} \qquad \text{(A1.64)}$$

Therefore from Equation (A1.57) and (A1.64) gives,

$$S_{di} = \frac{1}{1 + \psi_i\, B_{sat}} \qquad \text{(A1.65)}$$

For ISAT = 1

$$S_d = \frac{1}{1 + \psi_i\, B_{sat}} \qquad \text{(A1.66)}$$

$$S_q = 1 \qquad \text{(A1.67)}$$

For ISAT = 2

$$S_d = S_q = \frac{1}{1 + \psi_i\, B_{sat}} \qquad \text{(A1.68)}$$

It must be noted that the calculation of ψ_i is different in Region 2 and Region 3.

A1.6 Calculation of the steady state exciter output

Figure (A1.8) gives the phasor diagram of the synchronous machine under steady state. The equivalent field current (i_f) required to maintain the steady state terminal voltage (v_t) is given by
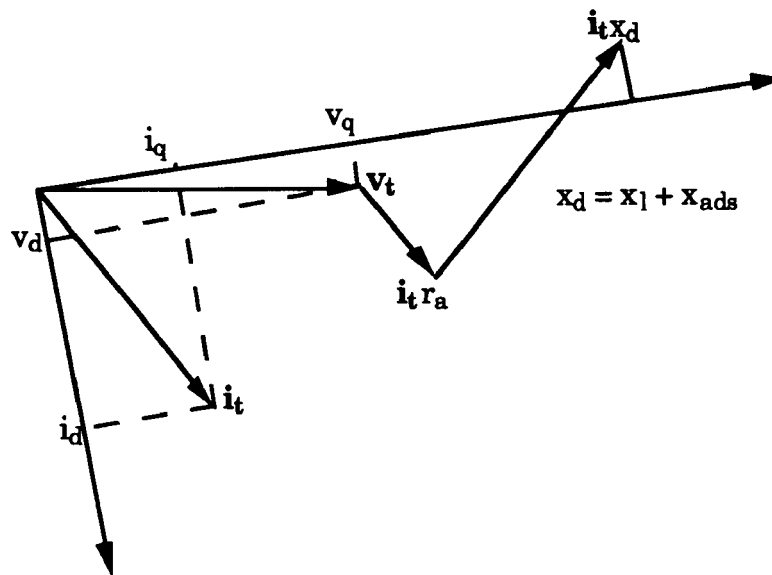
Figure (A1.8) Phasor diagram to determine field current.

$$i_f = \frac{v_q + i_q \, r_a + i_d \, x_d}{x_{ads}} \qquad\qquad \text{(A1.69)}$$

Therefore, the field voltage is,

$$Efd = i_f \, x_{ad} \qquad\qquad \text{(A1.70)}$$

A1.7 Network reduction

The final state matrix [A] of the power system takes the form:

$$[A] = [A_{st}] + [B_{st}] \, [Y_N + Y_{st}]^{-1} \, [C_{st}] \qquad\qquad \text{(A1.71)}$$

It is seen that the derivation of the state matrix involves the matrix inversion of the interconnecting network. For large networks this inversion process will be coputationaly costly. Compared to the number of buses present in the network, the number of buses to which devices are connected is small. This is used to advantage in reducing the network to only the device buses and then inverting the resulting matrix. The general form of the equation describing the linearized network is given below in partitioned form depending on the type of bus i.e. device bus, remote sensing bus or load bus.

$$
\begin{bmatrix} \Delta i_d \\ \Delta i_r \\ \Delta i_l \end{bmatrix} = \begin{bmatrix} Y_{dd} & Y_{dr} & Y_{dl} \\ Y_{rd} & Y_{rr} & Y_{rl} \\ Y_{ld} & Y_{lr} & Y_{ll} \end{bmatrix} \begin{bmatrix} \Delta v_d \\ \Delta v_r \\ \Delta v_l \end{bmatrix}
\tag{A1.72}
$$

where,

$[\Delta i_d]$ = Vector of small changes in current injections into the system device buses from all the system devices.

$[\Delta i_r]$ = Vector of small changes in current injections into the system remote sensing buses.

$[\Delta i_l]$ = Vector of small changes in current injections into the system load buses.

$[\Delta v_d]$ = Vector of small changes in the device bus voltages.

$[\Delta v_r]$ = Vector of small changes in the remote sensing buses.

$[\Delta v_l]$ = Vector of small changes in the load buses.

The current injections into the remote sensing buses and the load buses are zero, since there is no source connected to them. hence,

$$[\Delta i_r] = [0] \tag{A1.73}$$

$$[\Delta i_l] = [0] \tag{A1.74}$$

Using Equation (A1.74), (A1.73) and (A1.72) one can represent the changes in the voltage of the remote sensing and load buses in terms of the changes in the voltages of the device buses i.e.

$$[\Delta v_l] = [Y_{LD}] [\Delta v_d] \tag{A1.75}$$

$$[\Delta v_r] = [Y_{RD}] [\Delta v_d] \tag{A1.76}$$

where,

$$[Y_{LD}] = - Y_{ll}^{-1} \{Y_{ld} - Y_{lr} [Y_{rr} - Y_{rl} Y_{ll}^{-1} Y_{lr}] [Y_{rd} - Y_{rl} Y_{ll}^{-1} Y_{ld}] \} \tag{A1.77}$$

$$[Y_{RD}] = - [Y_{rr} - Y_{rl} Y_{ll}^{-1} Y_{lr}] [Y_{rd} - Y_{rl} Y_{ll}^{-1} Y_{ld}] \tag{A1.78}$$

Now, $[\Delta i_d] \neq [0]$ and therefore the reduced network equation becomes:

$$[\Delta i_d] = [Y_{DD}] [\Delta v_d] \tag{A1.79}$$

where,

$$[Y_{DD}] = Y_{dd} + Y_{dr} Y_{RD} + Y_{dl} Y_{LD} \tag{A1.80}$$

Equation (A1.80) is finally used in the inversion process for obtaining the system state matrix. From Equation (A1.75) and (A1.76) the remote sensing and load bus voltages can be reconstructed once the device bus voltages are known.

A1.8 System stability - Eigenvalues & Eigenvectors; State participation factors

The stability of a system described by state space equations is determined by the eigenvalues of the system state matrix [A]. If all the eigenvalues have negative real parts then the system is said to be stable. The eigenvalues of a system state matrix are the same as the poles of the characteristic equation of the same system.

Consider the matrix [A] and one of its eigenvalues λ. Then the column vector [p] and row vector [q] are called the right and left eigenvector of the matrix [A] respectively, if they satisfy the following expressions,

$$[A] [p] = \lambda [p] \qquad\qquad (A1.81)$$
$$[q] [A] = \lambda [q] \qquad\qquad (A1.82)$$
$$[p] , [q] \neq 0$$

Each eigenvalue λ of the matrix [A] has a right [p], and a left [q] eigenvector. Let the matrix [A] have all its eigenvalues distinct, then the set of all the right eigenvectors are orthogonal with respect to each other.

Similarly, the set of all left eigenvectors, will also be orthogonal with respect to each other. The multiplication of any right eigenvector with any left eigenvector results in the following expression,

$$k = \sum_{m=1}^{n} p_{im} \, q_{jm} \tag{A1.83}$$

where, k is always zero except for the condition that i is equal to j. i.e. k is nonzero only when the right and left eigenvectors corresponding to the same eigenvalue are multiplied. In the above equation p_{im} and q_{jm} are the mth elements of the right and left eigenvectors respectively, corresponding to the ith eigenvalue. Also n is the size of the matrix [A].

The eigenvalues and right eigenvaectors of the state matrix [A] of the power system are calculated by routines from the eigensystem package EISPACK [21]. The right eigenvectors are then scaled so that their infinite norm is unity. Let [P] be the matrix whose columns are the right eigenvectors of the matrix [A]. The matrix [Q] whose rows are the left eigenvectors of [A] are obtained by inverting matrix [P]. The left eigenvector matrix [Q] is obtained by inverting the right eigenvector matrix [P]. i.e.

$$[Q] = [P]^{-1}. \tag{A1.84}$$

Diagonalization

Let [P] and [P]$^{-1}$ be the right and left eigenvector matrices of [A] respectively and [Λ] be its eigenvalue matrix. Matrices [P], [P]$^{-1}$ and [Λ] may be complex. the eigenvalue matrix [Λ] is diagonal if the eigenvalues of matrix [A] are distinct. In power systems no two devices have exactly the same characteristics even if they are manufactured by the same company, at the same time. Hence one can say that the state matrix of the power system does not contain any repeated eigenvalues i.e. all the eigenvalues of the power system are distinct.

The diagonalization of matrix [A] can be achieved by the following operations on it as given below,

$$[Λ] = [P]^{-1} [A] [P]. \tag{A1.85}$$

State participation factors

The state participation factor is a sensitivity index. It is the sensitivity of the specified eigenvalue to changes in the diagonal element of the power system state matrix. The magnitude of these factors convey information of the amount of influence the corresponding system states have on a particular eigenvalue. Also, since these factors are non-dimensional, they do not have the scaling problems of the eigenvectors and are better at determining which states have a predominant influence on the

specified eigenvalue. The calculation of the state participation factors are described below.

Consider the system state matrix [A] and one of its eigenvalues λ. Cooresponding to the eigenvalue λ, let [p] and [q] be the corresponding right and left eigenvectors respectively. The right eigenvector [p] satisfies the following expression,

$$\lambda [p] = [A] [p] \tag{A1.86}$$

premultiplying both sides of the above equations with [q] gives,

$$\lambda [q] [p] = [q] [A] [p] \tag{A1.87}$$

From Equation (A1.85) it is seen that,

$$[q] [p] = 1.0 \tag{A1.88}$$

Therefore, Equation (A1.87) is rewritten as,

$$\lambda = [q] [A] [p] \tag{A1.89}$$

Taking the partial derivative of λ with respect to the diagonal element a_{ii} of the matrix [A] gives,

$$\frac{\partial \lambda}{\partial a_{ii}} = q_i \, p_i \tag{A1.90}$$

where, q_i is the ith element in the row vector [q], and p_i is the ith element in the column vector [p]. Equation (A1.90) gives the state participation factor of the ith state of the system to the eigenvalue λ.

Appendix 2 - System Data

A2.1 Network data

Table (A2.1): Network data in per unit (Base-100MVA, 100 KV)

From Bus No.	To Bus No.	Ckt I.D	r (p.u.)	x (p.u.)	B (p.u.)
1	2		0.0035	0.0411	0.6987
1	39	1	0.0020	0.0500	0.3750
1	39	2	0.0020	0.0500	0.3750
2	3		0.0013	0.0151	0.2572
2	25		0.0070	0.0086	0.1460
2	30		0.0000	0.0181	0.0000
3	4		0.0013	0.0213	0.2214
3	18		0.0011	0.0133	0.2138
4	5		0.0008	0.0128	0.1342
4	14		0.0008	0.0129	0.1382
5	6		0.0002	0.0026	0.0434
5	8		0.0008	0.0112	0.1476
6	7		0.0006	0.0092	0.1130
6	11		0.0007	0.0082	0.1389
6	31	1	0.0000	0.0500	0.0000

243

Table (A2.1) Network data (Contd.)

6	31	2	0.0000	0.0500	0.0000
7	8		0.0004	0.0046	0.0780
8	9		0.0023	0.0363	0.3804
9	39		0.0010	0.0250	1.2000
10	11		0.0004	0.0043	0.0729
10	13		0.0004	0.0043	0.0729
10	32		0.0000	0.0200	0.0000
12	11		0.0016	0.0435	0.0000
12	13		0.0016	0.0435	0.0000
13	14		0.0009	0.0101	0.1723
14	15		0.0018	0.0217	0.3660
15	16		0.0009	0.0094	0.1710
16	17		0.0007	0.0089	0.1342
16	19		0.0016	0.0195	0.3040
16	21		0.0008	0.0135	0.2548
16	24		0.0003	0.0059	0.0680
17	18		0.0007	0.0082	0.1319
17	27		0.0013	0.0173	0.3216
19	20		0.0007	0.0138	0.0000
19	33		0.0007	0.0142	0.0000
20	34		0.0009	0.0180	0.0000
21	22		0.0008	0.0140	0.2565
22	23		0.0006	0.0096	0.1846

Table (A2.1) Network data (Contd.)

22	35		0.0000	0.0143	0.0000
23	24		0.0022	0.0350	0.3610
23	36		0.0005	0.0272	0.0000
25	26		0.0032	0.0323	0.5130
25	37		0.0006	0.0232	0.0000
26	27		0.0014	0.147	0.2396
26	28		0.0043	0.0474	0.7802
26	29		0.0057	0.0625	1.0290
28	29		0.0014	0.0151	0.2490
29	38		0.0008	0.0156	0.0000

A2.2 Dynamic device data

Generator Data:

All generating system data is on 100 MVA, 100KV base, all machines have one q-axis damper winding and the exciters are of either IEEE DC1 or ST1 type. Machine saturation is ignored. All data is expressed in per unit. H and D is the inertia constant and damping in per unit respectively. All data is with reference to the generator d-q equivalent circuits and the exciter block diagram.

Table (A2.2a): Generator data-machine & exciter data.

	G30	G31	G32	G33	G34	G35	G36	G37	G38
H	42.0	30.3	35.8	28.6	26.0	34.8	26.4	24.3	34.5
D	4.0	9.75	10.0	10.0	3.0	10.0	8.0	9.0	14.0
x_{ad}	0.087	0.26	0.22	0.232	0.616	0.232	0.263	0.262	0.181
x_{aq}	0.056	0.247	0.207	0.228	0.566	0.219	0.26	0.252	0.175
x_l	0.013	0.035	0.03	0.03	0.054	0.022	0.032	0.028	0.03
r_a	0.000	0.0	0.0	0.0	0.0	0.006	0.0	0.001	0.0
x_{fl}	0.0227	0.0404	0.0257	0.0149	0.0893	0.0318	0.0182	0.0326	0.0317
rf	2.85E-5	1.22E-4	1.14E-4	1.15E-4	3.47E-4	9.6E-5	1.32E-4	1.17E-4	1.18E-4
x_{klq1}	0.0	.2977	.0806	0.337	.1396	.0808	.3777	.0840	.0348
r_{kq1}	0.0	9.6E-4	5.1E-4	1.0E-3	4.25E-3	1.99E-3	1.13E-3	2.17E-3	2.84E-4

Table (A2.2a): Generator data-excter data.

Ka	25.0	6.0	5.0	5.0	40.0	5.0	40.0	5.0	40.0
Ta	0.06	0.05	0.06	0.06	0.02	0.02	0.02	0.02	0.02
Ke	*	-0.63	-0.02	-0.05	*	-0.04	1.0	-0.05	1.0
Te	*	0.41	0.5	0.5	*	0.47	0.73	0.53	1.4
Aex	*	0.705	.0184	.0035	*	.0021	0.493	.0028	0.61
Bex	*	0.288	0.625	0.82	*	0.857	0.311	0.837	0.3
Kf	*	0.25	0.08	0.08	*	0.075	0.03	0.085	0.03
Tf	*	0.5	1.0	1.0	*	1.25	1.0	1.26	1.0

* blocks with these parameters do not exist for IEEE ST1 type exciter.

SVC data:

The three SVCs are assumed to have identical parameters. The parameters are reference to the SVC block diagram.

Table (A2.2b): SVC Data

	S1,S16,S23
Base MVA	100.0
Base KV	100.0
Ksvc	50.0
T1	0.172
T2	0.216
T3	0.0
T4	0.0
T5	0.006
T6	0.016

A2.3 Nominal operating condition load flow data

Nominal operating condition load flow solution: loads, generation and voltage magnitude in per unit. (Base-100MVA, 100KV) (All lines in service.)

Table (A2.3): Nominal operating condition load flow solution

Bus No.	I V I	Angle	Load MW (p.u.)	Load Mvar (p.u.)	Generation MW (p.u.)	Generation Mvar (p.u.)
1	1.0362	-9.8009	0.0000	0.0000	0.0000	0.0000
2	1.0195	-7.0103	0.0000	0.0000	0.0000	0.0000
3	0.9917	-9.9973	3.2200	0.0240	0.0000	0.0000
4	0.9551	-10.8125	5.0000	1.8400	0.0000	0.0000
5	0.9540	-9.4724	0.0000	0.0000	0.0000	0.0000
6	0.9552	-8.6842	0.0000	0.0000	0.0000	0.0000
7	0.9472	-11.1386	2.3380	0.8400	0.0000	0.0000
8	0.9478	-11.7050	5.2200	1.7600	0.0000	0.0000
9	1.0083	-11.5817	0.0000	0.0000	0.0000	0.0000
10	0.9620	-6.0207	0.0000	0.0000	0.0000	0.0000
11	0.9584	-6.9312	0.0000	0.0000	0.0000	0.0000
12	0.9389	-6.9533	0.0850	0.8800	0.0000	0.0000
13	0.9603	-6.8301	0.0000	0.0000	0.0000	0.0000
14	0.9610	-8.7152	0.0000	0.0000	0.0000	0.0000
15	0.9694	-9.2229	3.200	1.5300	0.0000	0.0000

Table (A2.3): Nominal load flow (Contd.)

16	0.9888	-7.7104	3.2940	0.3230	0.0000	0.0000
17	0.9928	-8.8113	0.0000	0.0000	0.0000	0.0000
18	0.9909	-9.7269	1.5800	0.3000	0.0000	0.0000
19	0.9900	-2.5050	0.0000	0.0000	0.0000	0.0000
20	0.9869	-3.9118	6.8000	1.0300	0.0000	0.0000
21	0.9955	-5.1393	2.7400	1.1500	0.0000	0.0000
22	1.0217	-0.4338	0.0000	0.0000	0.0000	0.0000
23	1.0204	-0.6606	2.4750	0.8460	0.0000	0.0000
24	0.9970	-7.5855	3.0860	-0.9220	0.0000	0.0000
25	1.0282	-5.5577	2.2400	0.4720	0.0000	0.0000
26	1.0177	-6.8541	1.3900	0.1700	0.0000	0.0000
27	1.000	-8.9883	2.8100	0.7550	0.0000	0.0000
28	1.0191	-3.1303	2.0600	0.2760	0.0000	0.0000
29	1.0206	-0.2134	2.8350	0.2690	0.0000	0.0000
30	1.0475	-4.5818	0.0000	0.0000	2.5000	1.6170
31	0.9820	0.0000	0.0920	0.0460	5.7571	1.5291
32	0.9831	1.8803	0.0000	0.0000	6.5000	1.4862
33	0.9972	2.6913	0.0000	0.0000	6.3200	0.4796
34	1.0123	1.2673	0.0000	0.0000	5.0800	1.4031
35	1.0493	4.5403	0.0000	0.0000	6.5000	2.3080
36	1.0635	7.3558	0.0000	0.0000	5.6000	1.9720
37	1.0278	1.2455	0.0000	0.0000	5.4000	0.1635
38	1.0265	6.8654	0.0000	0.0000	8.3000	0.4751
39	1.0300	-11.4056	11.0400	2.5000	10.0000	2.1615

A2.4 Weakened operating condition load flow data

Weakened operating condition load flow solution: loads, generation and voltage magnitude in per unit. (Base-100MVA, 100KV) (line 21-22 out of service).

Table (A2.4): Weakened operating condition load flow solution

Bus No.	I V I	Angle	Load MW (p.u.)	Load Mvar (p.u.)	Generation MW (p.u.)	Generation Mvar (p.u.)
1	1.0335	-10.4328	0.0000	0.0000	0.0000	0.0000
2	1.0125	-7.6406	0.0000	0.0000	0.0000	0.0000
3	0.9764	-10.6621	3.2200	0.0240	0.0000	0.0000
4	0.9415	-11.4019	5.0000	1.8400	0.0000	0.0000
5	0.9447	-9.9425	0.0000	0.0000	0.0000	0.0000
6	0.9466	-9.1216	0.0000	0.0000	0.0000	0.0000
7	0.9387	-11.6363	2.3380	0.8400	0.0000	0.0000
8	0.9395	-12.2206	5.2200	1.7600	0.0000	0.0000
9	1.0049	-12.1604	0.0000	0.0000	0.0000	0.0000
10	0.9528	-6.4655	0.0000	0.0000	0.0000	0.0000
11	0.9493	-7.3746	0.0000	0.0000	0.0000	0.0000
12	0.9285	-7.4120	0.0850	0.8800	0.0000	0.0000
13	0.9490	-7.3002	0.0000	0.0000	0.0000	0.0000
14	0.9447	-9.2624	0.0000	0.0000	0.0000	0.0000
15	0.9378	-9.8841	3.200	1.5300	0.0000	0.0000
16	0.9512	-8.2920	3.2940	0.3230	0.0000	0.0000

Table (A2.4): Weakened load flow (Contd.)

17	0.9645	-9.4634	0.0000	0.0000	0.0000	0.0000
18	0.9675	-10.4110	1.5800	0.3000	0.0000	0.0000
19	0.9773	-2.9383	0.0000	0.0000	0.0000	0.0000
20	0.9796	-4.3918	6.8000	1.0300	0.0000	0.0000
21	0.9330	-10.6272	2.7400	1.1500	0.0000	0.0000
22	1.0220	17.6382	0.0000	0.0000	0.0000	0.0000
23	1.0034	14.2091	2.4750	0.8460	0.0000	0.0000
24	0.9537	-5.9548	3.0860	-0.9220	0.0000	0.0000
25	1.0217	-6.1979	2.2400	0.4720	0.0000	0.0000
26	1.0042	-7.5003	1.3900	0.1700	0.0000	0.0000
27	0.9794	-9.6779	2.8100	0.7550	0.0000	0.0000
28	1.0122	-3.7328	2.0600	0.2760	0.0000	0.0000
29	1.0159	-0.7932	2.8350	0.2690	0.0000	0.0000
30	1.0475	-5.1956	0.0000	0.0000	2.5000	2.0774
31	0.9820	0.0000	0.0920	0.0460	5.9866	1.9066
32	0.9831	1.5121	0.0000	0.0000	6.5000	1.9436
33	0.9972	2.2884	0.0000	0.0000	6.3200	1.3702
34	1.0123	0.8042	0.0000	0.0000	5.0800	1.8125
35	1.0493	22.6104	0.0000	0.0000	6.5000	2.2865
36	1.0635	22.3439	0.0000	0.0000	5.6000	2.6427
37	1.0278	0.6389	0.0000	0.0000	5.4000	0.4532
38	1.0265	6.3042	0.0000	0.0000	8.3000	0.7827
39	1.0300	-12.0199	11.0400	2.5000	10.0000	2.4131

References

[1]   Ontario Hydro, 'Small Disturbance Stability Analysis Program
        Package Development - Final Report'. EPRI Research project - 2447,
        1987.

[2]   R.T.Byerly, E.W.Kimbark (Editors), 'Stability of Large Electric Power
        Systems', IEEE Press, 1974.

[3]   Federal Power Commission, 'Prevention of power failures'. Vol I,II
        & III., 1967.

[4]   P.Kundur, 'Digital Simulation of Multi-Machine power systems for
        stability studies', IEEE Transactions on Power Apparatus and
        Systems, January 1968.

[5]   D.Y.Wong, G.J.Rogers, B.Poretta & P.Kundur, 'Eigenvalue analysis
        of Very Large Power Systems', IEEE Trans., PWRS-2,1988, pp 472-
        480.

[6]   P. Kundur et. al. 'Application of Power System Stabilizers for
        Enhancement of Overall System Stability', IEEE Trans., PWRS-4,
        May 1989, pp 614-621.

[7]   F.P. deMello, C. Concordia,'Concepts of Synchronous Machine
        Stability as Affected by Excitation Control', IEEE Trans., Vol. PAS-88,
        April 1969, pp. 316-329.

[8]   Yuan-Yih Hsu, et. al., 'Application of Power System Stabilizers and
        Static Var Compensators on a Longitudinal Power System',
        IEEE/PES Winter Meeting, 1988.

[9]   J.H.Chow, J.J.Sanchez-Gasca, 'Pole-Placement Designs of Power
        System Stabilizers', IEEE/PES Summer Meeting, 1988.

[10]   Nelson Martins, L.T.G.Lima, 'Eigenvalue and Frequency Domain
        Analysis of Small-Signal Electromechanical Stability Problems',
        IEEE Publication 90TH0292-3-PWR, pp 17-33.

[11]   I.J.Perez-Arriaga et. al, 'Selective Modal Analysis with Applications
        to Electric Power Systems-Parts 1,2', IEEE Trans., PAS-101,
        September 1982, pp. 3117-3134.

[12]   Nelson Martins, L.T.G.Lima; 'Determination of Suitable Locations of
        PSS & SVC for Damping Electromechanical Oscillations in Large
        Power Systems', Proc. of 1989 Power Industry Computer Application
        Conference, pp. 74-82, May 1989.

[13]   E.V.Larsen, D.A.Swann, 'Applying Power System Stabilizers. Parts 1,2,3', IEEE Trans., PAS-100, June 1981, pp. 3017-3046.

[14]   A.E.Fitzgerald, C.Kingsley. Jr, 'Eletric Machinery', McGraw-Hill Book Company Inc, 2nd Ed. 1961.

[15]   Yao-Nan Yu, 'Electric Power System Dynamics', Academic Press, 1983.

[16]   'Excitation System Models for Power System Stability Studies - IEEE Committee Report', IEEE Transactions on Power Apparatus and Systems, PAS-100, February 1981, pp. 494-507.

[17]   'Power System Stabilization via Excitation Control', IEEE tutorial course - 81 EHO 175-0 PWR.

[18]   J.F.Hauer,'Reactive Power Control as a Means for Enhanced Interarea Damping in the Western U.S. Power System - A Frequency Domain Perspective Considering Robustness Needs', IEEE Symposium on Application of SVS for System Dynamic Performance, Publication 87 TH0187-5-PWR, pp. 79-82,1987.

[19]   E.V.Larsen, J.H.Chow,'SVC Control Design Concepts for System Dynamic Performance', IEEE Special Symposium on Application of SVS for System Dynamic Performance, Publication 87TH0187-5-PWR, 1987.

[20] G.J.Rogers, P.Kundur,'Small Signal Stability of Power Systems',
      IEEE Publication 90TH0292-3-PWR.

[21] 'Matrix Eigensystem Routines - EISPACK Guide 2nd ed; vol 6 of
      Lecture Notes in Computer Science'. B.T.Smith, et. al. (New York:
      Springler-Verlag, 1976).

[22] Benjamin C. Kuo., 'Automatic Control Systems', Prentice-Hall of
      India, 1976.

[23] A.E.Hammad, 'A Fast Stability Program for Power Systems with
      Multi-terminal HVDC and Static Var Compensator', IEEE PICA-79,
      pp. 290-297, May 1979.

[24] IEEE Committee Report, 'Proposed Terms and Definitions for Power
      System Stability', IEEE Trans, Vol PAS-101 No. 7, July 1982.

[25] M.S.Moorty, 'Small Signal Stability (S3) program - User's Manual',
      PEARL, April 1990.